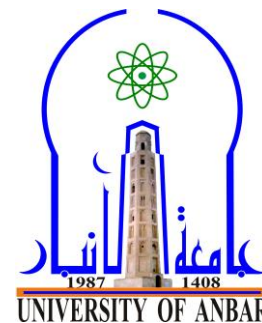Republic of Iraq
Ministry of Higher Education
And Scientific Research
University of Anbar
College of Sciences
Department of Chemistry

Removal of Some Pollutants from Aqueous Solutions Using Ultrasonic Technique and Prepared Multi Walled Carbon Nanotubes

A Thesis Submitted to

The College of Sciences - University of Anbar

as a Partial Fulfillment of the Requirements

for the Degree of Doctor of Philosophy

in Chemistry

By

Ahmed Mishaal Mohammed Farhan AL-Kubasi

BSc. Chemistry / University of Anbar (2000)

MSc. Chemistry / University of Anbar (2002)

Supervised by

Prof. Dr. Ismail K. Al-Khateeb   **Prof. Dr. Adawiya J. Haider**

College of Sciences   Nanotechnology and Advanced Materials Center

2013 A.C   1434 A.H.

بسم الله الرحمن الرحيم

﴿أَوَلَمْ يَرَ الَّذِينَ كَفَرُوا أَنَّ السَّمَوَاتِ وَالْأَرْضَ كَانَتَا رَتْقًا فَفَتَقْنَاهُمَا وَجَعَلْنَا مِنَ الْمَاءِ كُلَّ شَيْءٍ حَيٍّ أَفَلَا يُؤْمِنُونَ﴾

سورة الأنبياء

الاية ﴿30﴾

Summary

Activated carbon is characterized as being of special importance for its large use in industry field and for purposes of the pollution control. Removal of the pollutants which are benzene, o-xylene and sulfide ion is a main goal of the present research. The present investigation included the use of:

1. Non-activated carbon, activated carbon and multi-walled carbon nanotubes (MWCNT) synthesized from fuel oil wastes.

2. Ultrasonic technique.

In the first part the non-activated and activated carbons were prepared from the wastes of fuel oil through calcination and activation processes by using 20% of anhydrous zinc chloride. A novel MWCNT was synthesized from activated carbon by ultrasonic technique. Identification of MWCNT is achieved by using different techniques such as FE-SEM, TEM, AFM, XRD and FT-IR. Additional physical evaluations of the samples were also conducted such as the surface area, pH, density, moisture and ash content.

The prepared carbon types were tested to remove benzene, o-xylene and sulfide ion from aqueous solutions with using normal equilibration for sulfide ion, while benzene and o-xylene by using a new circulating system. Evaluation and efficiency of MWCNT and of activated and non-activated carbon samples were concerned through adsorption of benzene, o-xylene and sulfide ion from aqueous solution. Adsorption process on carbon for benzene, o-xylene and sulfide ion solutions was investigated at concentrations of (50, 100, 150, 200, 250, 300) ppm at four different temperatures (283, 293, 313 and 333) K and at different periods of time. Equilibrium adsorption study was done by using a new circulating system and isothermal models which are Langmuir, Freundlich and Temkin. Kinetic and thermodynamic parameters were also calculated.

Specific adsorption percentages of benzene and o-xylene were highly affected by the addition of activator and decreased with increasing

temperature compatible to that of non-activated carbon. The adsorption rate was increased by increasing benzene and o-xylene concentrations. A complete removal of benzene and o-xylene concentrations were achieved for initial concentrations of (50,100) ppm by MWCNT at temperature of 283 K. As such, it is clearly proved that benzene and o-xylene adsorption by synthetic MWCNT suits fair enough with the adsorption models. It clarifies that benzene and o-xylene adsorption by synthetic activated carbon and non-activated carbon agrees fair enough with the Freundlich and Temkin adsorption models and it poorly fits with Langmuir isotherm model. The negative value of enthalpy (ΔH^o) indicates that the adsorption process is exothermic and physical in nature, while the negative values of (ΔS^o) are explained on the basis of decrease in order at adsorption system. The negative value of (ΔG^o) indicates that the adsorption process could occur spontaneously. Kinetic study of the considered compounds on carbon showed that the adsorption system fits the pseudo first order model.

In the second part, degradation of benzene and o-xylene in an aqueous solution by ultrasonic has been done at different temperatures with initial concentrations of 100 and 200 ppm. Kinetic and thermodynamic degradation parameters of benzene and o-xylene were investigated, while, the mechanism of benzene and o-xylene sonolysis were proposed and discussed.

The degradation rate of benzene and o-xylene increased with the increasing of electric power, sonication time and decreased with increasing liquid volume, temperature and initial concentration of benzene and o-xylene. The beneficial effect of power on removal rates is believed to be due to increased cavitational activity occurring at higher levels of power. Thermodynamic parameters indicated that benzene and o-xylene degradation was spontaneous and exothermic in nature. Data obtained were fit with the pseudo-first order model.

LIST OF CONTENTS

LIST OF FIGURES

LIST OF TABLES

LIST OF IMAGES

List of Symbols and Abbreviations

Abbreviation	Name
ppm	Part per million
O-xylene	Ortho xylene
AC	Activated Carbon
CNT	Carbon Nanotubes
SWCNT	Single Walled Carbon Nanotubes
MWCNT	Multi Walled Carbon Nanotubes
CVD	Chemical Vapor Deposition
ΔG	Change of Gibbs Free Energy (kJ mol^{-1})
ΔS	Change in Entropy (J mol^{-1} K^{-1})
ΔH	Change in Enthalpy (kJ mol^{-1})
K_L	The Langmuir constant related to energy of adsorption (L /mg)
Q_o	The Langmuir constant related to maximum adsorption capacity
C_e	Concentration of adsorbate solution at equilibrium (mg/L)
C_o	Initial concentration of adsorbate solution (mg/L)
Q_e	The amount adsorbed per unit mass of adsorbent at equilibrium (mg/g).
K_f	The Freundlich constant related with adsorption capacity (mg/g)
n	The Freundlich constant related with adsorption intensity
q_t	Amount of adsorbate adsorbed at time t (mg /g)
V	Volume of adsorbate put in contact with the adsorbent (L)
M	Weight of adsorbate (g)
A, B	Temkin constants
COD	Chemical Oxygen Demand
g	Gram
BET	Brunauer, Emmett & Teller
nm	Nanometer
ASTM	American Standard for Testing Material
M	Molar

List of Symbols and Abbreviations

Abbreviation	Name
hr.	hour
min	Minute
TCD	Thermal Conductivity Detector
λ_{max}	Maximum Wave Length
UV – Vis.	Ultraviolet – Visible
Abs	Absorbance
SAOB	Sulfide Anti-Oxidant Buffer
FE-SEM	Field Emission Scanning Electron Microscopy
TEM	Transmission Electron Microscopy
AFM	Atomic Force Microscopy
HR-XRD	High Resolution X-Ray Diffraction
θ	The Angle between X-ray Beam and Reflecting Planes
FT-IR	FT-IR Fourier Transmission Infrared Analysis
k	The pseudo-first-order rate constant (min^{-1})
Eq.	Equation
N.A.C	Non-activated carbon
cm^{-1}	Unit of wave number
R^2	Correlation coefficient
R^*	Universal gas constant (8.314 J mol^{-1} K^{-1})
T	Temperature
t	Time
Conc.	Concentration
K	Equilibrium constant

CHAPTER ONE

1. Introduction

1.1. Overview

Pollution is one of the most serious problems affecting our environment, and life aspects. It is one of the most worldwide serious issues. With time, pollution problems increase with the growth of population and the increasing demands for water and food supplies which places an increasing stress on the ground and surface water quality and quantity [1-2].

1.2. Fuel Oil

Most petroleum products can be used as fuels, but the phrase "fuel oil", if ever used without qualification, may be interpreted differently depending on its context. However, because fuel oils are complex mixture of hydrocarbons, they can not be classified or defined precisely by chemical formula or definite physical properties. The arbitrary division or classification of fuel oils is based on their applications rather than on their chemical or physical properties. However, two broad classifications are generally recognized: (1) distillate fuel oil and (2) residual fuel oil [3].The conventional description of "fuel oil" is generally associated with the black, viscous residual material isolated as the result of refinery distillation of crude oil either alone or as a blend with light components used for steam generation and various industrial processes [4].

1.2.1. Residual Fuel Oil

The phrase "fuel oil" is applied not only to distillate products but also to residual materials, which are distinguished from distillate type fuel oil by boiling range and, hence, is referred to as residual fuel oil .Thus residual fuel oil is the fuel oil that is manufactured by the distillation residuum. The phrase includes all residual fuel oils, and fuel oil obtained by vis

breaking as well as by blending residual products from other operations [5]. Various grades of heavy fuel oils are produced to meet rigid specifications to ensure suitability for their intended usages. Detailed analysis of residual products, such as residual fuel oil, is more complex than the analysis of lower molecular weight liquid products. As with other products, there are a variety of physical property measurements that are required to determine whether the residual fuel oil meets specification or not. Yet, the range of molecular types presents in petroleum products increases significantly with the increase in the molecular weight (i.e., an increase in the number of carbon atoms per molecule). Therefore, characterization can not, and does not, focus on the identification of specific molecular structures but on molecular classes (paraffins, naphthenes, aromatics, polycyclic compounds, and polar compounds). Several tests that are usually applied to the lower-molecular-weight colorless and/or light-colored products can not apply to residual fuel oil [6, 7].

1.3. Effects of Organic and Inorganic Compounds on Human Health
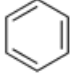
Organic and inorganic contaminants from industrial waste streams that seriously threaten the human health and the environment has been recognized as an issue of growing importance in recent years. The volume of waste water from domestic and industries is increasing yearly, the pollutants in the industrial waste water depend on the type of industries, the suitable treating processes and the type of the pollutants [8]. Harmful effects of benzene, o-xylene and sulfide ion prevalent in this study are as follow:

1.3.1. *Benzene*

Benzene is one of the major volatile organic compounds that are widely used in many industries as a solvent for organic synthesis, equipment cleaning and other processing purposes that exists in many fuels such as petroleum[9]. Petrochemical waste water introduces pollutants in the environment [10-12]. However, this compound has highly health concern causing cancer, irritation of mucosal membranes, hematological changes,

impairment of the central nervous system, respiratory problems and disruption of liver and kidney [13]. Therefore, the removal of this pollutant has a highly potential research in environmental treatments.
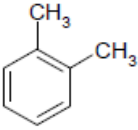
Table (1-1): Physiochemical properties of benzene compound [14]

Characteristics	Benzene
Chemical formula	C_6H_6
Chemical structure	
Polarity	Non-polar
Molecular weight (g/mol)	78.12
Density(g/cm^3)	0.876
Color	Colorless
Physical state	Liquid
Water solubility at 20 ^{o}C (mg/l)	1780
Boiling point (^{o}C)	80
Melting point (^{o}C)	5.5
Vapor pressure at 25 ^{o}C (mmHg)	95

1.3.2. *O-xylene*

Xylene has been widely used as a solvent in a variety of industries and commercial processes, such as chemical production, printing, paint, synthetic resin, rubber, automobiles emission [15]. However, the xylene is a volatile organic compound, which is produced by petroleum industries and presented in many petroleum derivatives, such as fuel oil and gasoline [16,17]. Xylene is a very risky organic compound as an environmental pollutant which penetrates human systems through ingestion, inhalation or absorption. Concerning healthy aspects, it might cause some problems in the liver, kidneys, heart, lungs and nervous system, including neurological diseases or cancer [18]. Therefore, the removal of these pollutants is an important target for environmental treatment systems.

Table (1-2): Physiochemical properties of o-xylene compound [14]

Characteristics	O-xylene
Chemical formula	$C_6H_4(CH_3)_2$
Chemical structure	
Polarity	Non-polar
Molecular weight (g/mol)	106.18
Density(g/cm^3)	0.880
Color	Colorless
Physical state	Liquid
Water solubility at 20 $^\circ$C (mg/l)	178
Boiling point ($^\circ$C)	144.41
Melting point ($^\circ$C)	-25.2
Vapor pressure at 25 $^\circ$C (mmHg)	6.61

1.3.3. *Sulfide Pollution*

Most of the hydrogen sulfide in raw waters is derived from natural sources and industrial processes [19]. A rotten egg odor characterizes H_2S in low concentrations. Some people can detect the gas by its odor at low concentrations. Human health is affected through exposure to hydrogen sulfide, by having irritating eyes and respiratory tract. Photophobia may persist for several days as conjunctivitis, pain, lacrimation, coughing, pain in breathing, pain in nose and throat. Repeated exposure causes headache, dizziness and digestive disturbances. Collapse and death may result from acute exposure to levels above 1000 ppm [20-22].

1.4. Water Pollution

Water pollution is of widespread national concern since different industrial activities generate a large number and variety of waste products. The problem of adequately handling of industrial waste waters is more

complex and difficult because industrial waste water vary in nature rating from relatively clean rinse waters to waste liquors than are heavily laden with organic or mineral matter or corrosive poisonous, inflammable or explosive substances [2].

As a result of rapid industrial growth following World War II, the amount of waste material generated by industries has increased manifold. The treatment of removal of these contaminants from the natural systems which they are released from has established into a special science, involving chemical, mechanical and biological processes. Impure water containing inorganic salts, organic compounds, microbial contamination and turbidity disturbs the natural hydrologic cycle (water cycle). The hydrologic cycle can be maintained by the removal of toxic chemicals by many scientifically simple and sometimes complex technological methods.

Hydrologic cycle which is one of the most important and yet highly unevenly distributed use of water with subsequent addition of contaminants has been disturbing the environmental balance. To prevent this disturbing, there are many techniques available for decontamination of waste water with the aim of minimizing waste and toxicity rates. Thus, if these methods are implemented correctly, development and growth can be sustained without destabilizing the hydrologic cycle. Preventing an effluent from entering into a large natural water source is the best option to control or limit its impact followed by minimization of the contaminants in it [23].

1.5. Waste water Treatment Methods

Techniques of organic and inorganic pollutants removal from aqueous systems are very important due to their high toxic nature even at very low concentrations. A wide range of methods are available for the removal of organic and inorganic compounds from aqueous solutions. These techniques includes ion exchange, microbial degradation [24,25], chemical oxidation and reduction, filtration, electrochemical treatment, cementation, evaporation [26], photo catalytic degradation [27], ultrasonic degradation [28],

enzymatic polymerization[29], membrane separation (reverse osmosis) [30], solvent extraction [31] precipitation and adsorption [32].

However adsorption methods were found to be more effective and attractive due to their lower costs and the higher efficiency for pollutants removal from waste water [33].

1.6. Activated Carbon (AC)

1.6.1. *AC Properties*

AC has been the most efficient and commonly used adsorbent in water purification all over the world [34-36]. The reason that AC is such an effective adsorbent material is due to its high surface area, porous structure, and high degree of surface activity [37, 38]. AC is also highly inert, thermally stable and can be used over a broad pH range [34].

1.6.2. *Historical Use of AC*

The use of carbon for water purification extends far back into history. The Egyptians used carbonized wood as a medical adsorbent and purifying agent [39]. Ancient Hindus filtered their drinking water with charcoal [40]. In 1901, scientists developed ways to synthesize AC from coal [41]. AC was first introduced industrially in the first part of the 20th century, when activated carbon from vegetable material was produced for use in sugar refining, since then, AC has been used in many industries [39].

1.6.3. *AC Application*

There are many applications for activated carbon in different fields, including separation and purification processes of gases and liquids [42-46], food and pharmaceutical industries [43, 47]. AC is also used as catalyst and catalyst support [42].

1.6.4. *AC Efficiency*

AC efficiency for removing a given pollutant depends on both its surface chemistry and its adsorption capacity [48]. The AC adsorption capacity is usually attributed to its internal pore volume that may be distributed throughout the solid as pores ranging in width from micro-pores to

macrospores [22, 48]. When the pore size of the activated carbon is in the range of the molecules, adsorption process will be enhanced and is expected to be efficient [39]. Adsorption capacity of the finished activated carbons also depends essentially on the type of the activation methods and on the structural properties of the original precursor material [49].

1.6.5. *Precursors of the AC*

Activated carbon is a relatively costly adsorbent [50]. Therefore, researchers are looking for new low-cost sources of AC. In addition to cost, there are many reasons which should be taken into account while choosing the precursors of activated carbon, such as abundance, purity, manufacturing process and further application of the product [37, 51].

Precursors of activated carbons are organic materials with high carbon content [52]. The most widely used carbonaceous materials for the industrial production of activated carbons are coal, wood and coconut shell [44, 53].

Recently, many agricultural by-products have been used as sources for activated carbon production [35, 36, 43, 54]. They have attracted considerable attention because they are widely available [44], renewable sources and their products give an economic gain [43]. Also by choosing these precursors some polluting wastes were removed from environment [54].

Many agricultural by-products were used for activated carbon preparation such as; peach stones [55], apricot stones [56], cherry stones [57], date stones [49, 58] , waste apple pulp [59], nut shells [37], pecan shell [60], walnut shells [61], almond shells [62], oil palm waste [63], rice husks [64], tea waste [65], coffee bean and grounds [52], corncob [66], cotton stalks [67] , and olive waste [43, 44, 68, 69].

1.7. Carbon Activation

In addition to the nature of the precursor, the activation process affects carbon characteristics [37, 44]. Different methods are used to prepare carbon with good affinity for adsorption by developing excellent surface properties and specific functionalities [39]. The main methods for the preparation of

activated carbons can be divided into physical and chemical activations [37, 70-73].

1.7.1. Physical Activation

The physical activation process involves two steps: firstly, is the carbonization (so-called pyrolysis) of the carbonaceous precursor [70] at elevated temperatures (500-1000°C) under inert atmosphere in order to eliminate oxygen and hydrogen elements as far as possible [49]. Many of the non-carbon elements, mainly volatiles, are removed during this process [49-51, 68, 72] yielding a solid residue (char) with carbon content is considerably higher than that of the precursor [68]. High-porosity carbons can be obtained only at high extents of char burn-off [72]. The second stage involves thermal activation of this char. Activation is a sequence process to enhance the char porosity and to clean out the tar-clogging pores; thus increasing the total surface area of the produced activated carbon [74]. The precursor and preparation methods (activation) not only determine its porosity but also the chemical nature of its surface, which consequently establishes its adsorptive and catalytic characteristics. Activation can be done either physically, chemically or by combination of both, known as physiochemical method. Physical activation is the gasification of the resulting char with activating agent such as carbon dioxide [68], steam or air [70] at high temperatures (800-1000 °C) [35, 68, 75]; developing a porous structure. The most activating agent widely used is steam because at a given temperature, the production has larger adsorptive capacity and wider pore size distribution compared to that of produced by CO_2.

1.7.2. Chemical Activation

In comparison with physical activation, chemical activation has two important advantages when a lignocellulose material is especially used as a raw material. One is the lower temperature (400-500) °C at which the process is accomplished making the process more economic compared to physical activation. The other is that the yield of chemical activation is

relatively higher, since carbon burn-off char is not required [37, 72, 76]. The formation of tar and other by-products is inhibited by the chemical agent [75, 76].

1.7.3. Operation of Chemical Activation

In chemical activation, the carbonaceous precursor is impregnated with an activating agent. Carbonization and activation are carried out simultaneously. The impregnated material is carbonized in an inert atmosphere [35, 72, 76]. There will be a reaction between the precursor and the activating agent used in activation, leading to developments in porosity [37].

The chemical activating agents act by dehydration of the sample during the chemical treatment stage and inhibit the formation of tar and volatiles and thereby increase the product yield [77].

1.7.4. Activating Agents

The chemical groups found on an activated carbon surface are directly attributed to the method of activation [16], type and concentration of the activating agents [37, 44, 77], pyrolysis temperature [44, 77], activation time [37, 78] and any additional treatment conditions [78]. Chemical activation involves impregnation of the raw material with chemicals that generally act as dehydrating materials and promote the pyrolytic decomposition and the formation of cross-links and inhibit formation of tar [37, 79].

Among the numerous activating agents the most widely used chemicals are zinc chloride [76, 77] and phosphoric acid [52]. These compounds are considered more effective and less expensive activating agents [80].

1.8. Surface Functional Groups of the Activated Carbon

The adsorption capacity of an AC is determined by the chemical nature of its surface. The surface of activated carbons is heterogeneous and it consists of faces of graphite sheets and edges of such layers. The edge sites are much more reactive than the atoms in the interior of the graphite sheets; chemisorbed foreign heteroatom, mainly containing nitrogen, hydrogen, halogen and particularly oxygen, are predominantly located on the edges

[81]. Oxygen in the surface oxides is bound in the form of various functional groups. The surface chemical functional groups mainly derive from activation process, precursor, heat treatment and post chemical treatment. The surface functional groups can be classified into two major groups; acidic groups consisting mainly carboxylic, lactones and phenols, and basic groups such as pyrone, chromene, ethers and carbonyls Fig .(1-1) [82].

In the case of liquid phase adsorption, the type of surface functional groups influences the process to a large extent causing a change in character of interactions between the solute molecules and carbon surface [83, 84]. Thus, the acidic or basic complexes formed on adsorbent surface determine the charge, the hydrophobicity, and the electronic density of the graphite layers, explaining the differences of adsorbent activity towards various substances.

An increase of adsorption is observed with the decrease of concentration of acidic surface groups [83, 85]. The increase of acidic surface function groups reinforces the hydrophilic nature of carbonic and thus decreases its affinity to non-polar organic compounds and conversely increases the adsorption capacity for polar molecules [86]. On the other hand, basic function groups lead essentially to hydrophobic carbons and display a strong affinity for organic molecules which have a limited solubility in water, like phenols [87].
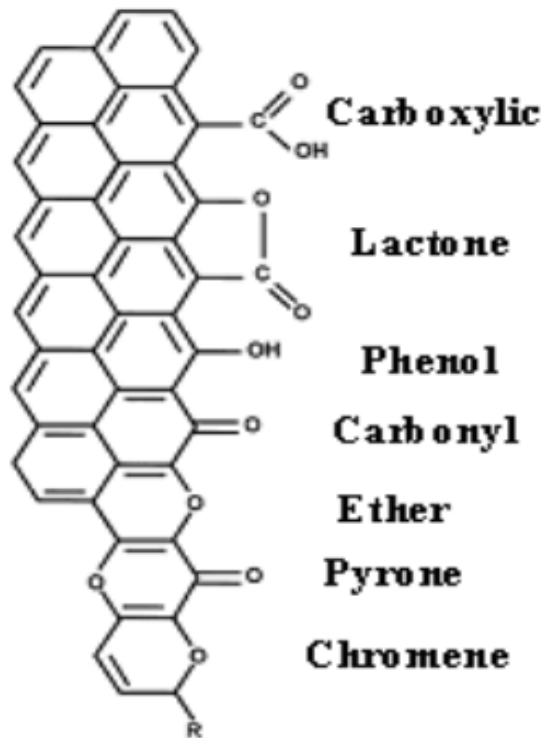
Fig. (1-1): Surface functional groups of the activated carbon

1.9. Carbon Nanotubes

Carbon nanotubes (CNT) rank among the most exciting new developments in modern science and engineering. They have attracted particular interest because they are predicted, and indeed observed, such small dimensions as extremely high strength, lightweight, elasticity, high thermal and air stability, high electric and thermal conductivity, and high aspect ratio offer crucial advantages. The potential utility of carbon nanotubes in a variety of technologically important applications such as molecular wires and electronics, sensors, high strength materials, and field emission has been well established [88, 89].

In the past 10 years, carbon nanotubes witnessed significant progress in both synthesis and investigations on their electrical, mechanical, and chemical properties [90]. This has been largely driven by the exciting science involved and numerous proposed applications of carbon nanotubes due to their unique chemical and electronic properties and nanometer sizes. Their large length (up to several microns) and small diameter (a few nanometers)

result in large ratio of about 1000, so they can be considered a two-dimensional structure (quantum wires) [91, 92].

Carbon nanotubes regarded as another form of pure carbon are perfectly straight tubules and their properties are close to those of an ideal graphite fiber. These tubes seamless cylindrical tubes, it is consisting of carbon atoms arranged in a regular hexagonal structure. It is considered as the ultimate engineering material because of its unique and distinct electronic, mechanical and material characteristics [93, 94].

1.10. Types of Carbon Nanotubes

Carbon nanotubes are classified into two main categories: single-walled carbon nanotubes (SWCNT) and multi-walled carbon nanotubes (MWCNT) depending on whether the tube walls are made of one layer (graphene tubes) or more (graphitic tubes). Iijima and co-workers [95] discovery consists of mainly the graphitic multi-walled nanotubes. In the mean time, CNT have emerged to be one of the most intensively investigated nanostructure materials [96].

1.10.1. *Single Walled Carbon Nanotubes* (SWCNT)

SWCNT are regarded cylindrical in shape and composed of singular graphene sheet rolled in cylinder walls with diameters ranging from 0.4 to 3 nm. Their physical and chemical properties differ due to difference in the length and diameter. It consists of two separate regions, with distinct physical and chemical properties. The first is the side wall of the tube and the second is the two hexagon cups [97].

Three types of single wall carbon nanotubes are possible: armchair, zig-zag and chiral nanotubes, depending on the way the two dimension graphene sheets are rolled up. By rolling a graphene sheet into a cylinder and capping each end of the cylinder with half of a fullerene molecule, a fullerene derives tubule and one atomic layer is formed as shown in Fig. (1-2). This direction in a graphite sheet and the nanotube diameter are derived from a pair of integers (n, m) [91].
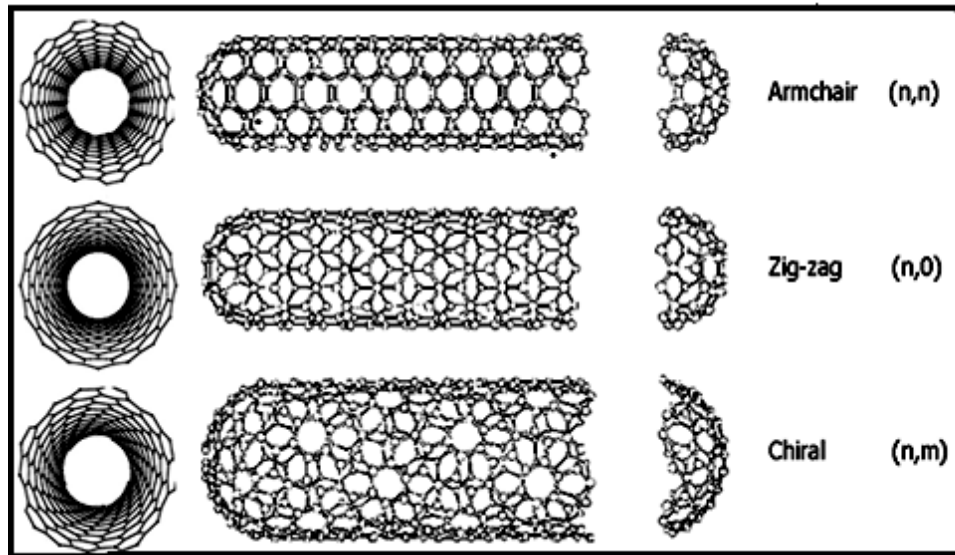
Fig. (1-2): Schematic theoretical model for a single walled carbon nanotubes [91]

1.10.2. *Multi Walled Carbon Nanotubes* (MWCNT)

MWCNT, which are the most general case, are a group of concentric SWCNT often capped at both ends with different diameters ranging from several nanometers up to 200 nm Fig. (1-3). These concentric nanotubes are held together by vander waals bonding. MWCNT form complex systems with different wall numbers, structures, and additional features such as: tips, internal closures within the central part of the tube. Compared with multi walled carbon nanotubes, SWCNT are expensive, clean and difficult to obtain; but they have been of great interest owing to their expected novel electronic, mechanical, and gas adsorption properties [98].
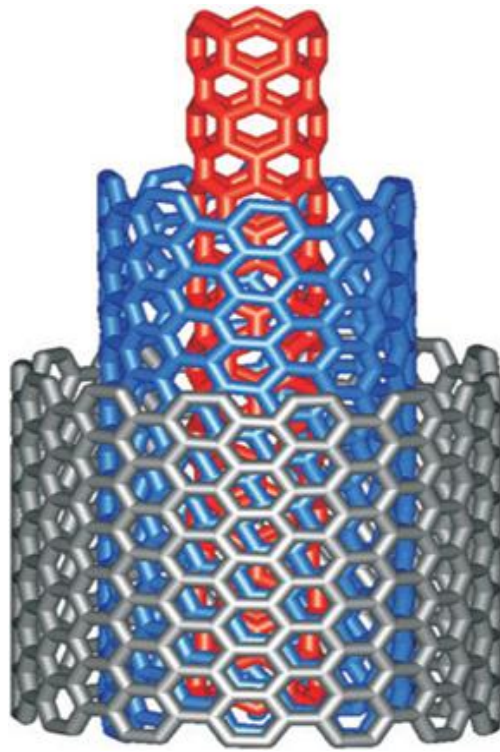
Fig. (1-3): Theoretical model for multi walled carbon nanotubes [98]

1.11. Carbon Nanotubes Synthesis

Carbon nanotubes can be synthesized using different techniques involving gas phase processes. These processes provide access to the high synthetic temperatures required for carbon nanotubes production. Three main methods are used to produce carbon nanotubes: the electric arc discharge [99], laser vaporization and chemical vapor deposition (CVD) [100, 101]. Other techniques include electrolytic synthesis, solar production method ….. etc. are being developed to find more economic ways of producing the unique and novel materials.

1.12. Applications of Carbon Nanotubes

Carbon nanotubes have evoked much interest since their discovery in 1991, due to their small size and unique electronic, mechanical and thermal properties. Many different applications have been proposed to exploit these unique properties, including energy storage [99], molecular electronics [102, 103], nano-probes [104], nano sensors [100, 105], nanotube composites and nanotube templates ….. etc. [99, 104].

1.13. Adsorption

The adsorption is usually associated with the transfer from a gas or liquid to a solid surface, or any other transformation, the substance being concentrated on the surface is defined as the adsorbate and the material on which the adsorbate accumulates as the adsorbent such as charcoal, silica-gel, zeolite, and porous clays [106].

The reason for adsorption phenomenon is the existence of some unsaturated forces on the adsorbent due to the incomplete coordination or insufficient material surface particles, like the liquid or solid phase adsorption which leads to saturate those forces on the adsorbent surface.

Decreasing in surface free energy (ΔG°) is occurred during the adsorption process, and decreasing in entropy (ΔS°) at the surface that the adsorption takes place, due to losing the degree of freedom possessed before adsorption. The decreasing of free energy and entropy at the same time will cause decreasing in heat content (ΔH°) according to the thermodynamic relation (exothermic change) [107]:

$$\Delta G^\circ = \Delta H^\circ - T \, \Delta S^\circ \, \ldots\ldots\ldots \quad (1\text{-}1)$$

So single partial layer may be formed at the adsorbed surface and in this case is called unimoleculer adsorption. Also multilayer may be formed at the adsorbed surface and known as multimolecular adsorption. On the other hand the penetration process of a particle in the phase of adsorbent is called absorption and the process of absorption and adsorption process together are called "sorption" [108]. This process usually takes place on the porous surface adsorbents. The enthalpy of this process is positive (endothermic process), because the distribution inside the adsorbent needs energy [109].

Adsorption is used in gas purification processes, such as in the removal of sulfur dioxide from a stack gas, and as a means of fractionating fluids which are difficult to separate by other separation methods. Oil and chemical industries make extensive use of adsorption in the cleanup and purification of waste water streams, and for the dehydration of gases.

However, the amount of adsorbate that can be collected on a unit of surface area is small .Thus a porous adsorbent with a large internal surface area is typically selected for industrial applications[110].

1.13.1. Types of Adsorption

The selection of an adsorbent includes a consideration of surface area as well as the type of solute and solvent involved in the adsorption process, since these relate to the types of forces (Vander Waals, dissociation, neutralization, oxidation) that are formed between the adsorbate and the surface, adsorption is described as either   physical adsorption (physisorption) or chemical adsorption (chemisorption) [110].

The primary difference between physisorption and chemisorption is the nature of bond that is formed between the adsorbed molecule and the adsorbent surface. Although chemical and physical adsorption are characterized by different thermal effects, a clear line between the two adsorption mechanisms does not exist. A large displacement of the electrons cloud toward the adsorbent and the sharing of electrons often result in about the same heat effects [109,110].

1.13.1.1. *Physisorption*

Physisorption results when the adsorbate adheres to the surface by Vander Waals, forces and electrostatic forces between adsorbate and adsorbent molecules. Although a displacement of electrons may exist, electrons are not shared between the adsorbent and adsorbate. The quantity of heat released for physisorption is approximately equal to the heat of condensation physisorption is often described as a condensation process. As expected, the quantity of material physically adsorbed increases as the adsorption temperature decreases.

The nature of Vander Waals, adsorption it is possible to adsorb much larger quantities which form layers several molecules in thickness or result in capillary condensation as shown in Fig.(1-4) [110,111].

1.13.1.2. *Chemisorption*

Chemisorption is characterized by a sharing of electrons between the adsorbent and adsorbate which result in the liberation of a quantity of heat that is approximately equal to the heat of reaction. Chemisorption involve ionic or covalent bond formation between the adsorbate molecules and the atoms of the functional groups of the adsorbent. Chemisorption occurs only on specific active centers which may represent only a small fraction of total surface. On this basis the maximum capacity of a surface for a specific chemisorption is frequently much less than the amount of adsorbate required to form a monomolecular layer as shown in Fig.(1-4), and because the sharing of electrons with the surface, chemisorbed materials are restricted to the formation of monolayer [112]. The quantity of adsorbate chemisorbed on surface increases with increased temperature [110, 111].

(a)   *(b)*
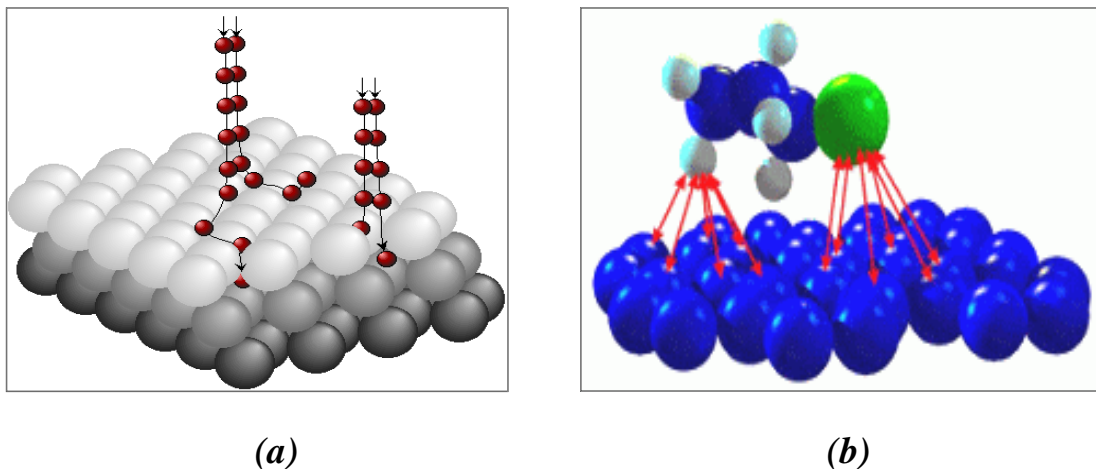
Fig. (1-4): The schematic representation of Physisorption (a) and Chemisorption (b) processes.

1.14. Adsorption Isotherm

Adsorption equilibrium studies are used to determine the distribution of adsorbate between the bulk fluid phase and the phase adsorbed on the surface of a solid adsorbent. The equilibrium distribution is generally measured at constant temperature and is referred to as an equilibrium isotherm. A number of mathematical models has been proposed to describe

the adsorption process. In addition to monolayer and multilayer adsorption, models have been developed to describe situations in which the adsorbate occurs locally on specific sites; or is mobile over the surface of the adsorbent. Consideration has also been given to cases in which adsorbed molecules interact not only with the surface but also with each other [110].

1.14.1. *Langmuir Equation*

The Langmuir isotherm equation is the first theoretically developed adsorption isotherm. It still retains an important position in physisorption as well as chemisorptions theories. The American scientist I. Langmuir derived this equation based on following assumptions [110].

1. All the sites of the solid have the same activity for adsorption.
2. There is no interaction between adsorbed molecules.
3. All of the adsorption occurs by the same mechanism, and each adsorbent complex has the same structure.
4. The extent of adsorption is no more than one monomolecular layer on the surface.

The Langmuir equation is frequently expressed in terms of the weight of adsorbate on the surface and concentrations other than pressure [110].

$$\frac{Ce}{Qe} = \frac{1}{Q_oK_L} + \frac{Ce}{Q_o} \quad \ldots\ldots\ldots\ldots \text{ (1-2)}$$

Where:

C_e: is the equilibrium concentration of the adsorbate (mg/L)

Q_e: The amount adsorbed per unit mass of adsorbent at equilibrium (mg/g).

Q_o and K_L (L.mg^{-1}): Langmuir constants which correspond to the maximum adsorption capacity (mg/g) of adsorbent and energy of adsorption, respectively.

1.14.2. *Freundlich Equation*

It describes equilibrium on heterogeneous surfaces and hence does not assume mono layer capacity [113]. The well-known logarithmic form of the Freundlich isotherm is given by the following equation:

$$\text{Log } Q_e = \log K_f + 1/n \log C_e \quad \ldots\ldots\ldots (1\text{-}3)$$

Where:

C_e is the equilibrium concentration of the adsorbate (mg/L), Q_e is the amount of adsorbate per unit mass of adsorbent (mg/g), K_F and n are Freundlich constants with n giving an indication of how favorable the adsorption process. K_F is related with adsorption capacity of the adsorbent. The slope (1/n) ranging between 0 and 1 is a measure of surface heterogeneity, becoming more heterogeneous as its value gets closer to zero [114]. A value for (n) less than one indicates a normal Freundlich isotherm, while (n) above one is indicative of efficient adsorption [115].

1.14.3. *Temkin Equation*

The linear form of Temkin isotherm is expressed as.

$$Q_e = B \text{ Ln } A + B \text{ Ln } C_e \quad \ldots\ldots\ldots (1\text{-}4)$$

This model was obtained with consideration of adsorption interaction and adsorption substances which was attained by designing diagram Ln C_e based on Q_e enables the determinations of the isotherm constants A and B. Mehdi and *et. al.* [116], observe that there is an accessible competition between this model and Freundlich model.

1.15. Ultrasonic Cavitation - Sonication

Ultrasound is a term used to describe sound energy at frequencies above the range that is normally audible to human beings (i.e.>16 kHz). At its upper limit ultrasound is not well defined but is generally considered as 5MHz in gases and 500MHz in liquids and solids which are subdivided to reflect applications. The range 20 to 100 kHz (though in certain cases up to 1 MHz) is designated as the power ultrasound reason, while the frequencies up to 1 MHz are known as high frequencies or diagnostics frequencies [117].

Sound is composed from longitudinal waves comprising rarefactions (negative pressures) and compressions (positive pressures). It is these alternating cycles of compression and rarefaction that, in high power ultrasonic applications, can produce a phenomenon known as "cavitation".

Cavitation is the formation, growth and collapse of bubbles in the liquid [118]. This process occurs whenever a new surface, or cavity, is created within a liquid. A cavity is any bounded volume, whether empty or containing gas or vapor, with at least part of the boundary being liquid. The collapse of the bubbles induces localized supercritical conditions: high temperature, high pressure, electrical discharges, and plasma effects. It has been reported that the gaseous contents of a collapsing cavity reach temperatures of 5000 ^{o}C, and the liquid immediately surrounding the cavity reaches 2100°C. The pressure is estimated to be 500 atmospheres, resulting in the formation of transient supercritical water. Thus, cavitation serves as a means of concentrating the diffuse energy of sound into micro reactors. Even though the local temperature and pressure conditions created by the cavity implosion are extreme, as one can have good control over the sonochemical reactions. The intensity of cavity implosion, and the nature of the reaction, are controlled by such factors as acoustic frequency, acoustic intensity, bulk temperature, static pressure, and the choice of liquid or dissolved gas. The consequences of these extreme conditions are the cleavage of dissolved oxygen molecules and water molecules (into $^{\bullet}$H atoms and $^{\bullet}$OH radicals). From the reactions of these entities ($^{\bullet}$O, $^{\bullet}$H, $^{\bullet}$OH) with each other and with H_2O and O_2 during the quick cooling phase, $HO_2^{\bullet}$ radicals and H_2O_2 are formed. In this molecular environment, organic compounds are decomposed and inorganic compounds are oxidized or reduced [119].

Ultrasound has been widely known to induce radical reactions. Considerable interest has been shown in the application of an innovative treatment for hazardous chemical destruction, including the degradation of volatile organic compounds based on the use of ultrasound. Although ultrasonic irradiation is employed in a variety of industrial processes (including welding of metals, homogenization of emulsions, dispersion of paints, cleaning and degreasing, synthesis of chemicals, catalysis, improved

extraction, crystallization, modification of enzyme and material processing [120], the chemical effects of ultrasound derived from acoustic cavitation (*i.e.* the formation, growth and implosive collapse of cavitation bubbles in liquid) cannot result from a direct interaction of sound with molecular species [121, 122]. These phenomena lead to sonolytic splitting of water as well as pyrolysis of a vaporized molecule [123].

Figure (1-5) shows that liquids irradiated with ultrasound can produce bubbles. These bubbles oscillate, growing a little more during the expansion phase of the sound wave than they shrink during the compression phase. Under the proper conditions these bubbles can undergo a violent collapse, which generates very high pressures and temperatures (cavitation). The compression of cavities when they implode in irradiated liquids is so rapid that little heat can escape from the cavity during collapse. The surrounding liquid, however, is still cold and will quickly quench the heated cavity [124].
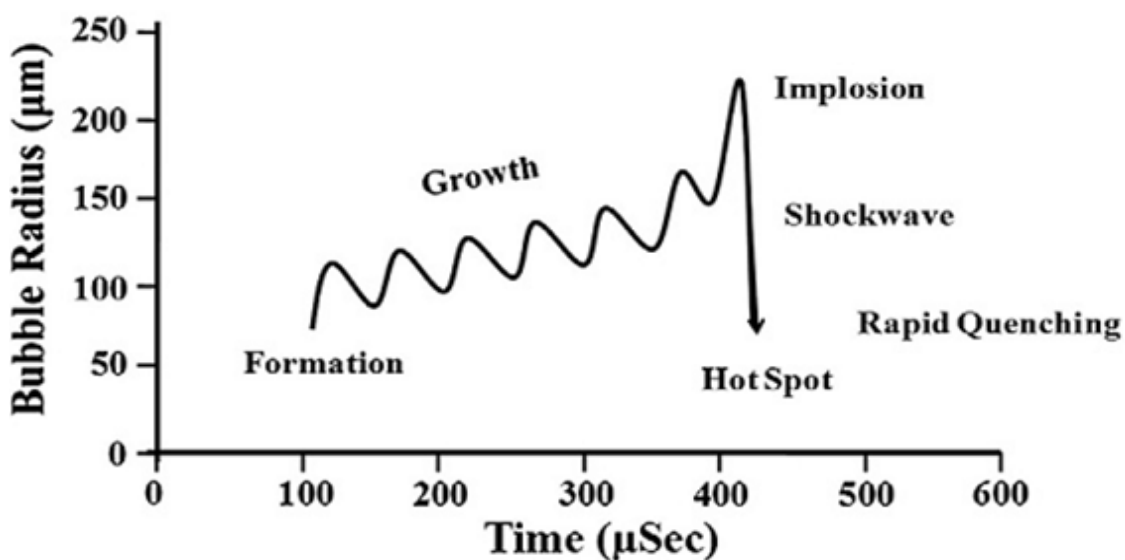
Fig. (1-5): Growth and implosion of cavitation bubble in aqueous solution with ultrasonic irradiation [124]

In aqueous phase sonolysis, there are three potential sites for sonochemical activity, namely:

(1) The gaseous region of the cavitation bubble where volatile and hydrophobic species are easily degraded through pyrolytic reactions as well as reactions involving the participation of hydroxyl radicals with the latter being formed through water sonolysis:

$$H_2O \rightarrow H^{\cdot} + OH^{\cdot}$$
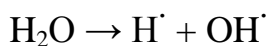
(2) The bubble-liquid interface where hydroxyl radicals are localized therefore, radical reactions predominate, while, pyrolytic reactions may be at less extent.

(3) The liquid bulk where secondary sonochemical activity may take place mainly due to free radicals that have escaped from the interface and migrated to the liquid bulk. It should be pointed out that hydroxyl radicals can recombine yielding hydrogen peroxide which may, in turn, react with hydrogen to regenerate hydroxyl radicals [125].

$$OH^{\cdot} + OH^{\cdot} \rightarrow H_2O_2$$

$$H_2O_2 + H^{\cdot} \rightarrow H_2O + OH^{\cdot}$$
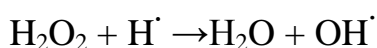
Table (1-3): Advantages of sonication [126]

No.	Advantages
1	Able to treat very toxic wastes at mild conditions.
2	Environmentally friendly technology using only electricity as a reactant.
3	The energy consumption depends on the chemical oxygen demand (COD).
4	The sono- treatment can be simply stopped by switching the power off.
5	Cost effective and safe.
6	Even effluents with low conductivity can be treated.
7	Sonochemical synthesis of chemicals

1.16. Literature Survey

The literature contains many research works concerning activated carbon, which may include source of the feed stock, the nature of

carbonization process, and type of activation carbon which are given as follows:

A. O'Grady and Wennerbery [127] prepared activated carbon having exceptionally high surface area over 2500 m^2/g and extraordinary adsorptive capacities. Carbon is made by a direct chemical activation in which petroleum coke and other carbonaceous sources are reacted with excess KOH at 400-600°C. Massoud, *et. al.*[128] produced low-cost adsorbent carbons from Illinois coal and evaluate the suitability of these materials for natural gas storage. Granular (20-100 mesh) activated carbons were produced by chemical activation with H_3PO_4. The product was characterized for its BET surface area, micropore volume, bulk density, and gravimetric-volumetric methane adsorption-storage capacities. Gracia, *et. al.*[129] prepared activated carbon from mixing pine wastes with KOH in a pilot gasifier, without any previous treatment. They employ different alkali-char ratios varied from 1:1 to 1:4 at 725-800°C. After the activation process, the sample was cooled under liquid N_2 and washed sequentially five times with (5%) NH_4Cl and finally with distilled water till neutral litmus paper is indicated. Then the sample dried at 110°C for 24 hour.

Aweed [130] prepared activated carbon from residual petroleum products such as that of Qaiyarah heavy crude oil (S about 7.45%) by employing direct oxidation with and/or by using certain type of catalysts ($CoCl_2$, $ZnCl_2$ and $FeCl_3$) at 350°C. Activation of the carbon after oxidation carried out at about 550±25°C by using different percentage of KOH. Catalysts used in the research ($CoCl_2$ & $ZnCl_2$) give a good result but not as the same as that of $FeCl_3$. Prinsloo and Jager [131] prepared activated carbon by the chemical and physical activation. Coke precursors (uncalcined) produced from waxy oil and medium temperature pitch were activated between 0.5 & 9 base coke ratio, 600-800°C heat treatment temperature, 1.5 and 12 hr. heat treatment time . All activation and cooling cycles were carried out under a constant flow of nitrogen. Kim, *et. al.*[132] prepared activated

carbon from rice husks by heating at a rate of 5°C up to 700°C and maintaining at 700°C for 2 hrs. The carbons obtained were subsequently activated at temperature between 750 and 900°C in a steam of moisture containing nitrogen.

Aweed [133] production of activated carbon by using different types of agricultural residues (sunflower shell, cocount shell, peanut shell, harvest hay and dates stones) by using excess amount of sodium hydroxide at 550°C for 3 hr. Rhamadhan, *et. al.* [134] prepared activated carbon from (Beje asphalt) using several percentage of V_2O_5 and in the presence of a stream of air or oxygen at 350°C for 3 hrs. Carbonization and activation were conducted at 550±25°C for 3 hrs. using excess NaOH. Al-Ghanam, *et. al.* [135] prepared activated carbon from (Heet asphalt) using several percentage of poly ethylene in the presence of air at 350°C for 3 hrs. and then completed the carbonization and activation at 550±25°C using excess NaOH. Al-Ghanam, *et. al.* [136] prepared activated carbon from heavy petroleum residue using chemical treatment. The activity of carbon was performed through adsorption of acids in aqueous. Al-Ghannam, *et. al.*[137] prepared activated carbon from Qaiyarah crude oil by chemical treatment and studied adsorption of some organic acids from aqueous solution at room temperature. Gonzalez-Serrano [138] showed that activated carbons with high BET surface area and a well-developed porosity have been prepared from pyrolysis of H_3PO_4 impregnated lignin precipitated from Kraft black liquors. Impregnation ratios within the range of 1-3 and activation temperatures of 623-873 K have been used, giving rise to carbons with different porous and surface chemical structure. Increasing the activation temperature and the impregnation ratio leads to a widening of the porous structure with a higher relative contribution of mesoporosity.

Ichcho, *et. al.* [139] studied the use of Moroccan oil shale for the preparation of adsorbents by chemical activation with phosphoric acid. The results indicate that this material is promising for this application. The

effect of different conditions of preparation on the yield and surface area is discussed. These parameters are H_3PO_4 shale weight ratio, carbonization temperature, carbonization time and concentration of H_3PO_4. Hamdon, *et. al.*[140] prepared activated carbon using oxidation condensation process and chemical treatment. The activated carbon was irradiated by gamma rays for different periods of time. The activity of activated carbon was studied by iodine number, methylene blue, density, ash content and humidity before and after irradiation.

Dusart, *et. al.* [141] studied adsorption of some amino acids on commercial activated carbon. Robabukhova, *et. al.*[142] studied adsorption of ethanol and butanol from aqueous solution on activated carbon. Al-Hyali, *et. al.* [143] have studied the adsorption of aromatic carboxylic acids and their relation to concentration, temperature and pH using activated carbon (commercial grade).

Punjaporn, *et. al.* [144] studied removal of benzene from waste water using aqueous surfactant two-phase extraction with cationic and anionic surfactant mixtures. Valente, *et. al.* [145] studied removal of phenol onto novel activated carbons made from lingo cellulosic precursors: Influence of surface properties. Chen, *et. al.*[146] studied adsorption of methyl tert-butyl ether using granular activated carbon and equilibrium, kinetic analysis. Muftah, *et. al.*[147] studied removal of phenol from petroleum refinery waste water through adsorption on data-pit activated carbon. Sze and Mckay [148] studied an adsorption diffusion model for removal of para-chlorophenol by activated carbon derived from bituminous coal. Salman, *et. al.* [149] studied batch and fixed-bed adsorption of 2, 4-dichlorophenoxy acetic acid onto oil palm frond activated carbon. Natalia, *et. al.*[150] studied high performance activated carbon for benzene-toluene adsorption from industrial waste water. Nourmoradi, *et. al.*[151] studied removal of benzene, toluene, ethylbenzene and xylene (BTEX) from aqueous solutions by

montmorillonite modified with nonionic surfactant: Equilibrium kinetic and thermodynamic study.

B. Iijima [152] was the first who discovered the MWCNT in the soot of negative graphite electrode produced by arc discharge. Ebbesen and Ajayan [153] achieved growth and purification of MWCNT and found that these nanotubes have diameters around 5-30 nm and lengths around 10μm. Iijima's group as well as Bethune, *et. al.* [154] found that the use of transition metal catalyst in the arc discharge leads to nanotubes with only single shell. Smalley's group [155] grew SWCNT using laser ablation technique on graphite rode.

Journet, *et. al.* [156] produced a large quantities of single walled carbon nanotubes by an arc discharge under helium pressure (660 Torr) between two electrodes of a graphite in which a hole in anode electrode had been drilled and filled with a mixture of metallic catalyst (Ni-Co, Co-Y, or Ni-Y) and graphite powders. The products were characterized by SEM, TEM, XRD and Raman spectroscopy analysis.

Zeng, *et. al.* [157] produced various forms of nanotubes by activated carbon arc discharge at low Helium gas pressure (140 Torr). They were showed that no nanotubes present in the soot and nanocapsul, carbon cone shape nanotube and the carbon toroidal nanotube which has a small length to diameter ratio. Kazaoui, *et. al.* [158] noticed that the optical absorption spectra of single-walled carbon nanotubes at peak 0.68 eV is attributed to the interband optical transition in semiconducting nanotubes.

Park, *et. al.* [159] purified multi-walled carbon nanotubes, prepared by electric arc discharge, through thermal annealing in air. The annealing apparatus consisted of two quartz tubes, whereby the inner tube, which contained the MWCNT, was simply rotated by the outer tube. The samples were annealed at 1033 K under ambient air with supply of sufficient amount of oxygen. Lee, *et. al.* [160] investigated large-scale synthesis of carbon nanotubes by plasma rotating arc discharge at helium pressure (500

Torr). The carbon nanotubes were formed by the condensation of high-density carbon vapor transferred out of the plasma region by the centrifugal force generated by the rotation of the electrodes.

Yu, *et. al.* [161] used coal or coke as source materials, to synthesize of carbon nanotubes, by plasma arcing technique. The use of coal for carbon nanotubes production over other materials may be more advantageous, because coal is cheap and abundant weak bonds in coal macromolecular structure may lead to more effective synthesis of nanotubes. Debasis, *et. al.* [162] synthesized CNT filled by Palladium nanoparticals using arc-discharge technique and show that the indexed diffraction pattern confirmed that the peak corresponding to carbon binding energy lie at 0.2846 eV.

Ambrosio, *et. al.* [163] grew MWCNT by CVD technique. They presented an investigation that the films have important photonic effect as a function of the wavelength in a large spectral interval (200-1800) nm. Yusa and Watanuki [164] examined the structural of multi walled carbon nanotubes powder under various hydrostatic pressure compressions using X-ray diffraction pattern at room temperature.

Pekker, *et. al.* [165] evaluated wide-range nanotube spectra in the near infrared, visible, mid and far infrared spectral region. They found that the far-infrared part of the spectrum is a more sensitive indicator of metallic tubes than in the visible peak. Hicks, *et. al.* [166] had fabricated diode SWCNT devices using Au and Al, as the asymmetric metal using chemical vapor deposition (CVD) process.

Also, Roy, *et. al.* [167] investigated the structure and composition of carbon nanotubes grown by arc-discharge technique using X-ray diffraction and x-ray photoelectron spectroscopy (XPS). They found a sharp diffraction peak corresponding to (002) for graphite powder and a fine line of binding energy of carbon equal to 0.285 eV from XPS measurements. Liao, *et. al.*[168] studied adsorption of resorcinol from water using multi-walled carbon nanotubes. Yang and Xing [169] studied adsorption of fulvic

acid by carbon nanotubes from water. Arasteh, *et. al.*[170] studied adsorption of 2-nitrophenol by multi-wall carbon nanotubes from aqueous solutions.

Su, *et. al.*[10] studied adsorption of benzene, toluene, ethylbenzene and p-xylene by NaOCl-oxidized carbon nanotubes. Yu, *et. al.*[171] studied adsorption of toluene ‹ethylbenzene and m-xylene on multi-walled carbon nanotubes with different oxygen contents from aqueous solutions. Yao, *et. al.*[172] studied equilibrium and kinetic of methyl orange adsorption on multi-walled carbon nanotubes. Bina, *et. al.*[173] studied removal of benzene has been investigated with highly significant approach using carbon nanotubes. Donglin, *et. al.* [174] studied the adsorption of methyl orange dye (MO) on MWCNT from aqueous solutions and the effects of temperature, stirring speed, MO concentration and MWCNT mass on MO adsorption. The results showed that the MO adsorption increased with its concentration and temperature in the aqueous solutions. The MO removal from the solution increased as MWCNT mass increases. The kinetic study demonstrated that MO adsorption on MWCNT was in a good accordance with the pseudo-second order kinetic model.

C. Many reports in the literatures have noted that a number of toxic or hazardous industrial chemicals could be destroyed by this novel technique. Following are some of the literatures:

Maezawa [175] studied the utilization of ultrasonic energy in a photocatalytic oxidation process for treating waste water containing surfactants. Kulkarni [176] has also concluded that the photocatalytic action with the ultrasound has resulted in higher degradation rates of the contaminants. This is due to the mechanical effects of cavitation involving photocatalyst surface cleaning and increased mass transfer of the polluting species to the powdered catalyst surface. Selli [177] reported that photocatalysis and sonolysis exhibit the synergistic effects in the degradation of organic acid in aqueous suspensions, when low ultrasound frequency is used. A comparative study between the sonolytic, photocatalytic

and sonophotocatalytic oxidation processes of aqueous solutions of malachite green was also carried out by Perez, N.J. and Herrera, M.F. showed the same results that the highest degradation was achieved in case of sonophotocatalytic treatment.

Vajnhandl and Marechal [178] in their paper reviewed some fundamentals of ultrasound, its broad applications and gathered some new research regarding its applications in textile wet processes, with the emphasis on textile dyeing and the decolorization- mineralization of textile waste waters.

Zeng and James [179] studied the degradation of pentachlorophenol (PCP) in aqueous solution by audible-frequency sonolytic ozonation. The first-order rate constant of PCP degradation by ozonation with sonication was found to be 15 times faster than that with bubbling ozone alone, while the rate constant with mechanical stirring was only four times faster. The hybrid effect of the irradiation by light and ultrasonic waves in conjunction with H_2O_2 was first confirmed to achieve the complete mineralization of propyzamide by Yano, *et. al.* [180].

A lot of research has been done on this technology in the recent years for the degradation of compounds like phenols and substituted phenols, alkyl halides, aromatics halides, substituted halides, inorganic chemicals, dyes, herbicides and pesticides etc. this treatment technology shows that it has potential for the degradation and mineralization of these recalcitrant compounds.

The degradation of malachite green (MG) in water by means of ultrasound irradiation and its combination with heterogeneous (TiO_2) photocatalysis was investigated by Berberidou, C. [181]. Eighty-kilohertz of ultrasound irradiation was provided by a horn-type sonicator, while a 9 W lamp was used for UV-irradiation. The extent of sonolytic degradation increased with increasing ultrasound power and decreasing initial concentration.

Selli [182] worked on the rate of 1, 4-dichlorobenzene (1,4-DCB) degradation and mineralization in the aqueous phase either under direct photolysis or photocatalysis in the presence of TiO_2, or under sonolysis at 20 kHz with different power inputs. Photocatalysis ensured faster removal of 1,4-DCB with respect to sonolysis and direct photolysis. The highest degradation and mineralization rate was attained with the combined use of photocatalysis and sonolysis, i.e. under sonophotocatalytic conditions. Mahvi [183] studied application of ultrasonic technology for water and waste water treatment. Qusay, *et. al.*[184] studied treatment of petroleum refinary waste water by ultrasound-dispersed nanoscale zero-valent iron particles. Xikui, *et. al.* [185] studied kinetics and mechanism of ultrasonic degradation of p-nitrophenol in aqueous solution with CCl_4 enhancement. Meral and Gonul [186] studied the sonolytic degradation of butyric acid and the effects of the ultrasonic power, the initial concentration of butyric acid, and the addition of H_2O_2 on the degradation of butyric acid. The results showed that the degradation of butyric acid increased with irradiation time.

1.17. Aim of Present Work

The main objective of this research is to explore and identify the use of a novel adsorbent to remove benzene, o-xylene, and sulfide from industrial waste water by adsorption onto activated carbon produced from fuel oil waste as the adsorbent and to evaluate a new circulating system and using it for water purification.

The novelty of our work can be restricted in the followings:

A- Synthesize a new MWCNT by ultrasonic probe technique of activated carbon synthesize from fuel oil wastes and to determine the optimum conditions for their preparation.

B- The purification system with more efficient and low cost of the first step is an unusual.

C- Using by-products of fuel oil coming from power plant as a source of carbon.

D- Using a new system in circulating processes to reach adsorption equilibrium in aqueous solutions.

E- The rules of environment cleaning

CHAPTER TWO

2. *Materials & Methods*

2.1. Chemical Materials

The following chemicals were used in this study (Table 2-1).

Table (2-1): The chemicals used in this study

No.	Materials	Formula	% Purity	Supplier From
1	Benzene	C_6H_6	99.5	Aldrich
2	O-xylene	$C_6H_4(CH_3)_2$	99	Aldrich
3	Zinc Chloride (anhydrous)	$ZnCl_2$	98	Aldrich
4	Hydrochloric Acid	HCl	36	BDH
5	Sulfuric Acid	H_2SO_4	98	BDH
6	Silver Nitrate	$AgNO_3$	99.5	Fluka
7	Sodium Nitrite	$NaNO_2$	98	GCC
8	Sodium Hydroxide	NaOH	99	Fluka
9	Calcium Hydroxide	$Ca(OH)_2$	99.5	BDH
10	Sodium Sulfide	Na_2S	98	BDH
11	Silica Gel	SiO_2	99	BDH
12	Sodium Chloride	NaCl	99.5	BDH
13	Nitric Acid	HNO_3	68	BDH
14	Buffer Powder pH = 7	-	-	Mettler-Toledo (Switzerland)
15	Ethanol	C_2H_5OH	99.98	GCC
16	Glass Wool	-	-	Fluka

2.2. Instruments and Apparatus

The following instruments and apparatus were used in this study (Table 2-2).

Table (2-2): Instruments and apparatus used in research

No.	Instruments	Productive Company	Source
1	Field Emission Scanning Electron Microscopy (FE-SEM)	FEI Nova Nano-SEM 450	Netherlands
2	Transmission Electron Microscopy (TEM)	Libra 120-Carl Zeiss	Germany
3	Atomic Force Microscope (AFM)	Advanced Angstrom Inc.	U.S.A
4	High Resolution X-Ray Diffraction (HR-XRD)	P analytical Company	Netherlands
5	Ultrasonic Probe	Sonicators	U.S.A
6	Surface Area Analyzer	Thermofinnigan - Co.	U.S.A
7	Fourier Transform Infra-Red Spectrophotometer (FTIR)	Shimadzu	Japan
8	UV-Visible Spectrophotometer	Shimadzu	Japan
9	Muffle Furnace	Carbalate	UK
10	Electrical Oven	Memmert	Germany
11	pH-Meter	Mettler-Toledo	China
12	Vacuums Pump	Barhant Company CE	Germany
13	Cleveland Open Cup Flash and Fire Points Tester	Chrom Tech	U.S.A
14	Thermostated Shaker Water Bath	Daiki	Korea
15	Water Bath	GFL	Germany
16	Sensitive Balance	Sartorius	Germany
17	Hot Plate with Magnetic Stirrer	Stuart Scientific	UK
18	Centrifuge	Hermle	Germany

No.	Instruments	Productive Company	Source
19	Peristaltic Pump	ISCO	U.S.A
20	Heating-Mantle	ERS	E.E.C.
21	Water Distillator	GFh	Germany
22	Desiccators	-	England
23	Homogenizer	-	India
24	Blender	Glassco	India
25	Ice Maker	Scotsman AF100	Italy

2.3. Physicochemical Properties of Fuel Oil

Physicochemical properties of fuel oil wastes are shown in Table (2-3).

Table (2-3): Physicochemical properties of fuel oil wastes

Property	Value
Density (g/cm^3)	0.855
Flash Point	170 ^{o}C
Fire Point	196 ^{o}C
Liquid Condensed %	36
Distillation Point	52-104 ^{o}C
Boiling Point	325 ^{o}C
Carbon %	10
Volatile Matter %	24.1
Un volatile Matter (wax) %	29.9

2.3.1. Distillation Point

The distillation tests give an indication of the type and the quality of the products that can be obtained from waste degradation. The basic method of distillation depends on characteristics of hydrocarbons and has an important effect on safety and performance, especially in the case of fuels and solvents (ASTM D-86) [187].

2.3.2. Flash Point & Fire Point

The flash point is the lowest temperature at atmospheric pressure (760 mmHg, 101.3 kPa) at which application of a test flame will cause the vapor

of a sample to ignite under specified test conditions. The fire point (open cup method) is also used for the determination of the fire point, the temperature at which the sample will ignite and burn for at least 5 s, (ASTM D-92, IP 36) [188].

2.4. Multi Walled Carbon Nanotubes (MWCNT) Synthesis

2.4.1. Vacuum Distillation of Fuel Oil Residue

The samples of fuel oil residue were collected from the power plant in Ramadi area, Iraq. The samples were placed under low pressure of 20 mmHg, heated at a range of 280-325 $^{\circ}$C to remove volatile substances and to get riding of additional quantity of liquid ingredients in waste oil and to ensure an increase of the density of carbon from fuel oil wastes. The refining operation was done by using laboratory apparatus as shown in Fig. (2-2) and Image (2-1). Distillation process continues reaching a highly dense mass, and becomes like solids.

1- Vacuum pump
2- Heating – mantle
3- Three- necked flask
4- Thermometer
5- Condenser
6- Stand-with-Clamp
7- Receiving flask
8- Water bath
9- Silicon tubes
10- Traps
11- Vacuum pump
12- Rubber
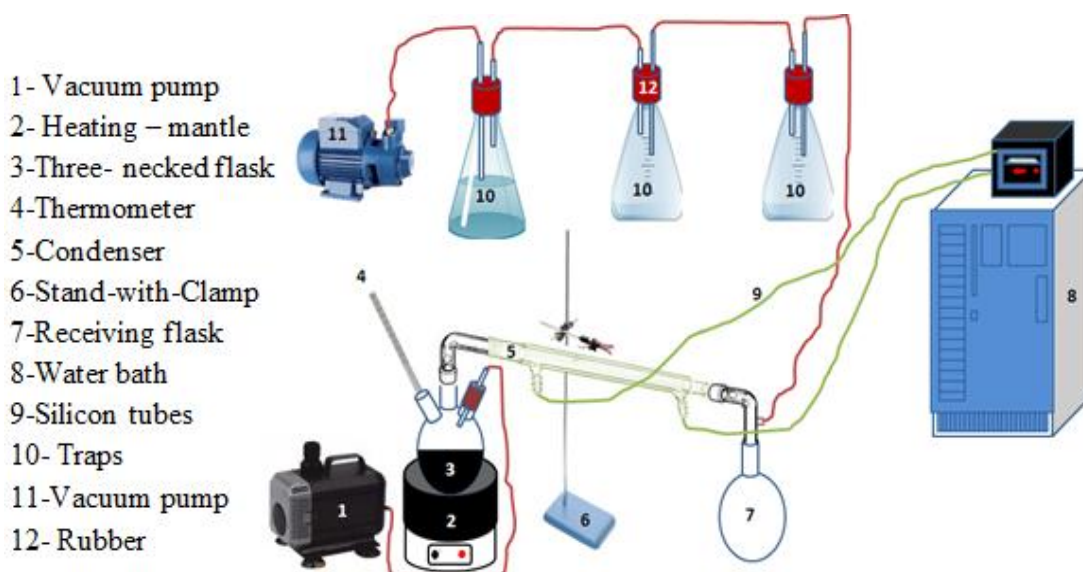
Fig. (2-2): Schematic diagram of vacuum distillation for the preparation of carbon from heavy fuel oil residues

Image (2-1): Apparatus used in vacuum distillation for the preparation of carbon from heavy fuel oil residues

2.4.2. Preparation of Activated Carbon

1- *Primary Carbonization*

Certain weights of the waste of the solid product of last step were taken and soaked with 20% (w/w) anhydrous zinc chloride ratio of 1:2. The mixture was heated at a temperature of 70 $^{\circ}$C gradually with continuous stirring for two hours by homogenizer and left standing for (48) hours and then transferred to step (2).

2- *Final Carbonization and Activation*

The produced materials burned at a temperature of 400-500 $^{\circ}$C in the muffle furnace under atmospheric pressure for two hours and then the sample was cooled to room temperature.

3- *Purification of Activated Carbon*

The sample washed with (0.1) M of hydrochloric acid, filtered and then washed with distilled water several times in order to eliminate the content of inorganic materials in the resulting carbon samples. To ensure the removal of chloride ion a solution of (0.1) M of silver nitrate was added drops to the filtrate once the turbidity disappears that indicate the total

removal Cl⁻ ion. The activated carbon was dried at 110-120 ^{o}C for 24 hours and then cooled, grinded, passed through sieves of (16-20) mesh and stored at desiccators.

2.4.3. Preparation of MWCNT by Sonication Probe

MWCNT prepared by a sonication technique which is performed in a probe-type operating at a fixed frequency of 22 kHz, amplitude of 100 μm and a power value of 100 W. Weight of 0.1g activated carbon sample was placed in 250 ml vessel containing 100 ml of deionized water. Samples were placed in thermostated circulating water bath at 25 ±1 ^{o}C during sonication for (1, 2, 3, 4 and 5) hr. Then the solution was centrifuged for 15 min at 6000 rpm, dried at 110-120 ^{o}C for 24 hr.

The synthesized materials were purified as follows. In order to obtain pure MWCNT, and removing the metal catalysts, the products were dissolving in 10% HCl solution for about 16 h at room temperature. Then the samples were washed several times with deionized water. In order to achieve extra purification, the prepared materials were dissolved in 5 M nitric acid for 3 h at 70 ^{o}C. After that, the washing step was repeated as mentioned above for the HNO_3 treatment process. Treated MWCNT were dried at 120 ^{o}C. In order to eliminate non-carbon elements, all of the purified materials were placed in the furnace at 400 ^{o}C for 30 min, cooled in a desiccator and then identified using FE-SEM, TEM, AFM, XRD and FT-IR.

2.5. Activated Carbon Characterization

A. *Measurements of pH*

The pH value of prepared activated carbon was determined by mixing 1.0 g of sample with 10 ml distilled water then shaked for 30 min, the solution was filtrated at room temperature and then measured by pH-meter.

B. *Determination of Ash Content*

The ash content was estimated by weight 1.0 g of activated carbon to crucible, heated in muffle furnaces at 1000 -1100 ^{o}C for three hours, cooled

in a desiccator. The remaining samples after combustion were supposed to be ash content then the percentage was calculated [189].

C. *Measurement of Moisture*

Moisture content was measured by heat 1.0 g of prepared activated carbon in an oven at 150 ^{o}C for four hours then cooled in a desiccator. The weight difference before and after heating was calculated [190].

D. *Measurement of Density*

The density of the prepared activated carbon was determined by weight 10 cm^3 of the carbon sample using graduated cylinder and the density was calculated [191].

$$Density\ (g/cm^3) = mass/volume$$

E. *Surface Area*

This measurement is based on the continuous flow method. For The Brunauer, Emmet and Teller (BET) surface area analysis, a mixture of nitrogen balance helium is passed through the reference channel of the thermal conductivity detector (TCD) detector to the sample housed within a flow-through glass cell and finally into the TCD analytical channel. Signals produced by the TCD detector are collected by the microprocessor control board, integrated and stored in the memory file.

The analytical procedure starts with the degassing of the sample with the carrier gas at programmable temperature. When the sample is dried, the operator simply transfers the sample holders to the analytical ports and fit them into place by means of quick fit connectors. Pressing the start button will automatically raise the liquid nitrogen flask carriage initiating the analysis.

The Brunauer, Emmet and Teller (BET) equation[192] for determming surface area is shown in its simplest form to be:

$$S_t = K\ (1\text{-}P/P_o)\ x\ V_a$$

Where:

S_t = Total surface area of sample being analyzed

K = A constant for nitrogen, assuming conditions = 4.03

P/P_o = 0.294 for a gas mixture of 30% N_2 and 70% He

V_a = Volume of gas (N_2) adsorbed.

2.6. Benzene and O-xylene Solutions

2.6.1. Preparation of Solutions

A 1000 ppm stock solution of (benzene and o-xylene) was prepared by dissolving 0.1 g of each compound in 100 g of distilled water in volumetric flask, thereafter solutions of (300, 250, 200, 150, 100 and 50) ppm were prepared by a subsequent dilution.

2.6.2. Determination of Maximum Wavelength (λmax)

To determine the wavelength of maximum absorption, an absorption spectrum for each compound by using UV-Vis has been recorded at the range (200-400) nm by using quartz cell of 1cm thickness (path length). The spectra are shown in Figs. (2-3) and (2-4).
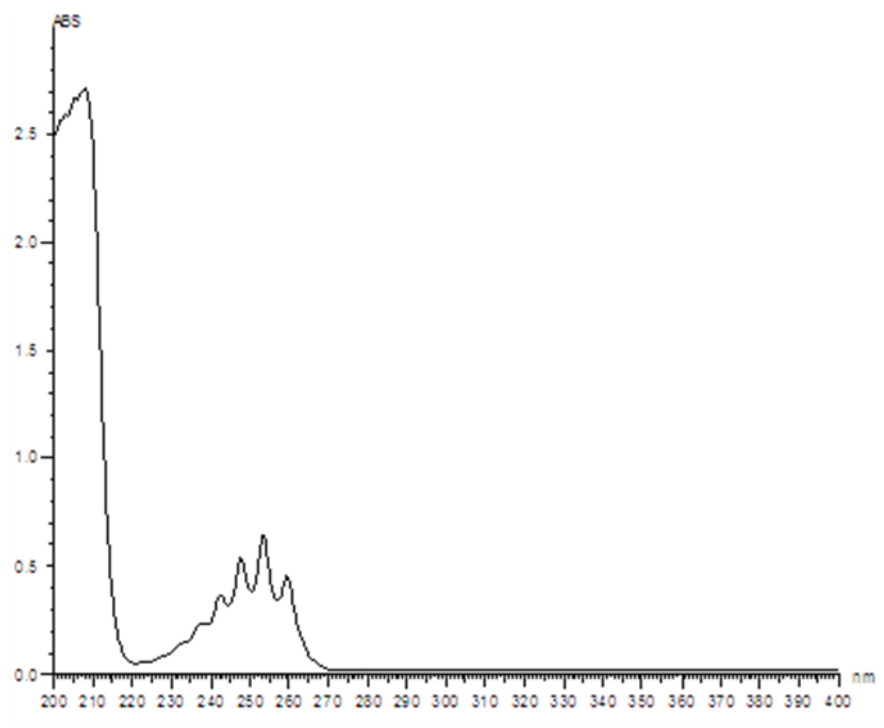
Fig. (2-3): Maximum wavelength for benzene (204 nm)
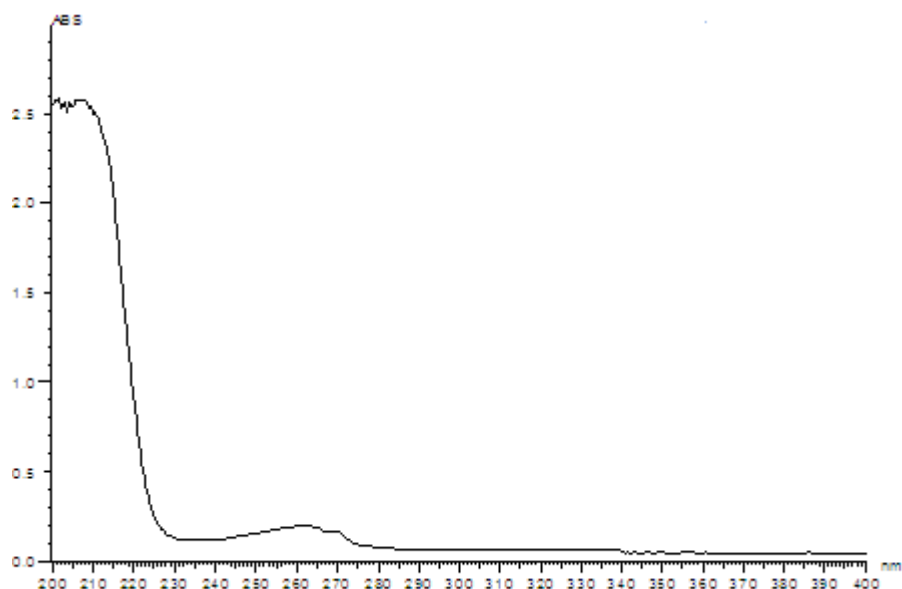
Fig. (2-4): Maximum wavelength for o-xylene (215 nm)

2.6.3. Calibration Curve

The calibration curve was graphed at fixing the λmax obeying the (Beer-Lambert law). Specific concentrations were prepared for each compound, the absorption has been recorded and the calibration curves were plotted between the absorption and concentration. The best line between points has been drawn using least square method (Figs. 2-5 and 2-6).

$$y = 0.0437x + 0.0014$$
$$R^2 = 0.9969$$
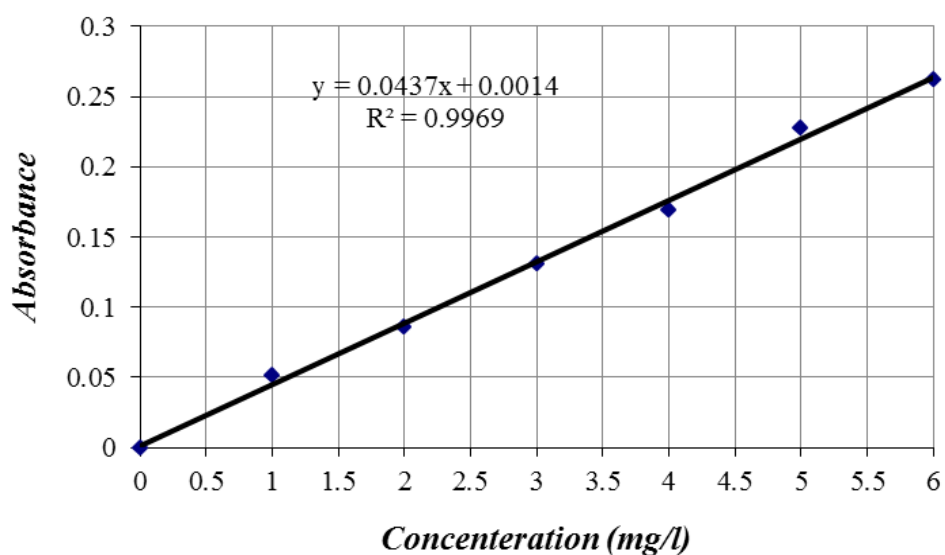
Fig. (2-5): Calibration curve for benzene
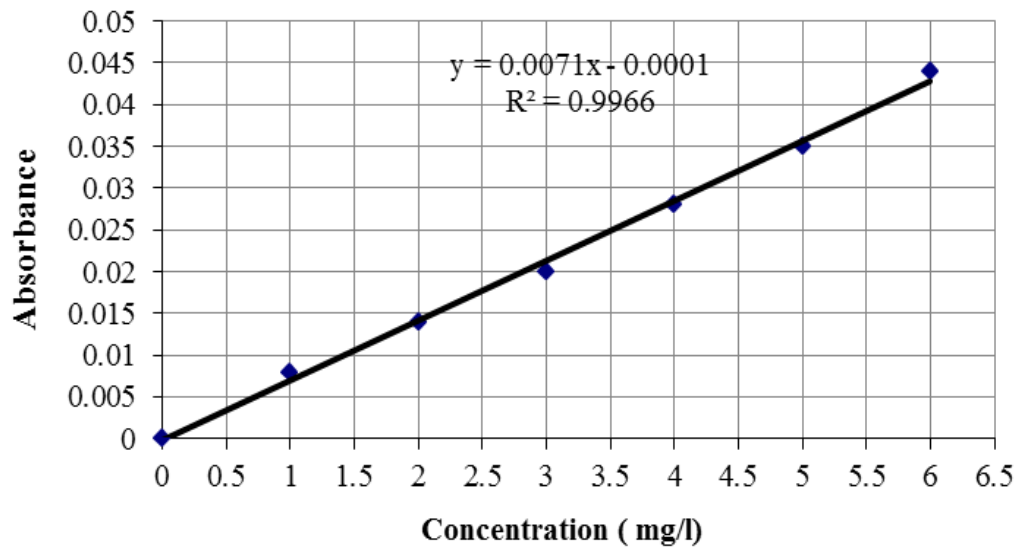
Fig. (2-6): Calibration curve for o-xylene

2.7. Adsorption Studies

2.7.1. New Circulating System

The adsorption process was done by using a new circulating system as described in Fig. (2-7) and Image (2-2). Five grams of activated carbon sample have been placed in separator funnel (No.6) fitted to a three-necks flask (No.5) containing 200 ml of solutions (benzene or o-xylene) with six different concentrations (50,100,150,200,250 and 300) ppm at temperatures of 283,293,313 and 333 K for 120 minutes using a thermostated water bath (No.3). The equilibrium time was achieved by a recycling solution using a peristaltic pump (No.4). To minimize the evaporation and contamination, a cooling system (No.7) and a trap (No.2) were in contact along with a cycling process. Four mL sample were taken for each 10 min from the valve (No.8). UV-Vis spectrophotometer has been used to measure the absorbance for benzene and o-xylene at equilibrated solutions at certain wavelength (204 nm) and (215 nm) respectively. The quantity of adsorbate was calculated by using the following formula [193]:

$$Q_e = V_{Sol} (C_o - C_e)/M \ldots\ldots (2\text{-}1)$$

Where:

Q_e = Quantity of adsorbate (mg/g).

V_{Sol} = Total volume of adsorbate solution (L)

C_o = Initial concentration of adsorbate solution (mg/L)

C_e = Concentration of adsorbate solution at equilibrium (mg/L)

M = Weight of adsorbent (g)

While the percentage removal of solutions and equilibrium adsorption q_e (mg/g) was uptake, using the formula.

$$\% \text{ adsorption Efficiency} = (C_o - C_e)/ C_o \times 100 \ \dots \ (2\text{-}2)$$
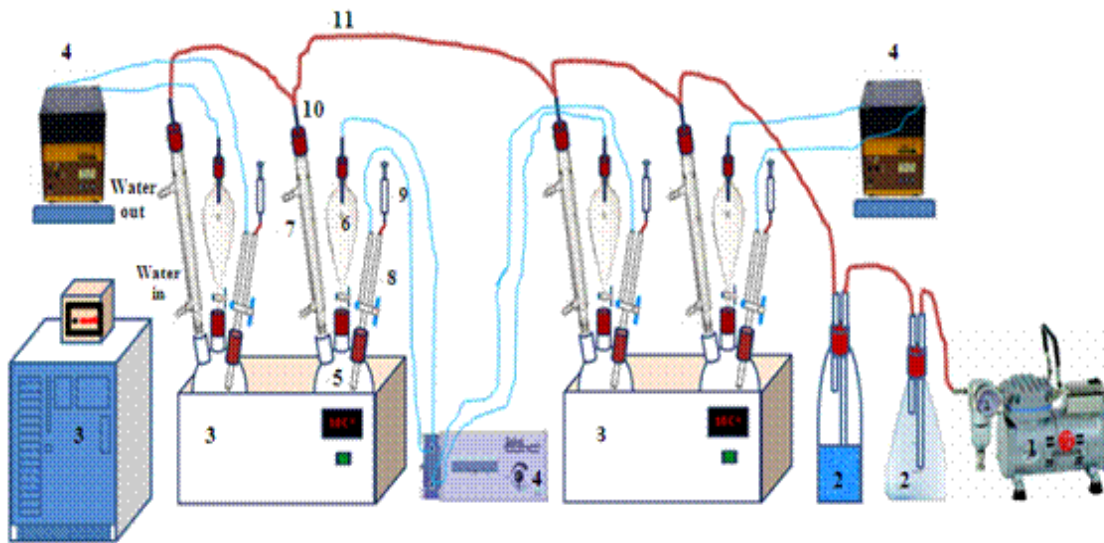
1-Vacuum pump 2- Traps 3- Water bath   4- Peristaltic pump 5- Three - necked flask
6- Separatory funnel   7- Cooling system (Condenser) 8- Control valve 9- Syringe
10- Rubber   11-Silicon tubes

Fig. (2-7): Schematic diagram of new circulation system for adsorption

Image (2-2): New circulation system for adsorption

2.7.2. Normal Equilibration

Determination of equilibration time for benzene, o-xylene adsorption on MWCNT was done by shaking 5 ml of solutions at concentrations of (50,100,150,200,250 and 300) ppm with 0.05 g of adsorbent at constant temperatures of 283,293,313 and 333 K for 120 min. Sub-sample were taken from each concentration at 10 to 120 min for kinetic studies and then filtrated. UV-Vis spectrophotometer has been used to measure the absorbance for equilibrated solutions at certain wavelength. The quantity of adsorbate was calculated by using the above mentioned equations (2-1) and (2-2).

2.8. Sampling for Sulfide

Sulfide samples were collected from Heet city-Al-Anbar area, Iraq and stored in polyethylene bottles with highly fit leds to prevent any evaporation and any contact with atmosphere.

2.8.1. Preparation of Standard Solution of Sulfide

A standard solution of 0.1 N was prepared by weight 0.305 g of Na_2S in volumetric flask of 50 ml using distillation water. The series of standard solutions of (10^{-6}, 10^{-5}, 10^{-4}, 10^{-3}, and 10^{-2}) N were prepared by a subsequent dilution by using solution of sulfide anti-oxidant buffer (SAOB) (20 g of sodium hydroxide with 10 g of sodium nitrite).

2.8.2. Calibration of Sulfide Electrode

Calibration curve for sulfide electrode was done by using standard solution of sulfide ion containing (SAOB) for pH elevation of solution, fixing ionic strength and preventing sulfide oxidation. The relation between electrical potential and concentration was done as shown in Fig. (2-8)
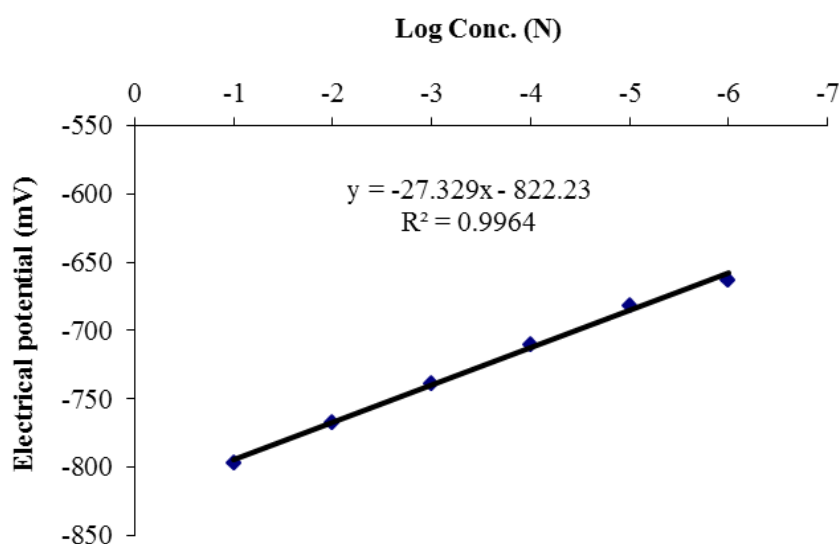
Fig. (2-8): Calibration curve for sulfide

2.8.3. Treatment for Sulfide Removal

The adsorption efficiency of carbon was determined by using sulfide solutions and spring water containing sulfide with addition of SAOB by the ratio of (1:1). Different ratios of sulfide solution and carbon sample were determined by weight 0.05 g of non-activated carbon, activated carbon and MWCNT at temperature of 298 K for (30, 60 and 90) min. Solutions were shaked, filtrated and sulfide concentration was estimated by using sulfide electrode.

2.9. Tools of Characterisations

The morphology and microstructure of MWCNT were investigated by field emission scanning electron microscopy (FE-SEM), transmission electron microscopy (TEM) and atomic force microscopy (AFM). A structure evolution of the prepared MWCNT was examined by X-ray diffraction (XRD). Fourier transforms infrared spectrometer (FT-IR) and surface area.

2.9.1. Field Emission Scanning Electron Microscopy (FE-SEM)

FE-SEM is one of the most powerful tools used to investigate the surface morphology of materials. It uses a field emission gun instead of typical electron gun sources used in an SEM system. The electron beam passes through electromagnetic lenses, focusing onto the sample, resulting in the reflection of different types of electrons. The high-energy electrons (backscattering electrons) are caused by the elastic collision in the deep level inside the sample; whereas the secondary electrons are produced from the inelastic collision on the sample surface or close to the surface [194]. The secondary electrons are then collected by the detector to obtain an image of the sample surface. In addition, choosing the suitable accelerator voltage is important to generate a high-resolution Image. (2-3) shows the schematic of FE-SEM system. An FE-SEM system (FEI Nova Nano-SEM 450) was used to study the morphology of the products Fig. (2-9).
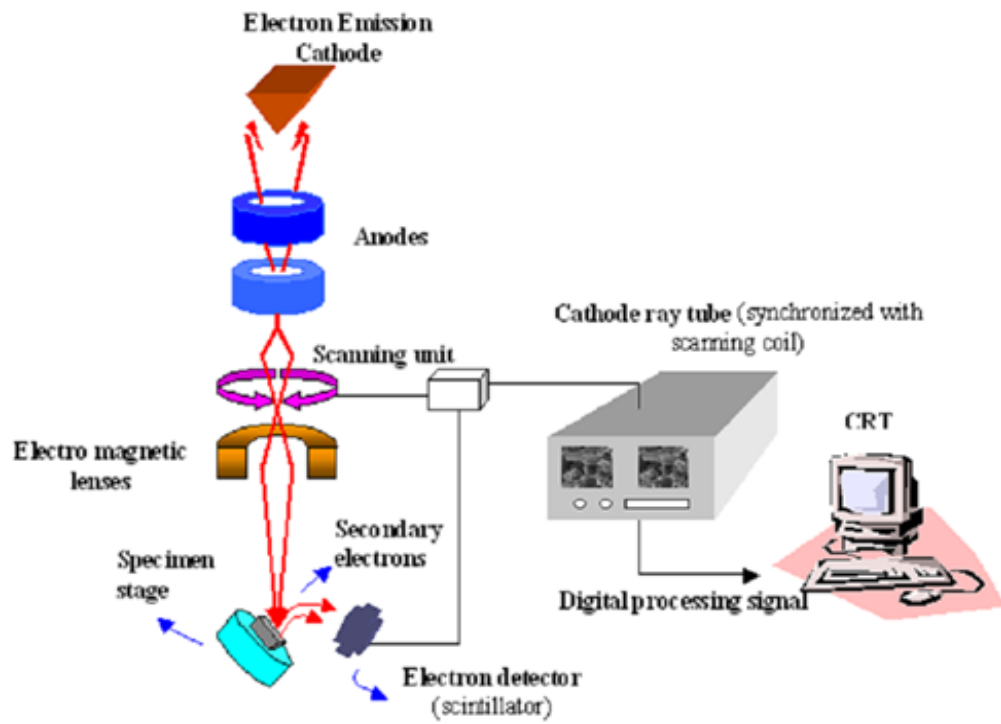
Fig. (2-9): Schematic diagram of FE-SEM system

Image (2-3): Field emission scanning electron microscopy system

2.9.2. Transmission Electron Microscopy (TEM)

The first transmission electron microscope was built in 1931 with a magnification of 16× [195]. Afterward, extensive efforts have been exerted to enhance the resolution of the transmission electron microscope. The principle behind TEM is similar to that of SEM, except that under TEM, the electron beam passes (transmits) through the specimen, requiring the detector to be fixed behind the sample holder. The electron density distributed behind the sample is focused on a fluorescent screen by lenses. Several methods are used to obtain the images such as exposing the photographic sensitive media. Given the strong interaction between the electron beam and the atoms of the samples by elastic and inelastic scattering, the specimen should be very thin, with thickness ranging from 5 nm to 100 nm [196]. Thus, the TEM sample should be in solution depots on a Cu grid and allowed to dry before measurement. In our study, the microstructure observation was performed using Libra 120-Carl Zeiss transmission electron microscope Image (2-4).
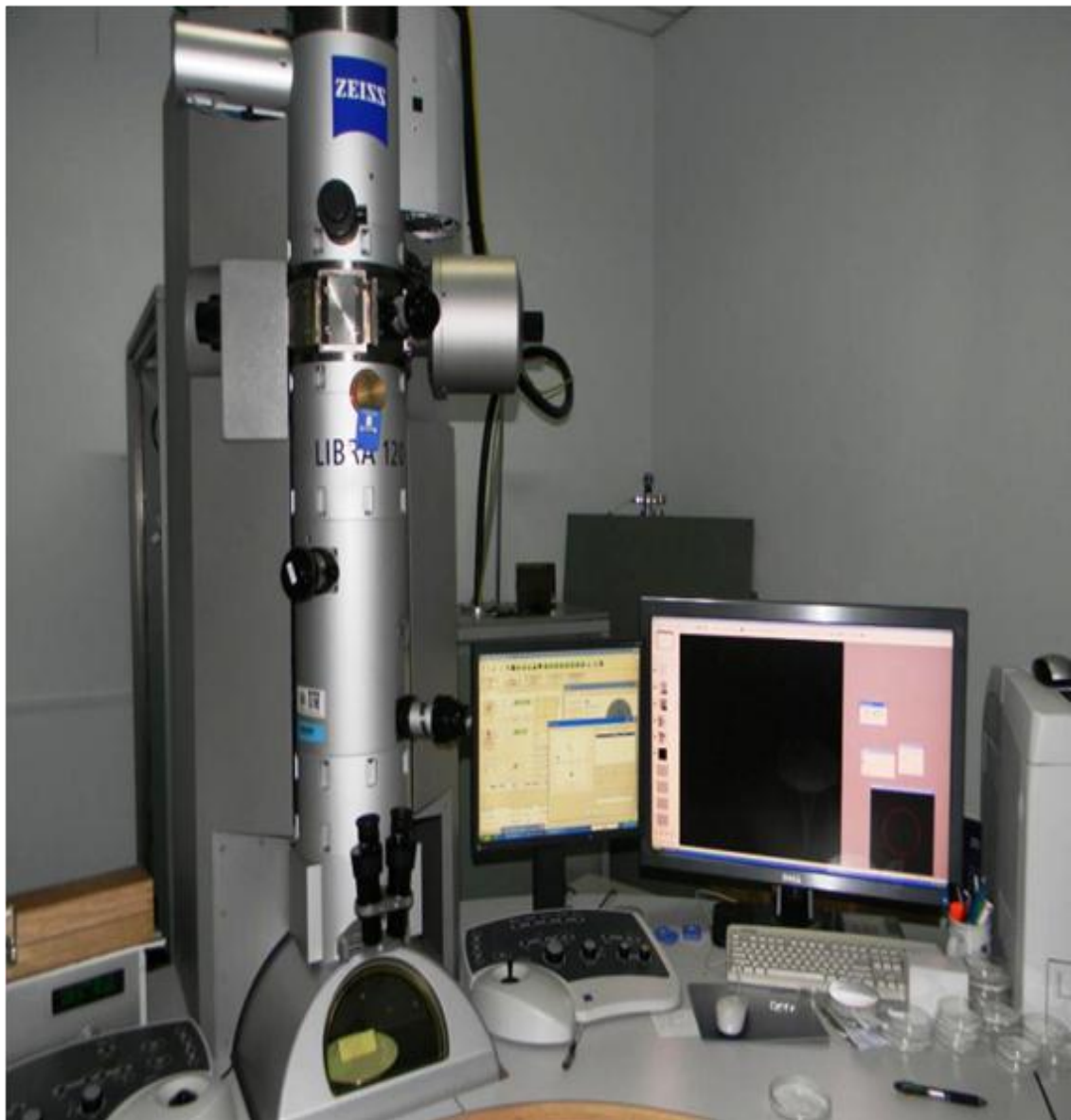
Image (2- 4): Libra 120-Carl Zeiss transmission electron microscope

2.9.3. Atomic Force Microscopy (AFM)

The surface structures of the prepared MWCNT were investigated using atomic force microscopy (AFM) (Nano-scope analysis) in a high-resolution nanometer range. AFM consists of a cantilever with a sharp tip is brought within close proximity of the sample, and scanned over it to map contours of the surface. In the AFM the signal is provided by variations in the force between the tip and the surface atoms Fig. (2-10). The most factors that AFM main function depends on its the force between the tip (probe) and the surface of the sample. The interaction forces between the tip and the

sample deflect the cantilever whenever the tip is near a sample surface, which is depend on the distance between the sample and the probe, the geometry of the tip, and the nature of the surface. The deflection is typically measured by a laser spot reflected as an array of photodiodes on the cantilever's top surface. The laser light from a solid-state diode is reflected back to the cantilever, and then collected by a position sensitive detector (PSD). There are two types of AFM operation: the contact and the non-contact mode. Although the non-contact mode has a lower resolution than the contact mode, the former is not as destructive to the sample surface as the former [197].
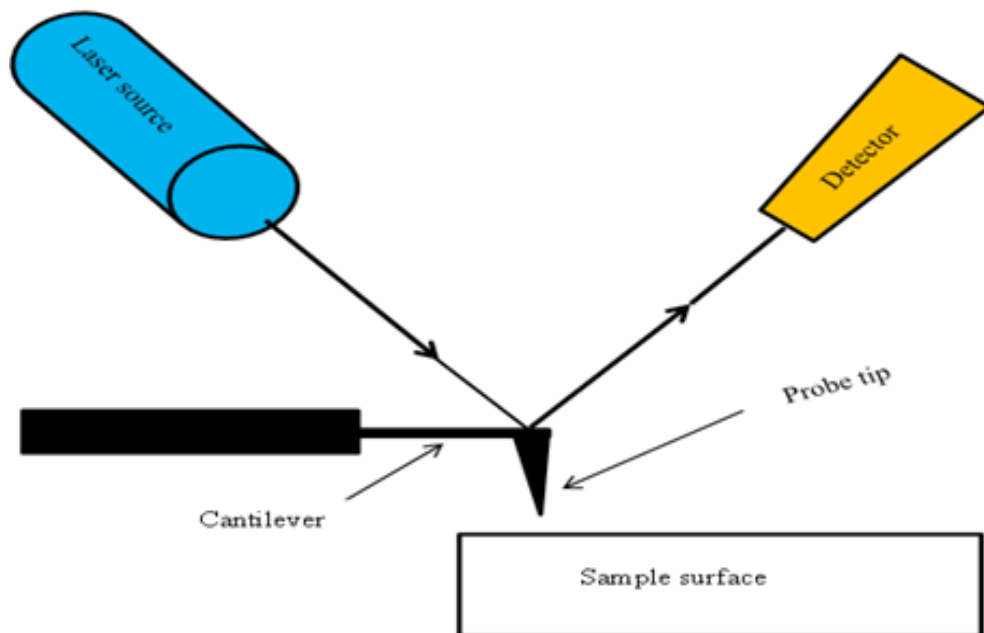
Fig. (2-10): Schematic diagram of the operation of an AFM [197]

2.9.4. High Resolution X-Ray Diffraction (HR-XRD)

The structure evolution of the as-prepared MWCNT were examined by high-resolution X-ray diffraction (HR-XRD) using X'Pert Pro MRD diffractometer (P analytical company) system equipped with Cu-Kα-radiation wavelength (λ=0.15418 nm) operating at 40 kV and 30 mA . The interaction between the X-rays and the sample crystal planes are elastica

scattering beam diffraction within the crystal structure of sample compounds is controal by Braggs law Fig.(2-11) and Image (2-5).
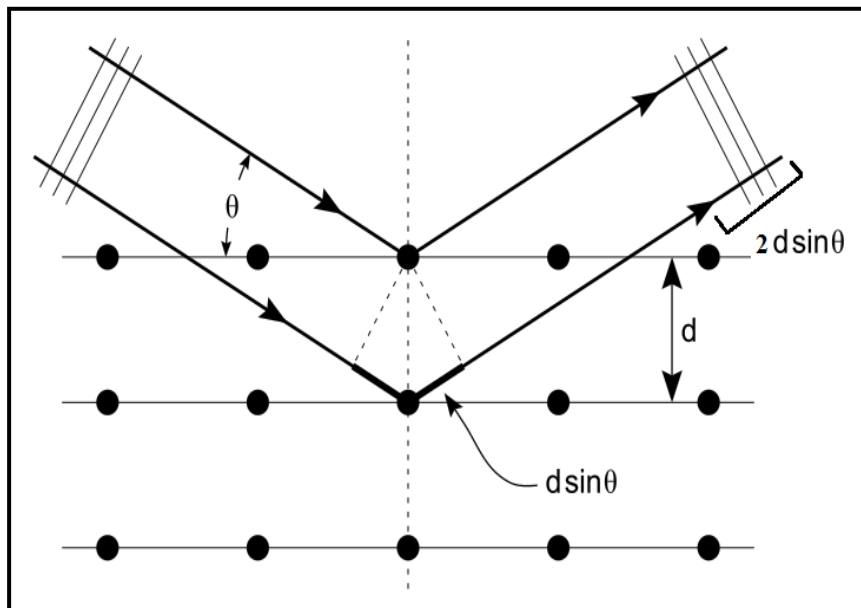
Fig. (2-11): Braggs diffraction from a cubic crystal lattice [198]

Image (2-5): High resolution X-ray diffraction equipment

2.9.5. FT-IR Analysis

The products for (non-activated carbon, activated carbon, and MWCNT) were characterized by fourier transform infrared to identify function groups.

2.10. Removal of Organic Pollutant by Ultrasonic

2.10.1. Degradation Experiments

Aqueous benzene and o-xylene solutions of 100 ppm and 200 ppm were prepared and used for degradation. Ultrasonic irradiation of the each compound solutions were carried out continuously with sonicators at a fixed frequency of 20 kHz Fig. (2-12). Samples of 100 ml for each compound were placed in 250 ml conical flask and placed in water bath at temperatures of (283, 293, 313 and 333) K under a sonication for 150 min. Four milliliters samples were withdrawn every 10 min for kinetic study. The amount of residual concentration of each compound in the solution was measured at certain wavelength using a UV-Vis spectrophotometer. The value of the absorbance obtained has been used to determine the equilibrium concentration from calibration curve according to Beer-Lambert law. The degradation percentage (% D) of each compound was calculated as follows.

$$\% \, D = (C_o - C_e) / C_o \times 100 \, \% \, \ldots\ldots\ldots \, (2\text{-}3)$$

Where C_o and C_e are the initials and remained concentration of each compound.
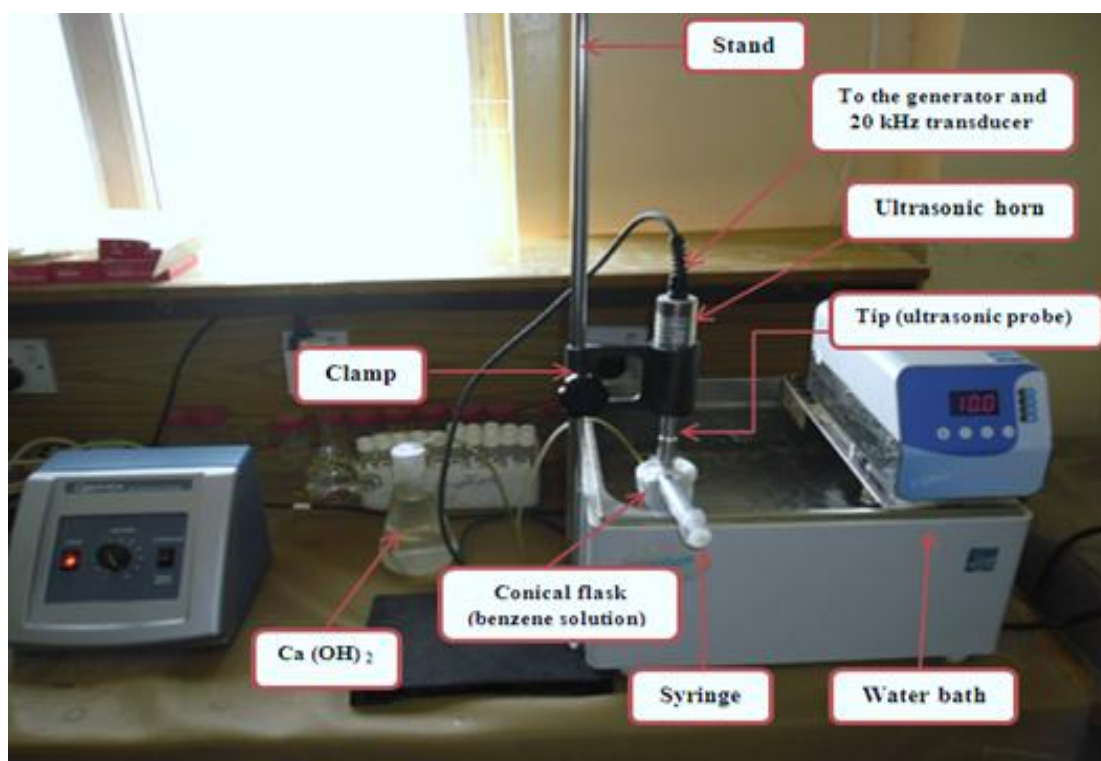
Fig. (2-12): Experimental setup of ultrasonic probe

2.10.2. Measurements of pH

The pH value was determined using pH-meter from each compound solution before and after degradation.

2.10.3. Qualitative Tests

Aromatics and aliphatics were identified. Ignition of aromatics produces a smoky soot while the aliphatic give un smoky blue flame.

Nitration was used to distinguish between aromatic and aliphatic compounds according to the following reaction

$$Ar\text{-}H + HNO_3 + H_2SO_4 \longrightarrow Ar\text{-}NO_2 \downarrow + H_2O$$

$$\quad\quad\quad 1ml \quad\quad\quad 1ml \quad\quad\quad \text{Yellow coloured compounds}$$
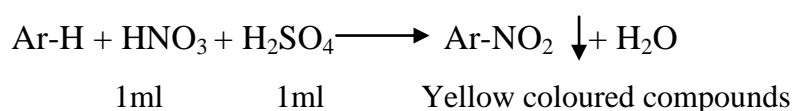
The yellow coloured products indicate the aromatic type while the disappearance of the colour reflects the aliphatic ones.

Detection of carbon dioxide produced from benzene and o-xylene after oxidation via clear water-lime gave turbid in the presence of CO_2 according to the equation.

$$CO_2 + Ca(OH)_2 \longrightarrow CaCO_3 + H_2O$$
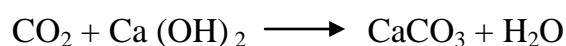
2.11. Kinetics Study

2.11.1. Reaction Order and Rate Constant

Reactors are used primarily to determine the rate law parameters for homogenous reactions. This usually achieved by measuring the concentration as a function of time then using the differential or integral method to determine the reaction order and reaction rate constant (k) [199].

The time-dependent experimental adsorption data are used for kinetic modeling the experimental work. The model equations used for fitting the data are:

- Zero order equation.
- 1st order equation.
- 2nd order equation.
- Pseudo 1st order model (Lagergren equation).

2.11.2. Pseudo 1st Order Model (Lagergren Equation)

The pseudo 1st order equation is generally expressed as [200]:

$$\frac{dqt}{dt} = k(qe - qt) \quad \ldots\ldots\ldots (2\text{-}4)$$

k is the rate constant of pseudo 1st order sorption (min^{-1})

After integration and applying boundary conditions from t = 0 to t = t and from $q_t = 0$ to $q_t = q_t$ Eq. (2-4) becomes

$$\ln(qe - qt) = \ln qe - kt \quad \ldots\ldots\ldots.. (2\text{-}5)$$

When the values of ln (q_e-q_t) non linear correlated with t, the plot of ln (q_e -q_t) versus t will give a linear relationships from which k and q_e can be determined from the slope and intercept of the graph respectively.

2.12. Thermodynamic Studies

The thermodynamic parameters including changes in standard free energy (ΔG^o), standard entropy (ΔS^o), and standard enthalpy (ΔH^o) for these adsorption processes are determined by using following equations [201].

$$\Delta G^o = -RT \ln K \qquad \ldots\ldots\ldots\ldots (2\text{-}6)$$

Where K is the thermodynamic equilibrium constant. The effect of temperature on thermodynamic constant is determined by:

$$\ln K = \Delta S^o / R^* - \Delta H^o / RT \quad \ldots\ldots\ldots.. (2\text{-}7)$$

Where ΔG^o is the free energy change (kJ/mol); R^* is the universal gas constant (8.314 J/mol K) and T (K) is the absolute solution temperature; ΔH^o change in enthalpy; ΔS^o is the change in entropy.

CHAPTER THREE

3. Results and Discussion

3.1. Physical Properties

Carbon is a very important industrial product due to its uses in various aspects of modern civilization. Some physical properties of the carbon produced by this study were mentioned in Table (3-1).

1. *Surface Area*

The BET isotherm method was used including adsorption of nitrogen gas to determine specific surface area. The surface area values of the resulting carbon prepared from fuel oil waste impregnated with concentrations of 20% $ZnCl_2$ solution is given in Table (3-1). The results showed that these values are equal to 399.75 m^2/g compared to that of non-activated 72.32 m^2/g. This value increases to reach a maximum value of 1050.4 m^2/g at MWCNT. These results indicated that MWCNT plays an important role in increasing the surface area.

2. *Density Measurement*

The density of the MWCNT derived from fuel oil waste source was 0.4908 g/cm^3 as shown in Table (3-1). Therefore, less density is causing greater pores and higher surface area.

3. *Ash Content Determination*

The prepared MWCNT has very low ash content 0.11% as shown in Table (3-1) which indicates a high purity for MWCNT. High ash content is undesirable for carbon since it reduces the mechanical strength and adsorptive capacity [202].

4. *pH Determination*

The average value of pH of MWCNT are 3.79 indicates more acidic compared with values of 6.15 and 5.53 for non-activated and activated carbon respectively as shown in Table (3-1). The surface acidity is due to the presence of carbon-oxygen surface chemical structures that have been

postulated as carboxyls and lactones. The activation process has increased the surface area and porosity as well as the surface acidity of carbon.

5. *Moisture Content Determination*

It is known that permissible range of moisture content of carbon is less than 10% [203]. However the moisture content of MWCNT is 1.6% as shown in Table (3-1) which indicates a very good property.

Table (3-1): Some physical properties of carbon samples used in the study

Samples	Surface area m^2/g	Density g/cm^3	Ash%	pH	Moisture %
MWCNT	1050.4	0.4908	0.11	3.79	1.600
A.C	399.75	0.5384	1.23	5.53	1.433
N.A.C	72.32	0.5834	2.61	6.15	0.773

3.2. Surface Morphology of MWCNT

3.2.1. *The Field Emission Scanning Electron Microscopy*

The field emission scanning electron microscopy (FE-SEM) technique is employed to observe the surface physical morphology of the MWCNT. Images (3-1) shows a typical surface of MWCNT prepared from fuel oil waste using ultrasonic probe with the uniform morphology. The MWCNT can be clearly recognized without showing any preferred direction. The individual MWCNT have a bamboo-like structure which is a typical feature of relatively 30-40 nm in diameter. The MWCNT are well dispersed and shows a sheet which is regarded as an entangled MWCNT network. The MWCNT sheets have high flexibility and are not easily broken during oxidation, washing and drying processes.
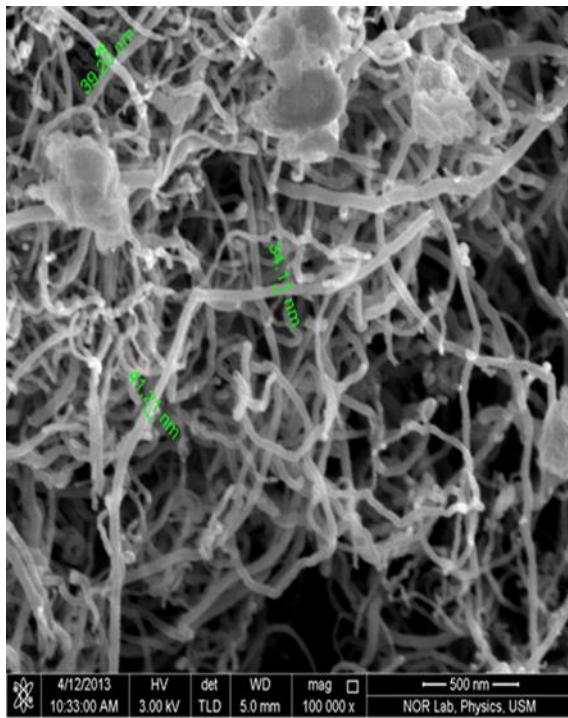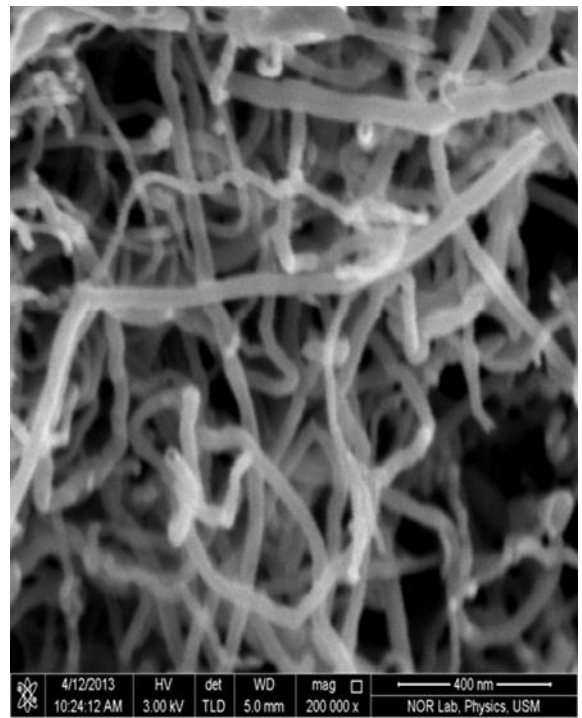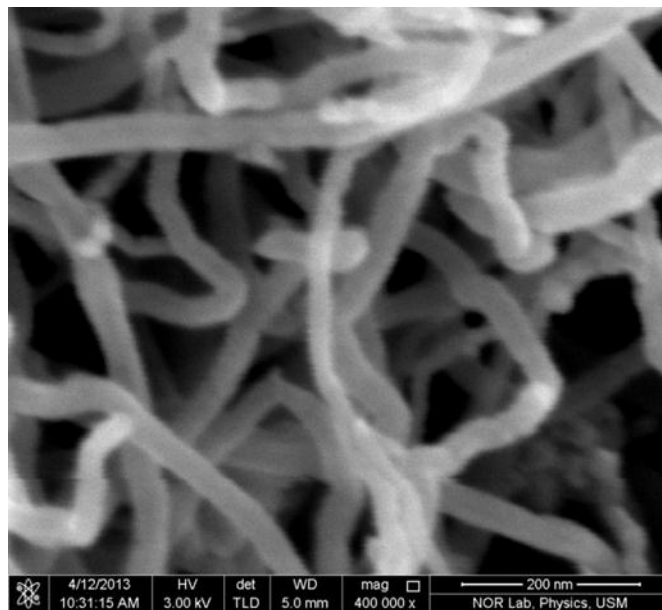
Images (3-1): FE-SEM of MWCNT obtained by fuel oil waste preparation using an ultrasonic probe technique **(A)** 100.000x **(B)** 200.000x **(C)** 400.000x

3.2.2. *Transmission Electron Microscopy (TEM) Analysis*

TEM is applied to analyze the particle size and structure of MWCNT. Images (3-2) shows TEM of the synthesized MWCNT as a powder grown by ultrasonic probe technique after purification.
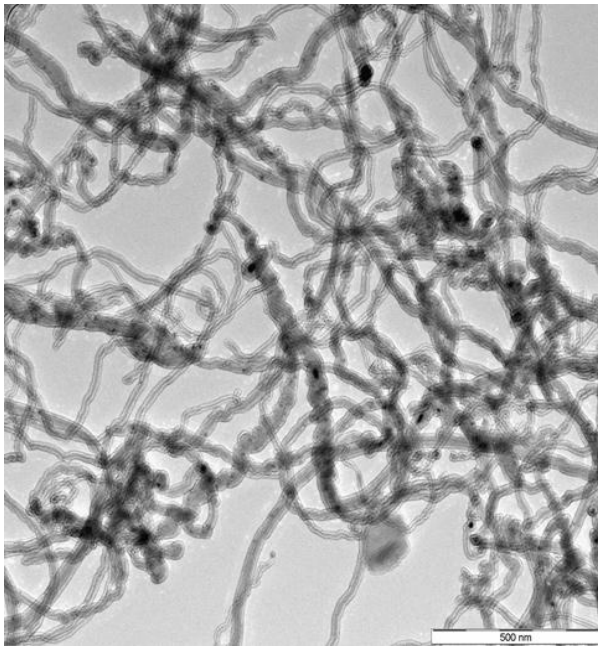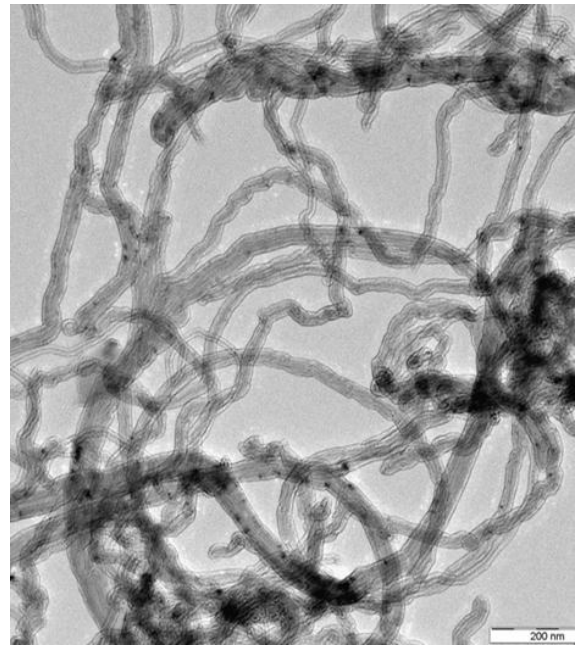
(A) **(B)**
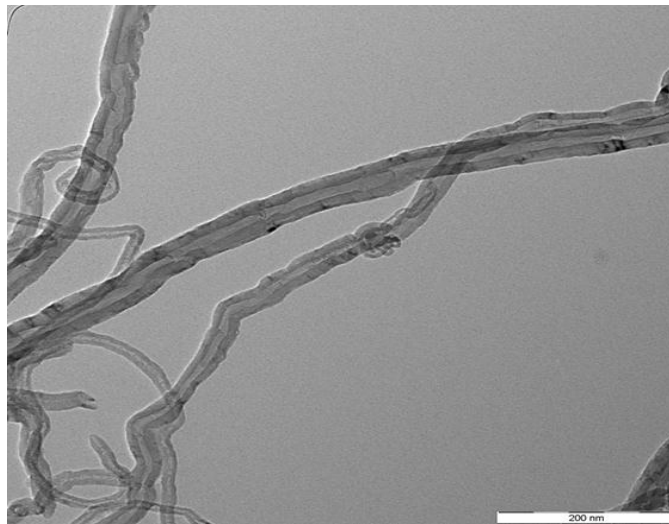
(C)

Images (3-2): TEM of MWCNT obtained by fuel oil waste preparation using ultrasonic probe technique with the diameter of MWCNT is around 20-30 nm and different magnifications **(A)** 500 nm **(B)** 200 nm for group of tubes **(C)** 200 nm for one tube

3.2.3. *Atomic Force Microscopy (AFM) Analysis*

The morphological characteristics of MWCNT have been studied using atomic force microscope (AFM) to observe nanostructure. Images (3-3) shows AFM present a two-dimensional and three-dimensional view of the surface structure of the MWCNT. The images confirmed that the MWCNT

have a roughness surface and small tube diameter distribution. The average tube of MWCNT is measured using AFM images. It can be observed that the average tube distribution of 66.36 nm as shown in Figure (3-1).
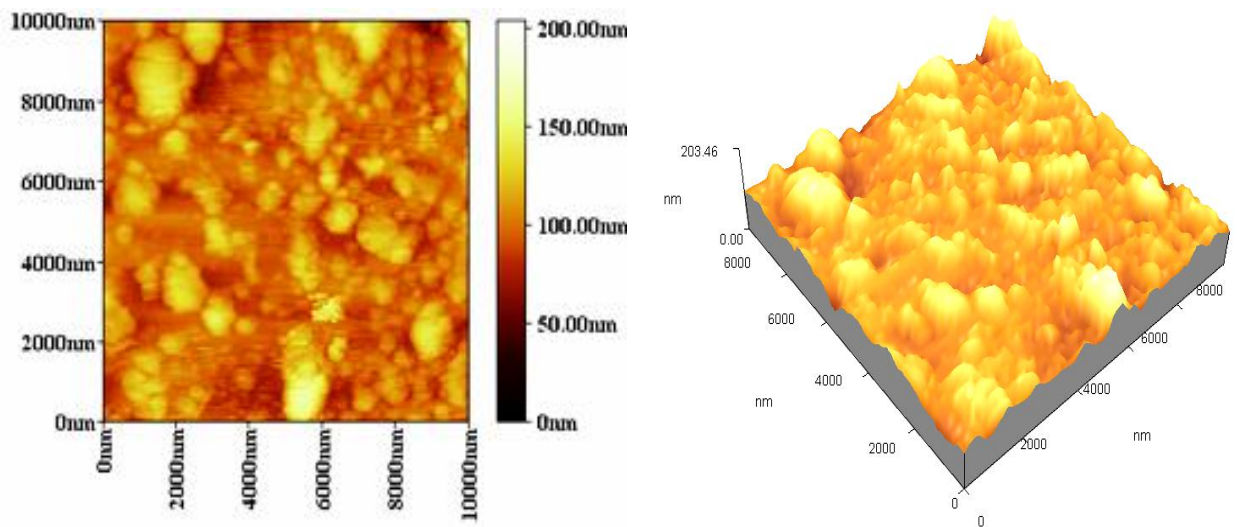
Images (3-3): AFM of 2-dimensional and 3- dimensional of MWCNT
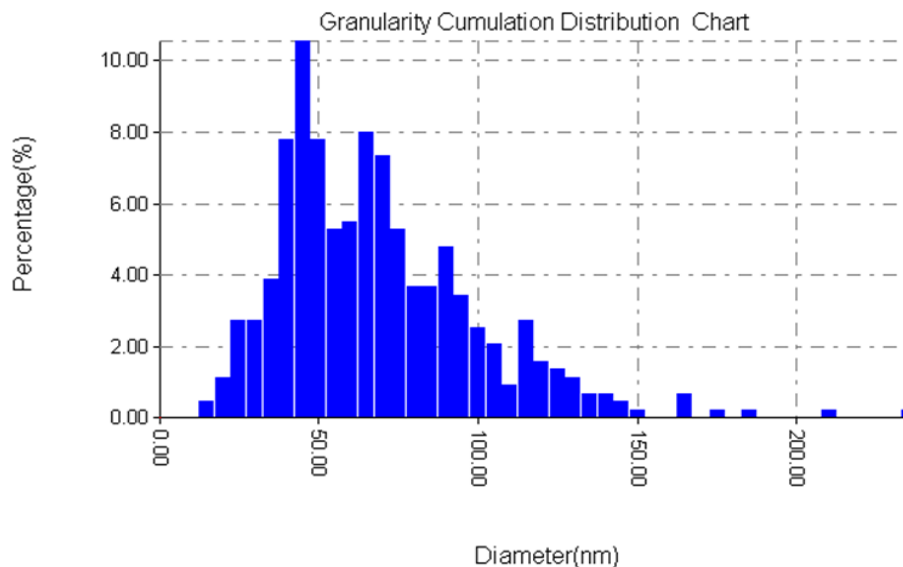
Fig. (3-1): The average tube distribution for MWCNT of diameter 66.36 nm

3.2.4. *X-Ray Diffraction Analysis*

X-ray diffraction may provide information about the structure of MWCNT. Fig. (3-2) shows the XRD pattern of the prepared MWCNT, which obtain that this powder is polycrystalline type with preferred (002) plane at $2\theta = 26.228^o$ and secondary peaks of (100), (123) and (113) at $2\theta = 31.589^o$, $2\theta = 34.605^o$ and $2\theta = 56.029^o$ respectively. These peaks identified to the reflection of hexagonal carbon structure. A fact confirmed

by using a standard card (No.00-046-0943). The other diffraction peak observed at $2\theta = 36.100^{o}$ could be identified to the reflection from the (101) plane of zinc oxide, confirmed by using a standard card (No.01-079-0208) which may be exist in row MWCNT material as activated. The preferred MWCNT peaks of (002) appear as a wide peak which means that the tube or grain size of prepared MWCNT is in the range of nanosize. According to the Debye-Shrerre formula give grain size of 16 nm value for the (002) direction. The grain size values obtained by XRD are agreed with which found by SEM, TEM and AFM techniques.
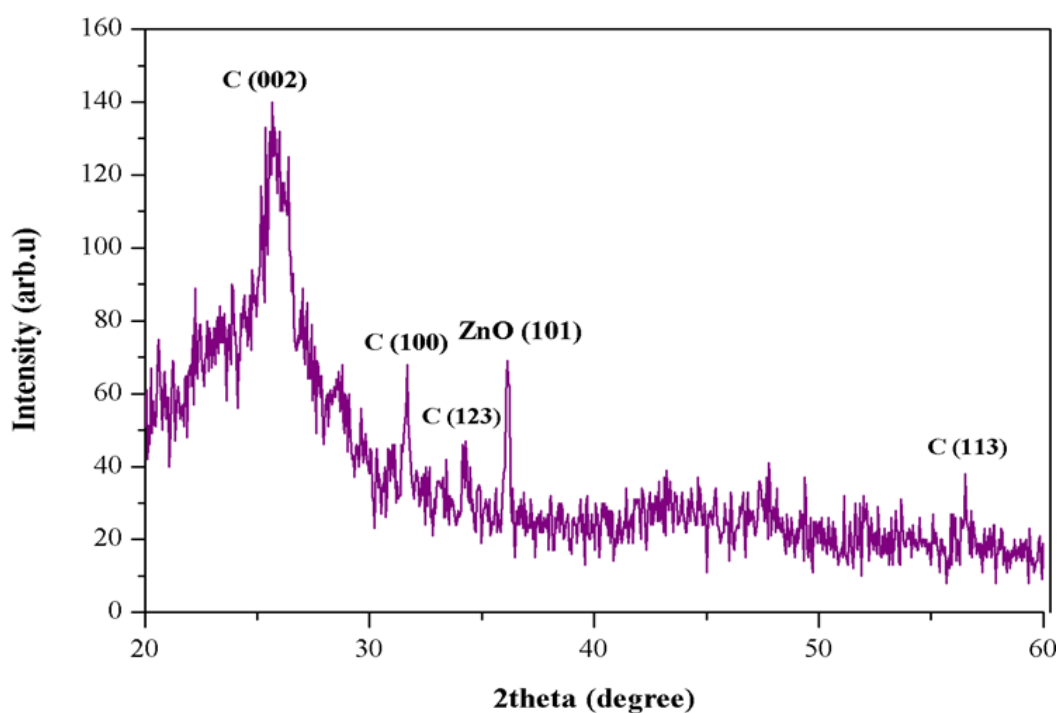
Fig. (3-2): X-ray diffraction patterns of MWCNT

3.2.5. *Fourier Transform Infra-Red Spectrophotometer (FT-IR)*

FT-IR spectroscopy is an important technique used in identifying characteristic surface functional groups. The adsorption capacity of carbon depends upon porosity as well as the chemical reactivity of functional groups at the surface. The functional groups on the adsorbent surface are identified by evaluating the spectra using available literature [204-206] (Fig. 3-3). The spectra showed that the peak at 3491 cm^{-1} could be ascribed to O-H stretching vibration of hydroxyl groups while the methylene group

is detected by C-H stretching at a wave number of 2877 cm^{-1}. The bands at 2000-2400 cm^{-1}, 1639 cm^{-1}, 1450 cm^{-1} and 1161 cm^{-1} can be attributed to C≡C, C=C or C=O, CH$_2$ bend and C-O respectively. The peak at 1161 cm^{-1} is usually assigned to C-O stretches in lactonic, ether and phenolic groups. The band at 650-1000 cm^{-1} is attributed to =C-H bend. Analysis of FT-IR shows that the (–OH, C-H, C≡C, C=O, C=C, C-C and C-O) groups contribute to the surface of adsorbent.
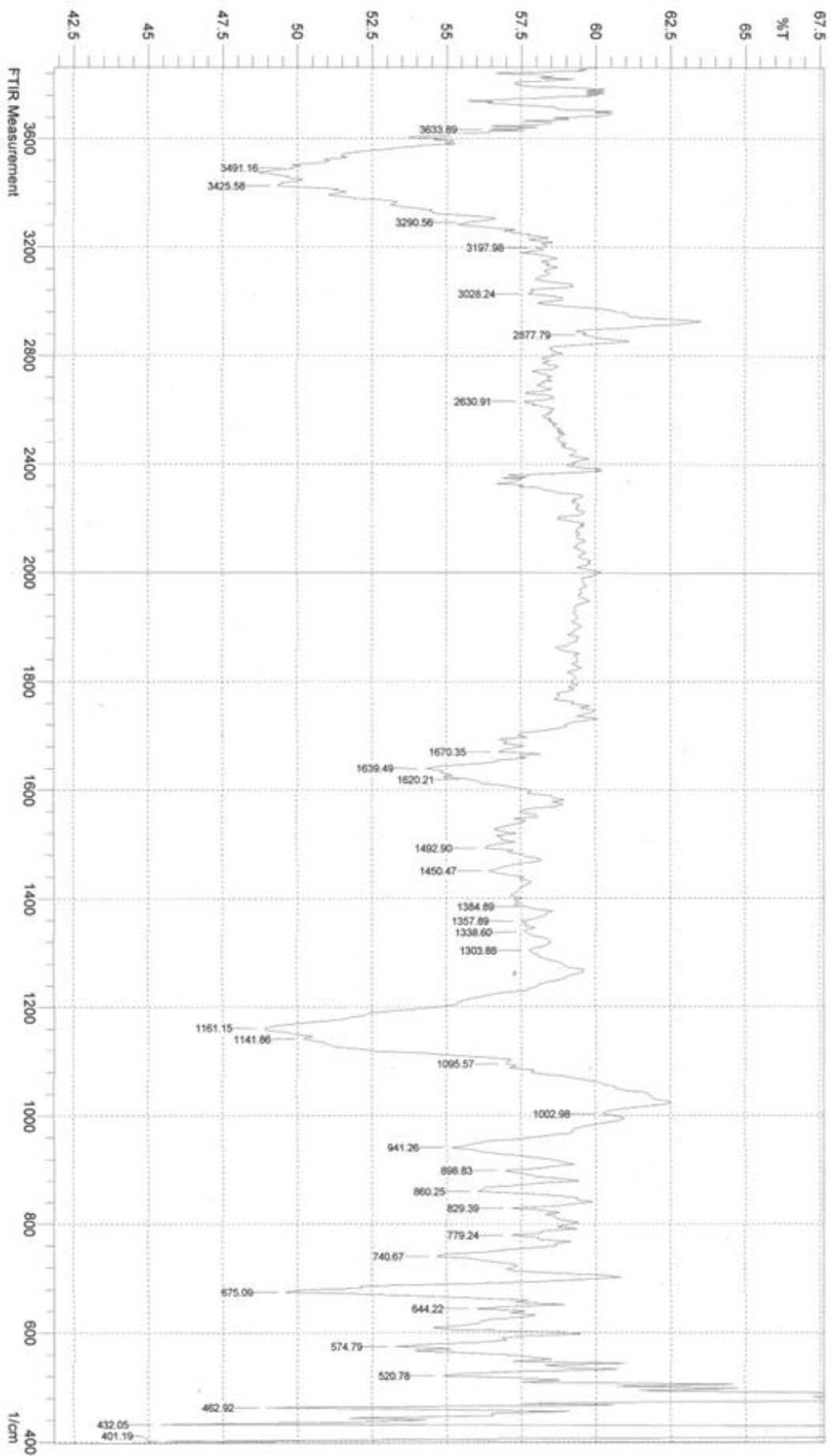
Fig. (3-3): FT-IR spectra of the prepared carbon

3.3. Removal of Pollutants by Adsorption Using Carbon

3.3.1. Equilibrium Adsorption

3.3.1.1. *Benzene Removal*

The isotherm of the benzene adsorption by synthetic non-activated carbon (N.A.C), activated carbon (A.C) and MWCNT were represented by applying the Langmuir, Freundlich and Temkin adsorption models. It was found that the adsorption process on the synthetic activated carbon and MWCNT fits very well with the isotherm models (Table 3-2).

The relations of equilibrium values of $\log Q_e$ vs. $\log C_e$, C_e/Q_e vs. C_e and Q_e vs. $\ln C_e$ for benzene adsorption isotherms using synthetic carbon powder at different temperatures are shown in Figures (3-4), (3-5), (3-6), (3-7), (3-8), (3-9), (3-10), (3-11) and (3-12) respectively.

The Freundlich linear isotherm is expressed in equation (1-3). This isotherm is usually used in special cases for heterogeneous surface energy and it is characterized by the heterogeneity factor 1/n. Q_e is the equilibrium value of benzene adsorbed per unit weight of synthetic activated carbon and MWCNT powder, i.e. a liquid-phase sorbate concentration occurred at equilibrium and K_F as the Freundlich constant. Freundlich constants are shown in Table (3-2) while the relations are clearly indicated that the Freundlich isotherm model fits the analyzed data according to its correlation coefficients (R^2). In general, the adsorption capacity of the adsorbent increases as the K_F value increases. On the average, a favorable adsorption tends to have Freundlich constant (*n*) between 1 and 10.

Larger value of *n* (smaller value of 1/*n*) implies stronger interaction between the adsorbent and the adsorbate [207]. From (Table 3-2) it can be seen that (*n*) value is between (1.767-5.587) showing favorable adsorption of benzene onto the MWCNT as compared to that of activated carbon and non-activated carbon.

The synthetic non-activated carbon, activated carbon and MWCNT powder takes up benzene on a heterogeneous surface by multilayer

adsorption as described by Langmuir. However, the Langmuir linear isotherm is expressed in equation (1-2). Where Q_o is the maximum amount of adsorption corresponding to complete monolayer coverage and K_L is the Langmuir constant. The fitting of adsorption data to Langmuir isotherm equation is investigated by plotting C_e/Q_e versus C_e. The result shows linear relationship between them as stated in Figure (3-7) for MWCNT as compared to that of benzene adsorption capacity on activated carbon and non- activated carbon (Table 3-2).

Negative values of activated carbon and non-activated carbon for Langmuir isotherm constants indicate the inadequacy of the isotherm model to explain this adsorption process [208].

Table (3-2) shows the calculated Langmuir constants and a maximum adsorption capacity for MWCNT, A.C and N.A.C.

The linear form of Temkin isotherm is expressed in equation (1-4). The adsorption data are analyzed according to eq. (1-4) and a plot of Q_e versus ln C_e enables the determinations of the isotherm constants A and B. The fitting of adsorption data to Temkin isotherm equation is investigated according to its correlation coefficients (R^2) (Table 3-2).
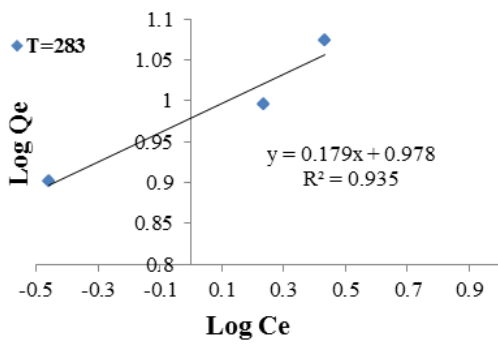
(A)
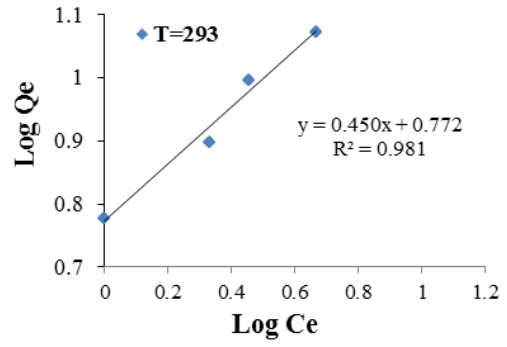
(B)
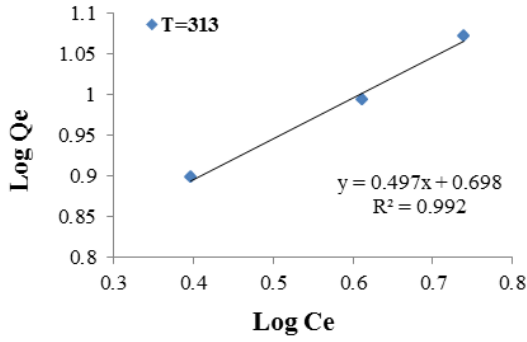
(C)
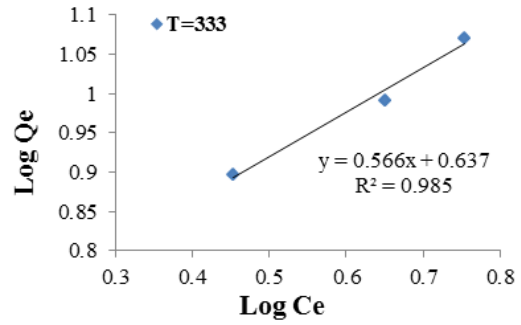
(D)

Fig. (3-4): Freundlich linear relationship for the adsorption of benzene solutions on MWCNT at different temperatures
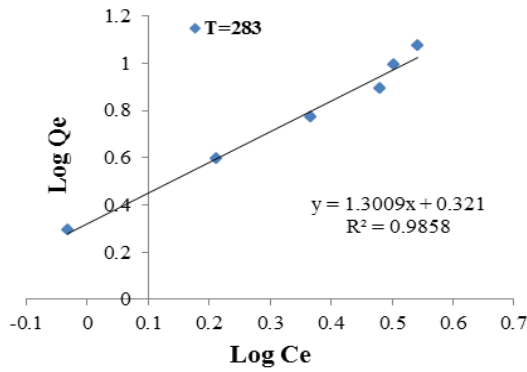
(A)
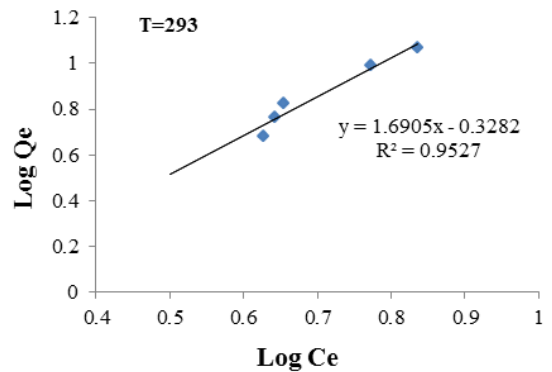
(B)
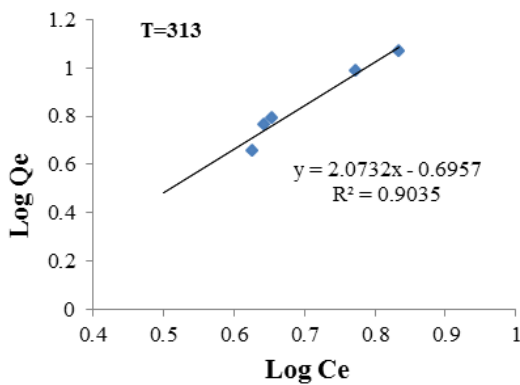
(C)
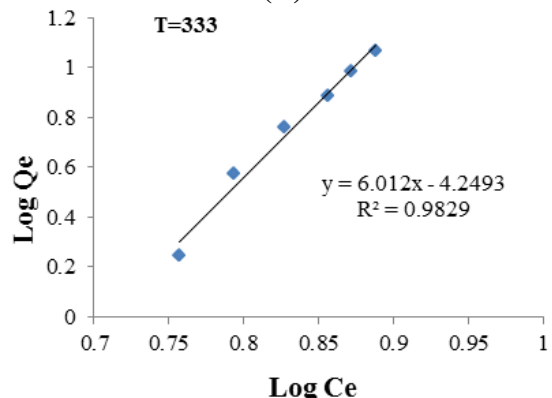
(D)

Fig. (3-5): Freundlich linear relationship for the adsorption of benzene solutions on activated carbon at different temperatures
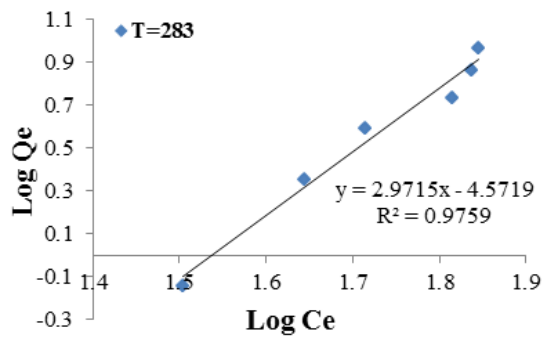
(A)
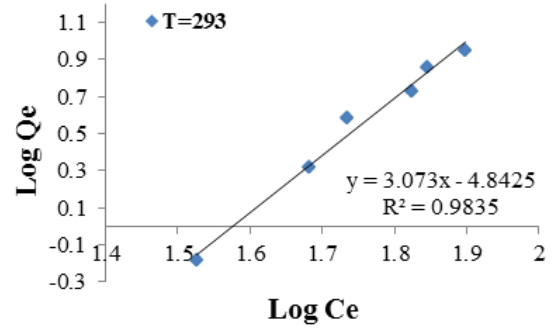
(B)
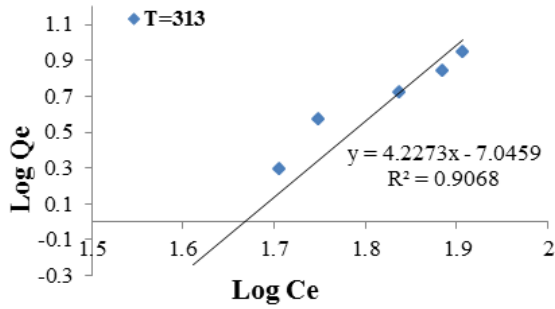
(C)
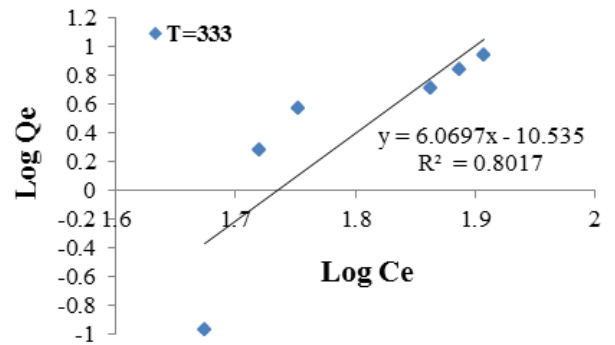
(D)

Fig. (3-6): Freundlich linear relationship for the adsorption of benzene solutions on non-activated carbon at different temperatures
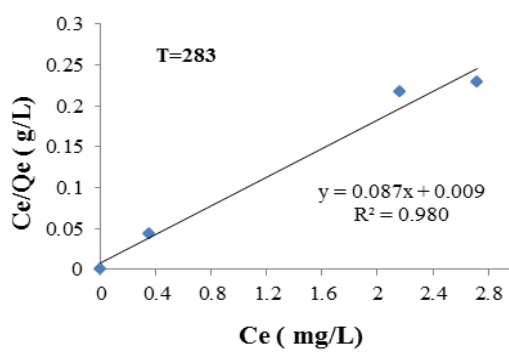
(A)
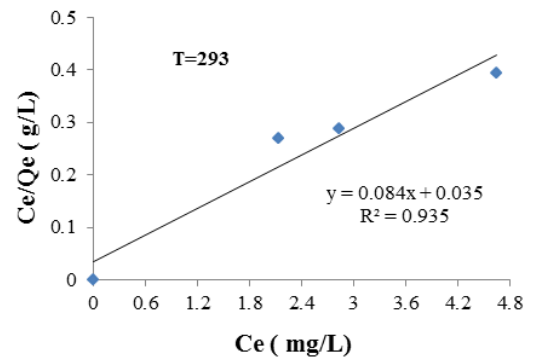
(B)
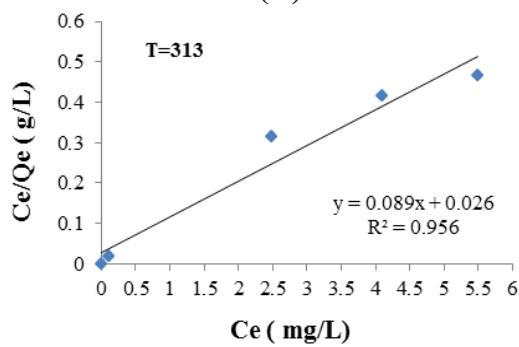
(C)
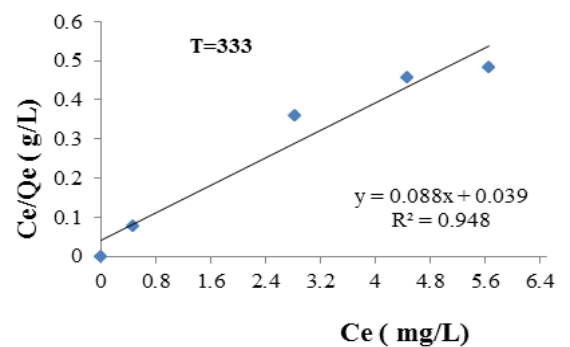
(D)

Fig. (3-7): Langmuir linear relationship for the adsorption of benzene solutions on MWCNT at different temperatures
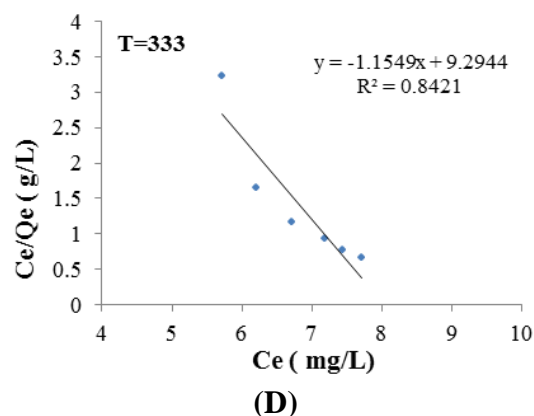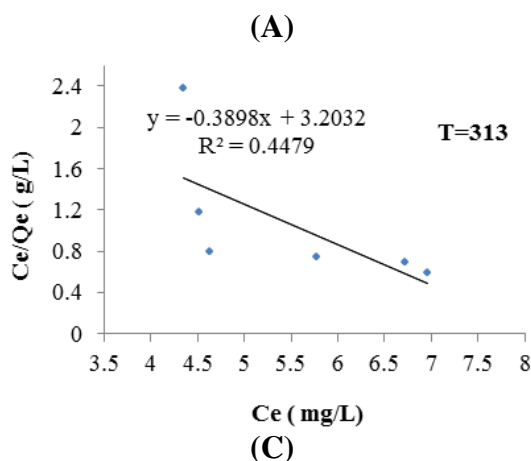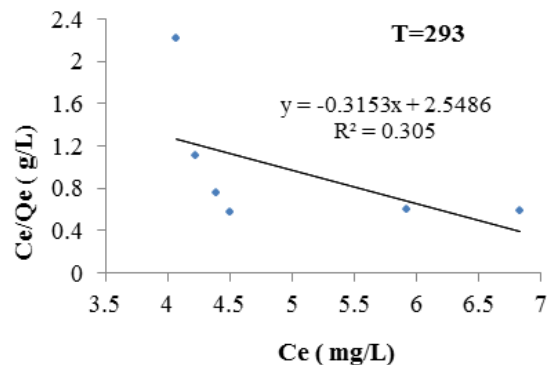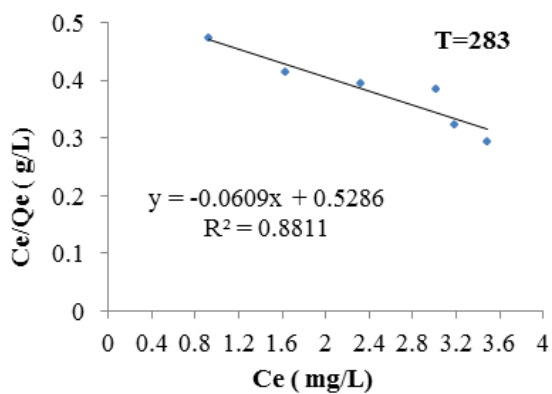
Fig. (3-8): Langmuir linear relationship for the adsorption of benzene solutions on activated carbon at different temperatures
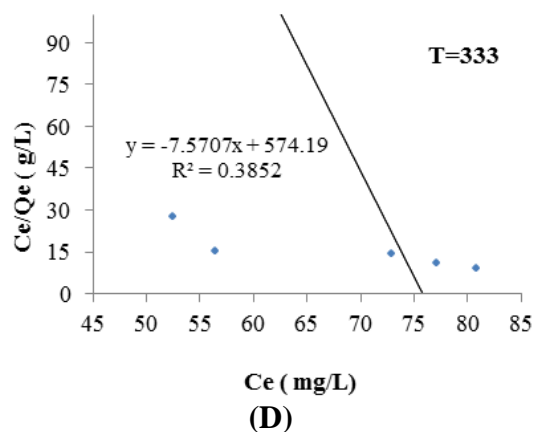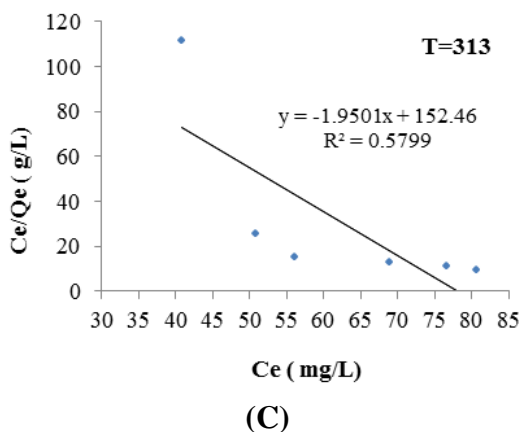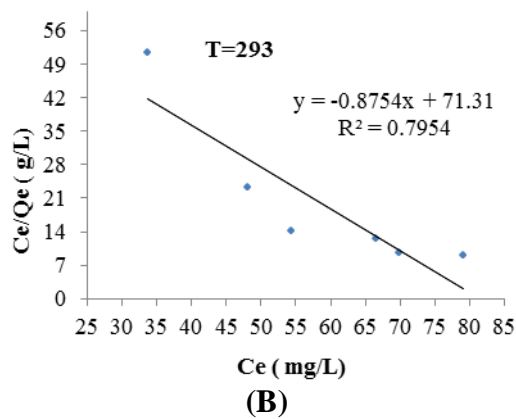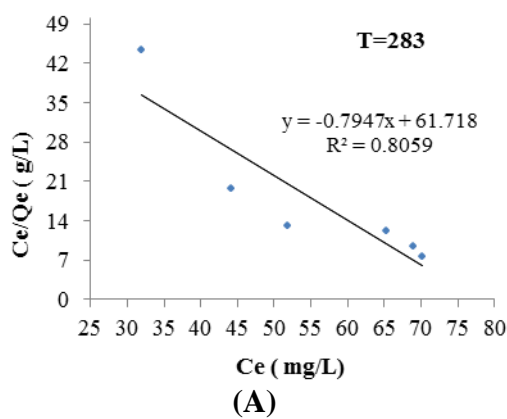
Fig. (3-9): Langmuir linear relationship for the adsorption of benzene solutions on non-activated carbon at different temperatures
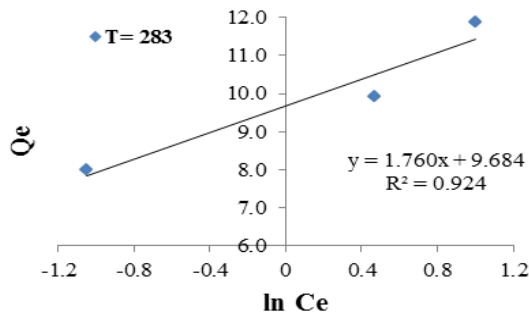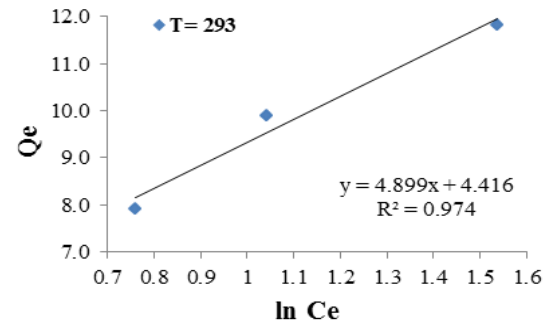
(A)   **(B)**
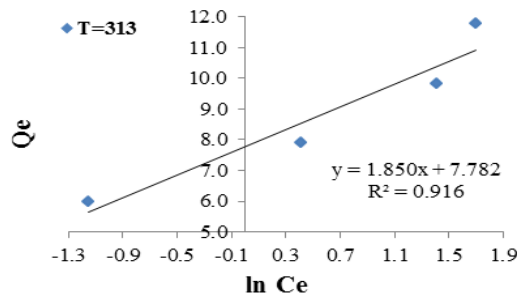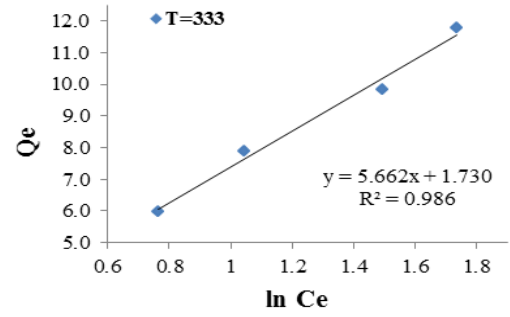
(C)   **(D)**

Fig. (3-10): The linear relationship of Temkin isotherm for the adsorption of benzene solutions on MWCNT at different temperatures
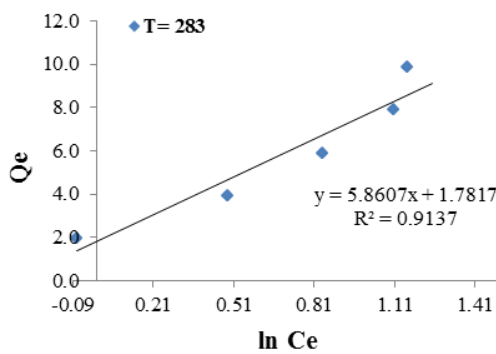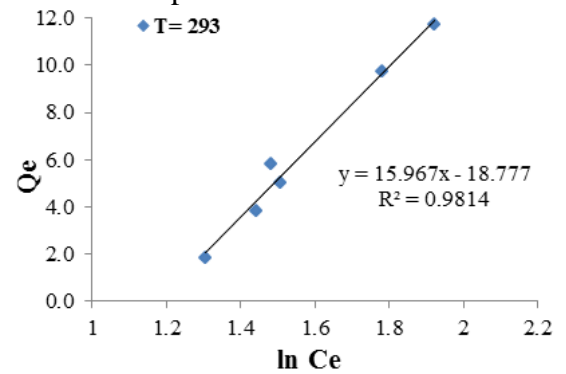
(A)   **(B)**
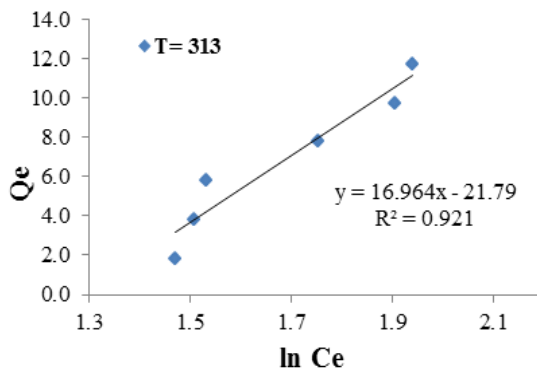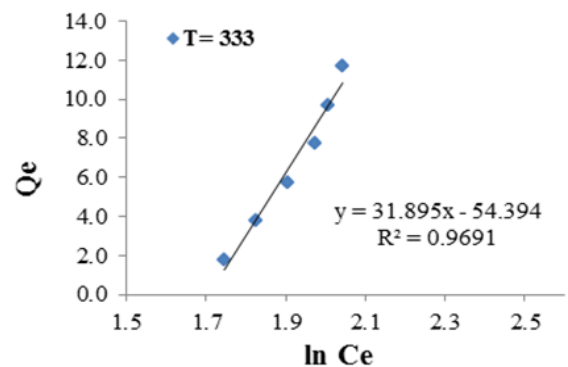
(C)   **(D)**

Fig. (3-11): The linear relationship of Temkin isotherm for the adsorption of benzene solutions on activated carbon at different temperatures
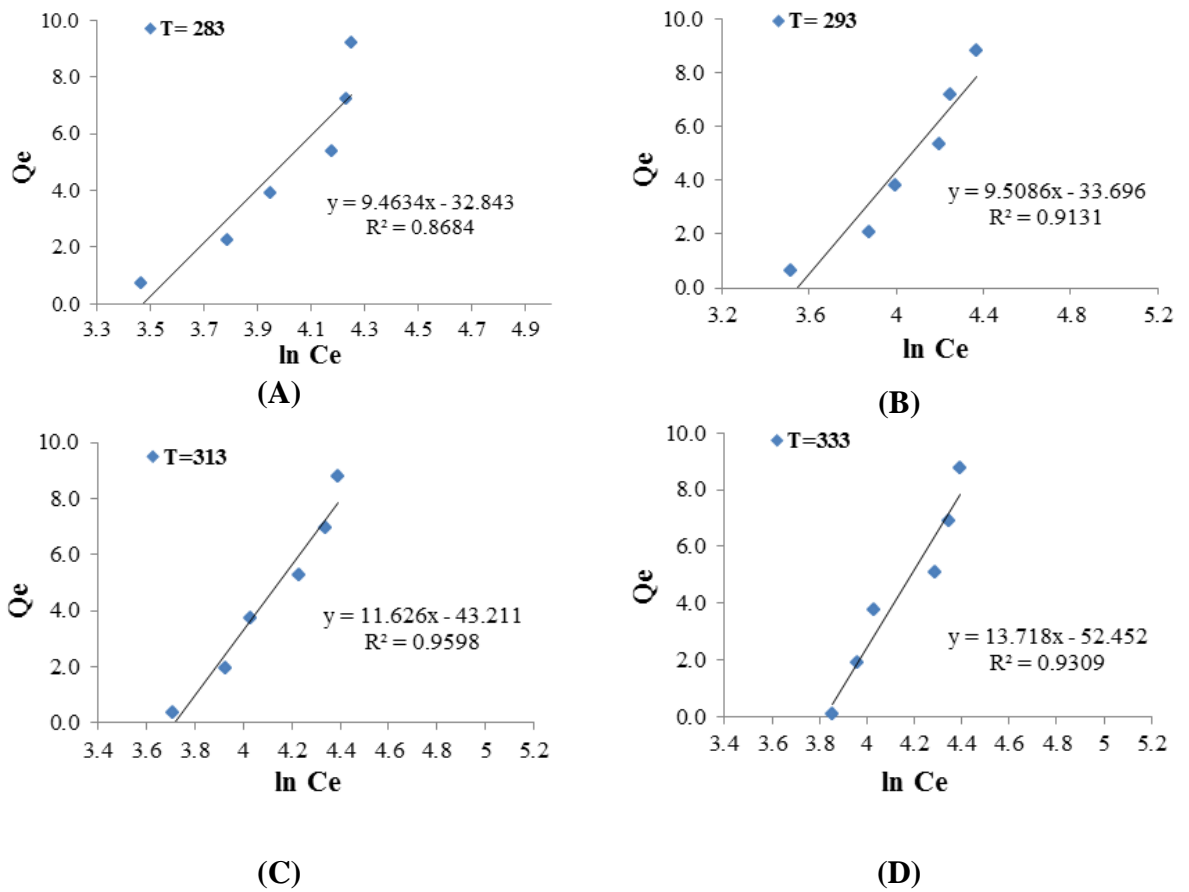
Fig. (3-12): The linear relationship of Temkin isotherm for the adsorption of benzene solutions on non-activated carbon at different temperatures

Table (3-2): The values of Freundlich, Langmuir and Temkin constants for benzene at different temperatures from Figs. (3-4), (3-5), (3-6), (3-7), (3-8), (3-9), (3-10), (3-11) and (3-12)

Samples	T (K)	Freundlich constants			Langmuir constants			Temkin constants		
		R^2	n	K_F	R^2	Q_o	K_L	R^2	B	A
MWCNT	283	0.935	5.587	9.506	0.980	9.667	111.11	0.924	1.760	245.25
	293	0.981	2.222	5.916	0.935	2.399	28.571	0.974	4.899	2.463
	313	0.992	2.012	4.989	0.956	3.423	38.461	0.916	1.850	67.12
	333	0.985	1.767	4.335	0.948	2.256	25.641	0.986	5.662	1.357
A.C	283	0.9858	0.769	2.094	0.8811	- 0.115	1.892	0.9137	5.861	1.355
	293	0.9527	0.592	0.470	0.305	- 0.124	0.392	0.9814	15.967	0.309
	313	0.9035	0.482	0.202	0.4479	- 0.122	0.312	0.9210	16.964	0.277
	333	0.9829	0.166	5.63×10^{-5}	0.8421	- 0.124	0.108	0.9691	31.895	0.182
N.A.C	283	0.9759	0.337	2.68×10^{-5}	0.8059	- 0.013	0.016	0.8684	9.463	0.031
	293	0.9835	0.325	1.44×10^{-5}	0.7954	- 0.012	0.014	0.9131	9.509	0.029
	313	0.9068	0.237	8.9×10^{-8}	0.5799	- 0.013	0.007	0.9598	11.626	0.024
	333	0.8017	0.165	2.917×10^{-11}	0.3852	- 0.013	0.002	0.9309	13.718	0.022

The adsorption rate of benzene increased with increasing concentration and the adsorption percentage decreases as temperature increases (Tables (3-3), (3-4), (3-5), (3-6), (3-7) and (3-8)). It can be seen that adsorption capacity increased until equilibrium concentration is obtained. A complete removal of benzene concentration is obtained for initial concentrations of (50,100,150) ppm in all temperatures for MWCNT. Hence, it is clearly proved that benzene adsorption by synthetic MWCNT agreed fair enough with the Langmuir, Freundlich and Temkin while the reduction of 98.84% is obtained in concentration of benzene at temperature 283 K. It is expressly established that benzene adsorption by synthetic activated carbon and non-activated carbon agreed fair enough with the Freundlich and Temkin adsorption models; and poorly fit with Langmuir isotherm model. The correlation coefficient was very high throughout the experimental range of benzene concentrations studied.

Table (3-3): The adsorption percentage of benzene with concentration 50 ppm at different temperatures

Temp. Time (min)	adsorption efficiency %											
	283K			293K			313K			333K		
	N.A.C	A.C	CNT	N.A.C	A.C	CNT	N.A.C	A.C	CNT	N.A.C	A.C	CNT
0	0.00	0.00	0.00	0.00	0.00	0.00	0.00	0.00	0.00	0.00	0.00	0.00
10	3.88	89.72	90.74	2.87	89.54	90.33	1.68	88.51	89.67	1.09	80.83	84.55
20	6.42	90.28	91.53	5.92	90.19	90.74	4.90	89.49	90.51	1.34	86.84	87.67
30	7.10	92.05	93.26	6.42	90.51	92.09	5.58	89.95	91.67	1.68	87.07	89.81
40	8.12	93.63	93.95	7.78	90.74	93.63	6.42	90.14	93.44	1.85	87.35	92.74
50	12.45	94.47	96.33	11.00	90.93	95.72	8.80	90.42	95.40	2.19	87.54	95.07
60	17.78	95.30	98.14	14.90	91.21	97.67	9.14	90.51	96.65	2.53	87.63	96.33
70	24.90	96.05	99.02	21.34	91.49	98.56	16.59	90.60	97.49	2.70	87.81	97.02
80	34.90	97.02	99.63	32.36	91.68	99.44	17.44	90.70	98.05	3.03	88.05	97.58
90	35.24	97.35	99.91	32.53	91.81	99.81	17.44	91.02	99.63	3.54	88.42	97.86
100	36.09	98.05	100.00	32.53	91.86	100.00	17.61	91.16	100.00	4.73	88.56	99.21
110	36.09	98.14	100.00	32.70	91.86	100.00	18.29	91.16	100.00	5.07	88.56	100.00
120	36.09	98.14	100.00	32.70	91.86	100.00	18.29	91.30	100.00	5.41	88.56	100.00

Table (3-4): The adsorption percentage of benzene with concentration 100 ppm at different temperatures

Temp.	adsorption efficiency %											
Time (min)	283K			293K			313K			333K		
	N.A.C	A.C	CNT	N.A.C	A.C	CNT	N.A.C	A.C	CNT	N.A.C	A.C	CNT
0	0.00	0.00	0.00	0.00	0.00	0.00	0.00	0.00	0.00	0.00	0.00	0.00
10	46.52	93.91	94.84	45.33	93.72	94.12	44.74	93.28	93.61	39.91	83.30	85.27
20	47.70	94.58	95.35	46.60	94.07	94.84	45.92	93.37	94.67	40.33	85.50	91.36
30	48.89	94.68	95.67	47.37	94.37	95.61	46.43	94.75	95.37	42.28	89.65	93.28
40	49.91	95.00	96.14	48.98	94.51	96.05	47.20	95.02	95.91	42.53	90.33	94.02
50	50.76	95.88	97.70	49.23	94.86	97.21	47.79	95.07	96.86	43.30	92.79	94.35
60	52.70	96.79	98.33	49.48	95.07	97.63	48.47	95.16	97.37	43.72	93.09	96.44
70	53.13	97.23	98.67	49.82	95.35	98.56	48.55	95.28	98.23	44.57	93.19	98.07
80	53.72	97.68	99.49	50.50	95.54	98.93	48.72	95.33	98.77	44.74	93.44	98.35
90	55.59	98.21	99.79	51.09	95.68	99.81	48.98	95.37	99.74	46.94	93.65	98.67
100	55.76	98.35	100.00	51.52	95.77	100.00	49.14	95.42	99.86	47.45	93.77	99.26
110	55.84	98.35	100.00	51.60	95.77	100.00	49.14	95.42	100.00	47.53	93.77	99.67
120	55.92	98.37	100.00	51.94	95.77	100.00	49.23	95.49	100.00	47.53	93.79	100.00

Table (3-5): The adsorption percentage of benzene with concentration 150 ppm at different temperatures

Temp.	adsorption efficiency %											
Time (min)	283K			293K			313K			333K		
	N.A.C	A.C	CNT	N.A.C	A.C	CNT	N.A.C	A.C	CNT	N.A.C	A.C	CNT
0	0.00	0.00	0.00	0.00	0.00	0.00	0.00	0.00	0.00	0.00	0.00	0.00
10	59.77	95.05	95.80	58.36	94.06	94.18	52.54	93.05	93.70	51.80	67.73	77.52
20	60.28	95.13	96.08	59.32	94.57	94.91	53.05	94.12	94.85	52.65	76.27	80.48
30	61.41	95.78	96.40	61.12	95.36	95.83	54.57	95.02	95.60	54.06	82.54	87.03
40	62.31	96.48	96.87	61.46	95.46	96.39	56.55	95.36	96.25	56.32	85.76	91.09
50	63.27	97.10	97.24	62.03	96.12	96.76	59.20	95.73	96.65	58.92	87.57	92.30
60	64.40	97.74	98.05	62.25	96.23	96.91	60.33	96.12	96.87	59.83	90.79	94.42
70	64.85	98.02	98.39	62.76	96.54	97.36	60.84	96.22	97.29	61.07	91.24	95.75
80	64.97	98.39	98.76	62.93	96.78	97.60	61.29	96.45	97.44	61.18	93.10	96.31
90	65.42	98.40	98.93	63.05	96.91	98.57	62.31	96.53	98.42	61.46	94.29	97.91
100	65.47	98.42	99.32	63.33	96.99	99.05	62.59	96.90	98.91	62.14	95.49	98.59
110	65.53	98.42	99.97	63.72	96.99	99.84	62.65	96.90	99.61	62.37	95.52	99.13
120	65.47	98.45	100.00	63.78	97.07	100.00	62.59	96.91	99.92	62.37	95.52	99.69

Table (3-6): The adsorption percentage of benzene with concentration 200 ppm at different temperatures

Temp. / Time (min)	adsorption efficiency %											
	283K			293K			313K			333K		
	N.A.C	A.C	CNT	N.A.C	A.C	CNT	N.A.C	A.C	CNT	N.A.C	A.C	CNT
0	0.00	0.00	0.00	0.00	0.00	0.00	0.00	0.00	0.00	0.00	0.00	0.00
10	64.53	91.61	96.64	63.51	91.14	91.23	59.61	90.38	91.14	59.32	72.79	77.41
20	64.57	93.60	96.97	63.60	91.78	93.86	62.16	91.27	93.14	61.78	77.20	82.55
30	64.70	94.53	97.28	64.15	93.05	95.27	63.98	91.82	93.64	62.20	82.92	85.45
40	65.00	95.67	97.59	64.32	93.94	96.18	64.32	93.77	94.32	62.41	87.07	87.55
50	65.12	96.52	97.87	65.17	96.06	96.74	64.66	95.63	96.14	62.58	89.95	91.14
60	65.63	96.76	98.29	65.50	96.55	97.16	64.74	96.51	96.77	62.71	91.39	92.73
70	66.27	97.01	98.55	65.59	96.86	97.54	64.83	96.88	97.43	62.79	93.39	94.95
80	66.39	97.33	98.85	65.97	97.12	97.69	64.91	97.06	97.69	62.96	94.53	96.69
90	66.73	97.64	99.06	66.06	97.34	98.28	65.04	97.09	98.12	63.43	94.95	97.14
100	67.33	97.87	99.23	66.56	97.42	98.57	65.34	97.10	98.34	63.56	95.76	97.67
110	67.41	98.48	99.51	66.56	97.43	98.74	65.59	97.10	98.52	63.56	95.80	97.99
120	67.37	98.49	99.83	66.70	97.51	98.93	65.59	97.12	98.76	63.56	96.40	98.58

Table (3-7): The adsorption percentage of benzene with concentration 250 ppm at different temperatures

Temp. / Time (min)	adsorption efficiency %											
	283K			293K			313K			333K		
	N.A.C	A.C	CNT	N.A.C	A.C	CNT	N.A.C	A.C	CNT	N.A.C	A.C	CNT
0	0.00	0.00	0.00	0.00	0.00	0.00	0.00	0.00	0.00	0.00	0.00	0.00
10	67.66	75.28	94.25	67.25	73.56	89.20	64.20	66.67	88.87	58.51	63.90	79.93
20	68.64	80.27	95.31	67.69	80.00	91.78	65.35	72.67	91.31	60.40	66.44	84.76
30	69.15	82.17	96.55	68.17	81.52	94.33	67.05	76.51	92.87	66.03	72.47	86.00
40	70.57	87.49	97.32	68.47	86.71	95.49	67.83	82.71	94.47	66.34	81.15	86.95
50	71.08	92.40	97.62	68.95	87.69	96.33	68.61	85.86	95.35	66.84	84.34	88.73
60	71.59	95.62	97.83	69.12	89.96	97.33	68.67	89.45	95.78	67.42	86.84	89.56
70	71.69	96.74	98.03	70.40	91.01	97.56	68.81	92.13	96.47	67.96	87.62	90.98
80	71.79	97.40	98.27	71.25	95.52	97.79	68.84	93.49	96.95	68.40	89.56	92.98
90	72.06	97.99	98.47	71.83	97.47	98.05	69.25	95.56	97.42	68.81	95.42	93.35
100	72.13	98.26	98.68	72.03	97.49	98.16	69.25	97.28	97.80	69.05	97.01	96.33
110	72.47	98.74	98.98	72.03	97.49	98.50	69.32	97.28	98.01	69.15	97.02	97.64
120	72.44	98.73	99.13	72.03	97.63	98.87	69.35	97.31	98.36	69.18	97.02	98.21

Table (3-8): The adsorption percentage of benzene with concentration 300 ppm at different temperatures

Temp. / Time (min)	adsorption efficiency %											
	283K			293K			313K			333K		
	N.A.C	A.C	CNT	N.A.C	A.C	CNT	N.A.C	A.C	CNT	N.A.C	A.C	CNT
0	0.00	0.00	0.00	0.00	0.00	0.00	0.00	0.00	0.00	0.00	0.00	0.00
10	69.46	77.29	95.03	69.29	76.70	88.97	65.62	69.80	87.24	62.09	67.34	81.52
20	70.96	79.29	95.73	70.03	77.82	91.49	68.78	76.38	90.18	66.75	69.46	85.58
30	71.13	84.88	95.86	70.65	83.25	92.03	70.51	80.20	91.52	69.69	73.44	87.06
40	74.43	89.52	95.97	71.44	87.82	93.00	71.33	85.51	92.49	71.01	77.71	88.49
50	74.74	92.37	97.73	71.86	89.18	94.18	71.47	87.85	93.49	71.35	79.74	90.27
60	75.17	95.00	97.93	72.71	91.16	95.03	72.20	90.79	94.12	71.75	82.12	90.85
70	76.10	96.92	98.17	73.02	93.53	95.79	72.77	92.43	94.49	72.00	91.65	92.24
80	76.38	97.73	98.42	73.36	95.31	96.36	72.79	93.92	95.30	72.65	93.79	93.30
90	76.58	98.29	98.55	73.50	96.18	98.05	72.91	95.84	96.36	72.94	94.91	94.76
100	76.58	98.47	98.79	73.56	97.71	98.19	73.05	97.67	97.45	72.99	97.16	95.64
110	76.58	98.83	98.98	73.61	97.72	98.33	73.08	97.68	97.89	73.02	97.42	97.79
120	76.64	98.84	99.09	73.61	97.72	98.45	73.10	97.68	98.17	73.05	97.43	98.11

3.3.1.2. *O-xylene Removal*

The isotherm of the o-xylene adsorption by prepared non-activated carbon (N.A.C), activated carbon (A.C) and MWCNT were represented by applying the Langmuir, Freundlich and Temkin adsorption models.

The relations of equilibrium values of $logQ_e$ vs. $logC_e$, C_e/Q_e vs. C_e and Q_e vs. lnC_e for o-xylene adsorption isotherms using synthetic carbon powder at different temperatures are shown in Figures (3-13), (3-14), (3-15), (3-16), (3-17), (3-18), (3-19), (3-20) and (3-21) respectively.

In this study, Freundlich, Langmuir and Temkin isotherm models were used to describe the relationship between the amounts of adsorbed o-xylene and its equilibrium concentration in solution. Adsorption isotherm for o-xylene onto activated carbon and MWCNT fitted adsorption data. Freundlich and Temkin isotherm equations were investigated by plotting log Q_e versus log C_e and Q_e versus ln C_e which are presented in Figures (3-13), (3-14) and Figures (3-19), (3-20) respectively. The adsorption isotherm parameters which were calculated from the slope and intercept of the linear plots using the linearized form of the Freundlich and Temkin equations, together with the R^2 values are given in Table (3-9). The Freundlich model assumes that the uptake of any adsorbate occurs on a

heterogeneous surface by multilayer adsorption and that the amount of adsorbate increases infinitely with an increase in concentration. From these assumptions, it can be concluded that synthetic activated carbon and MWCNT powder take up o-xylene on a heterogeneous surface by multilayer adsorption. The heterogeneity factor n was calculated and the estimated value ranged between (0.95 - 4.63) for MWCNT. It is will known that n value greater than 1.0 gives a favorable condition for adsorption.

The synthetic non-activated carbon, activated carbon and MWCNT powders take up o-xylene on a heterogeneous surface by multilayer adsorption as described by Langmuir. However, the Langmuir linear isotherm is expressed in equation (1-2). The fitting of adsorption data to Langmuir isotherm equation was investigated by plotting C_e/Q_e versus C_e the resulting graphs showed a linear relationship between them as stated in Figure (3-16) for MWCNT compared to that of o-xylene adsorption capacity on activated carbon and non- activated carbon (Table 3-9).

Negative values of activated carbon and non-activated carbon for Langmuir isotherm constants indicated that inadequacy of the isotherm model to explain this adsorption process [208]. It is clear from the R^2 values that the Freundlich and Temkin isotherm are fitted to the experimental data better than Langmuir isotherm model.
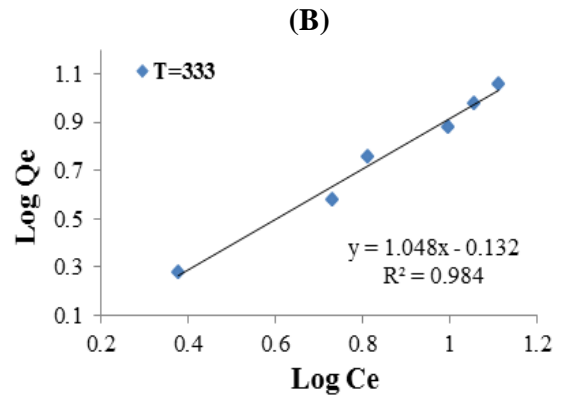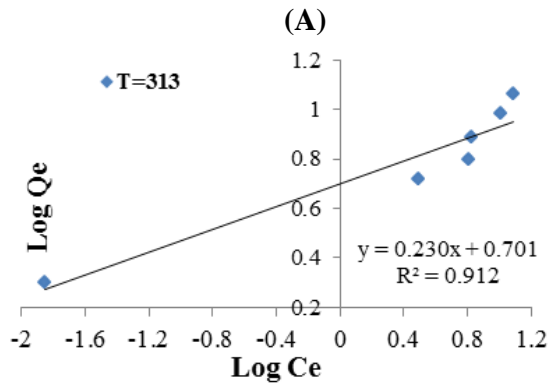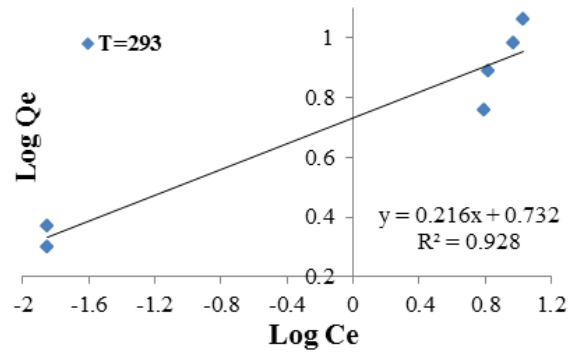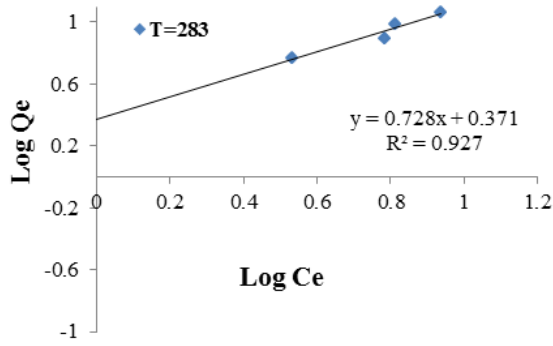
(A)

(B)

(C)

(D)

Fig. (3-13): Freundlich linear relationship for the adsorption of o-xylene solutions on MWCNT at different temperatures
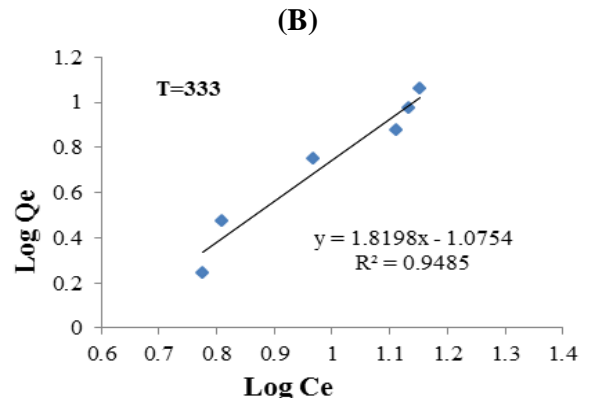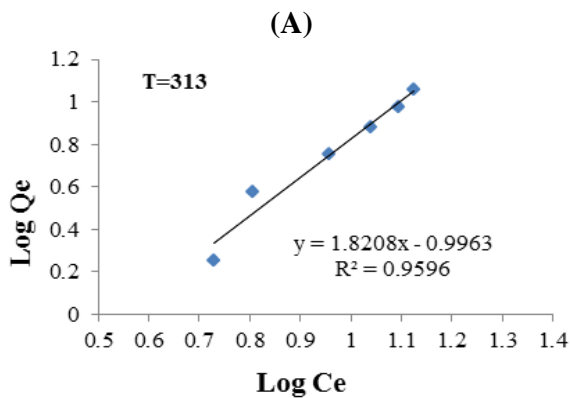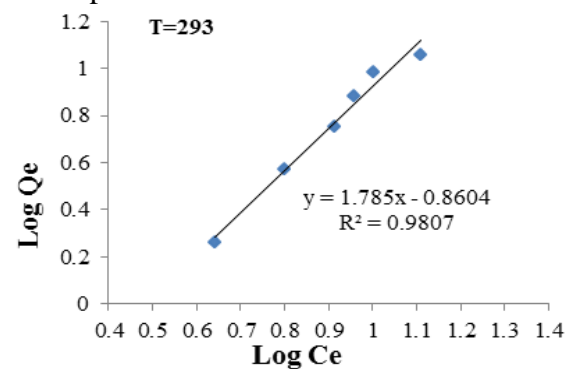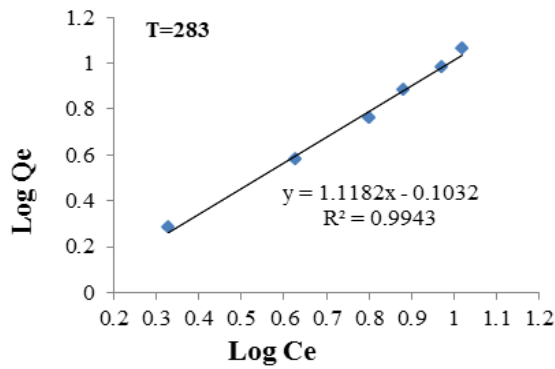
(A)

(B)

(C)

(D)

Fig. (3-14): Freundlich linear relationship for the adsorption of o-xylene solutions on activated carbon at different temperatures
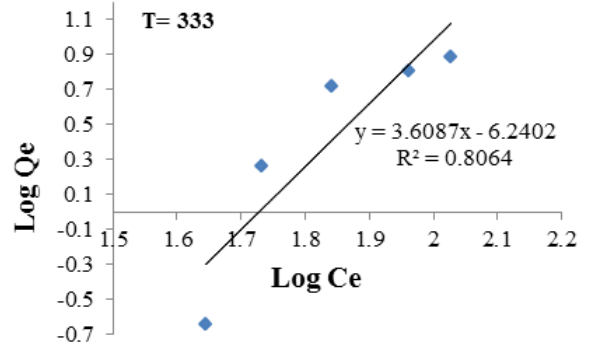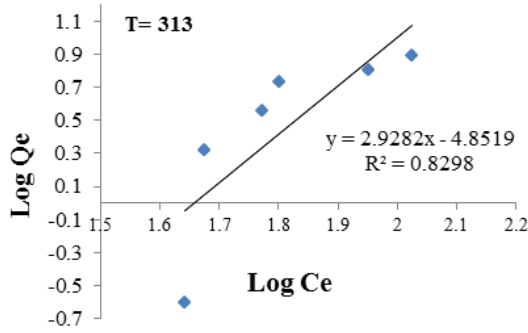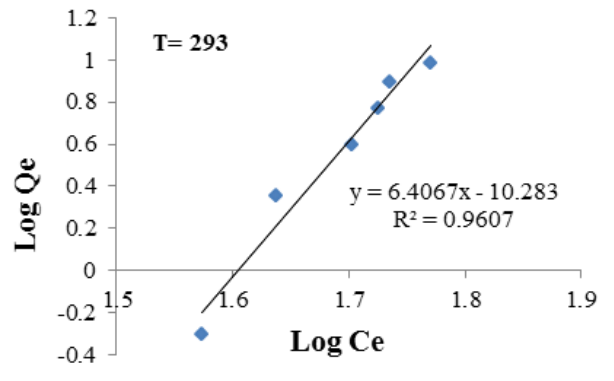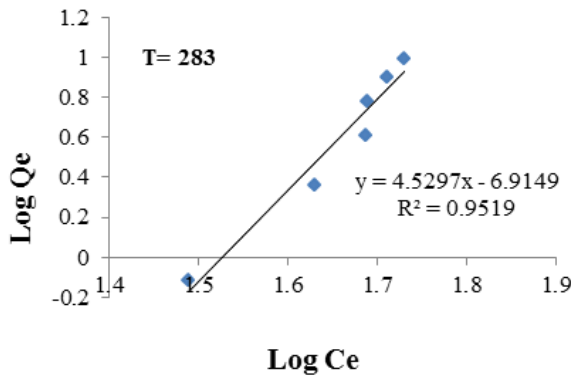
Fig. (3-15): Freundlich linear relationship for the adsorption of o-xylene solutions on non-activated carbon at different temperatures
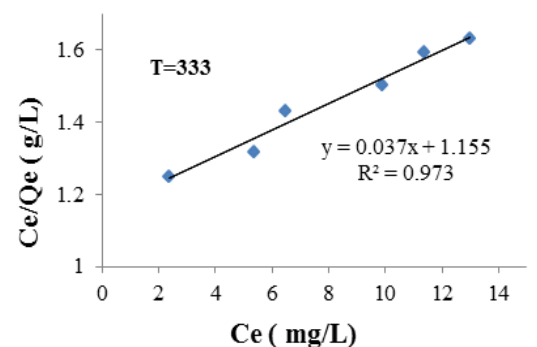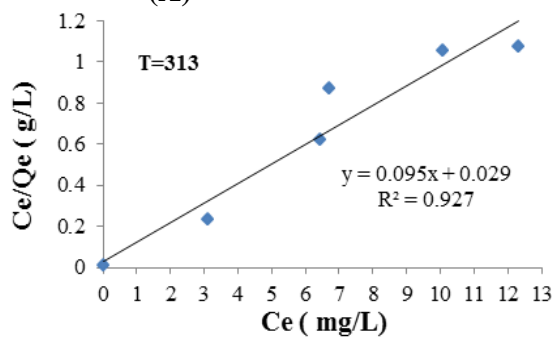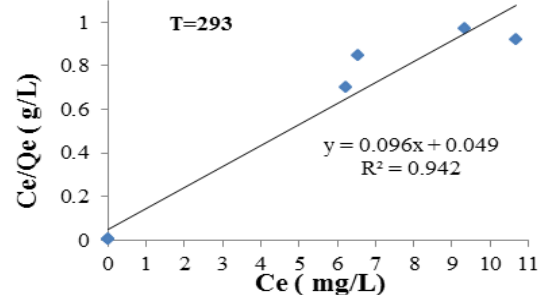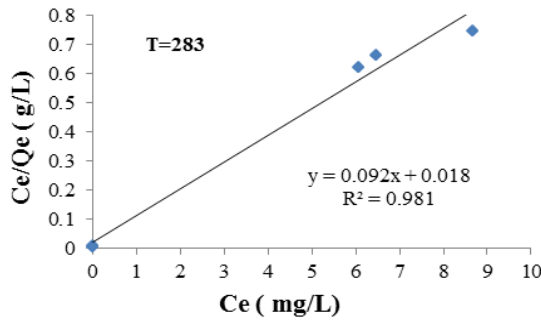
Fig. (3-16): Langmuir linear relationship for the adsorption of o-xylene solutions on MWCNT at different temperatures
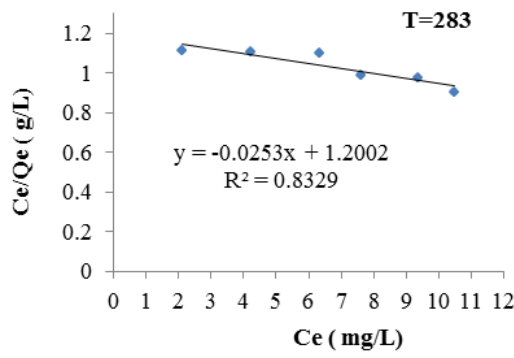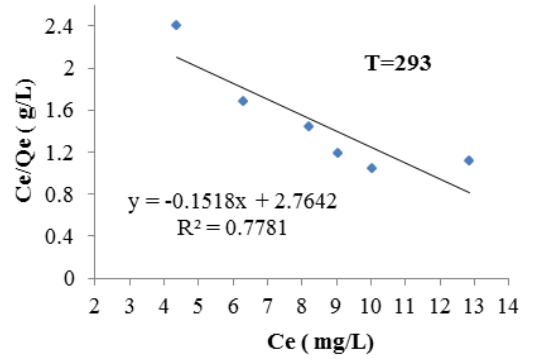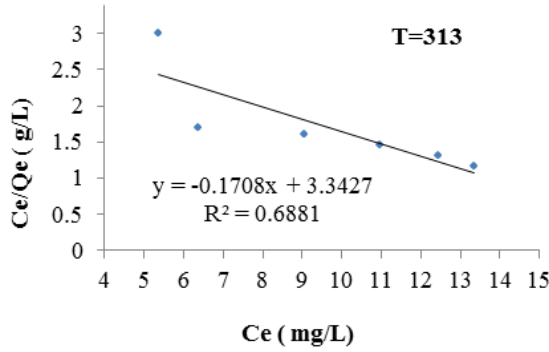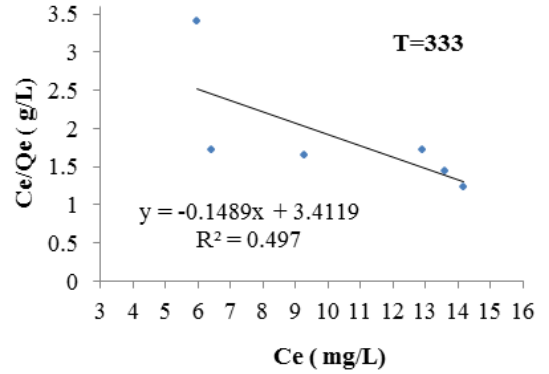
Fig. (3-17): Langmuir linear relationship for the adsorption of o-xylene solutions on activated carbon at different temperatures
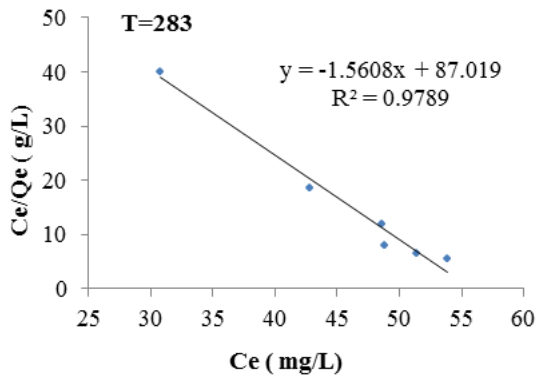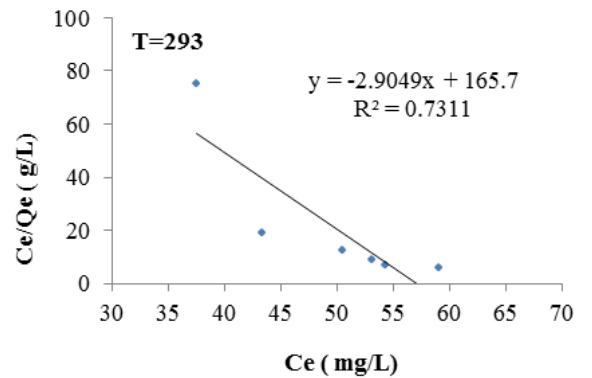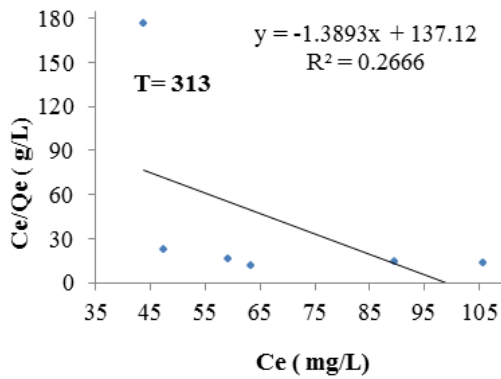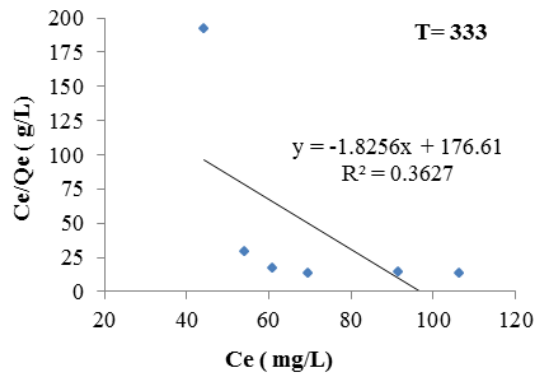
Fig. (3-18): Langmuir linear relationship for the adsorption of o-xylene solutions on non-activated carbon at different temperatures
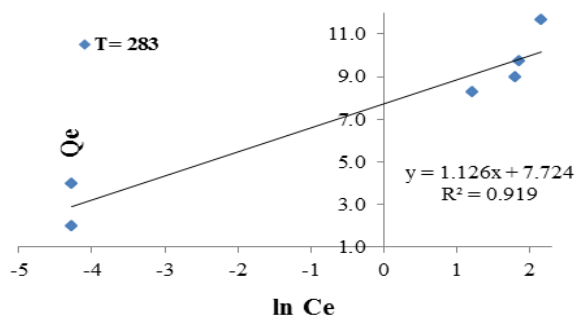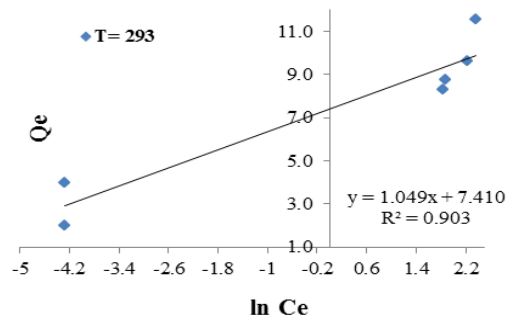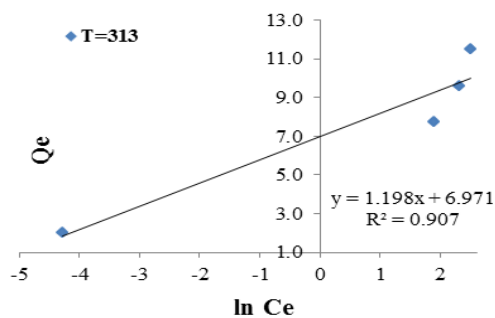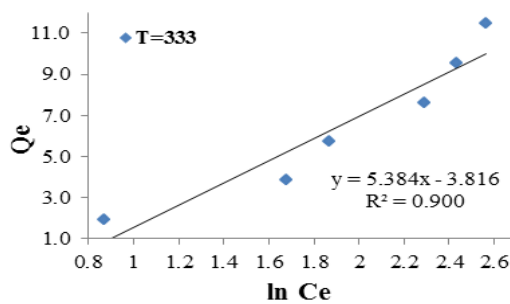
Fig. (3-19): The linear relationship of Temkin isotherm for the adsorption of o-xylene solutions on MWCNT at different temperatures
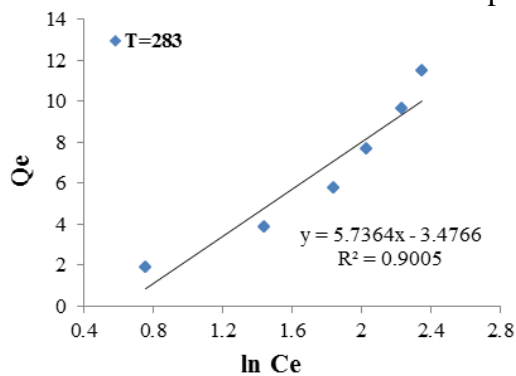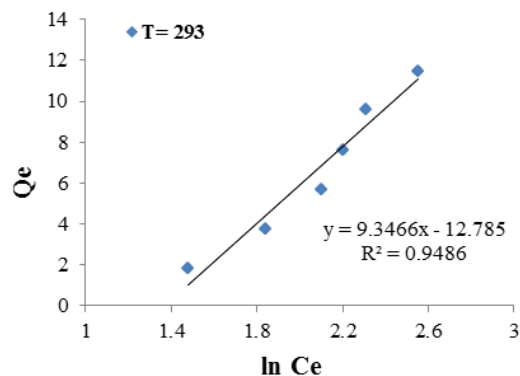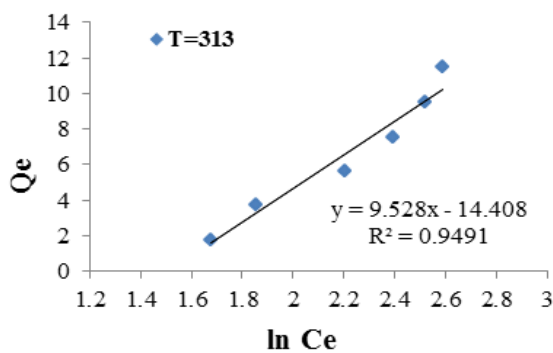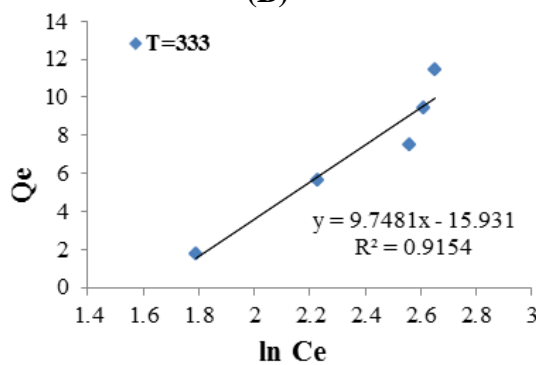
Fig. (3-20): The linear relationship of Temkin isotherm for the adsorption of o-xylene solutions on activated carbon at different temperatures
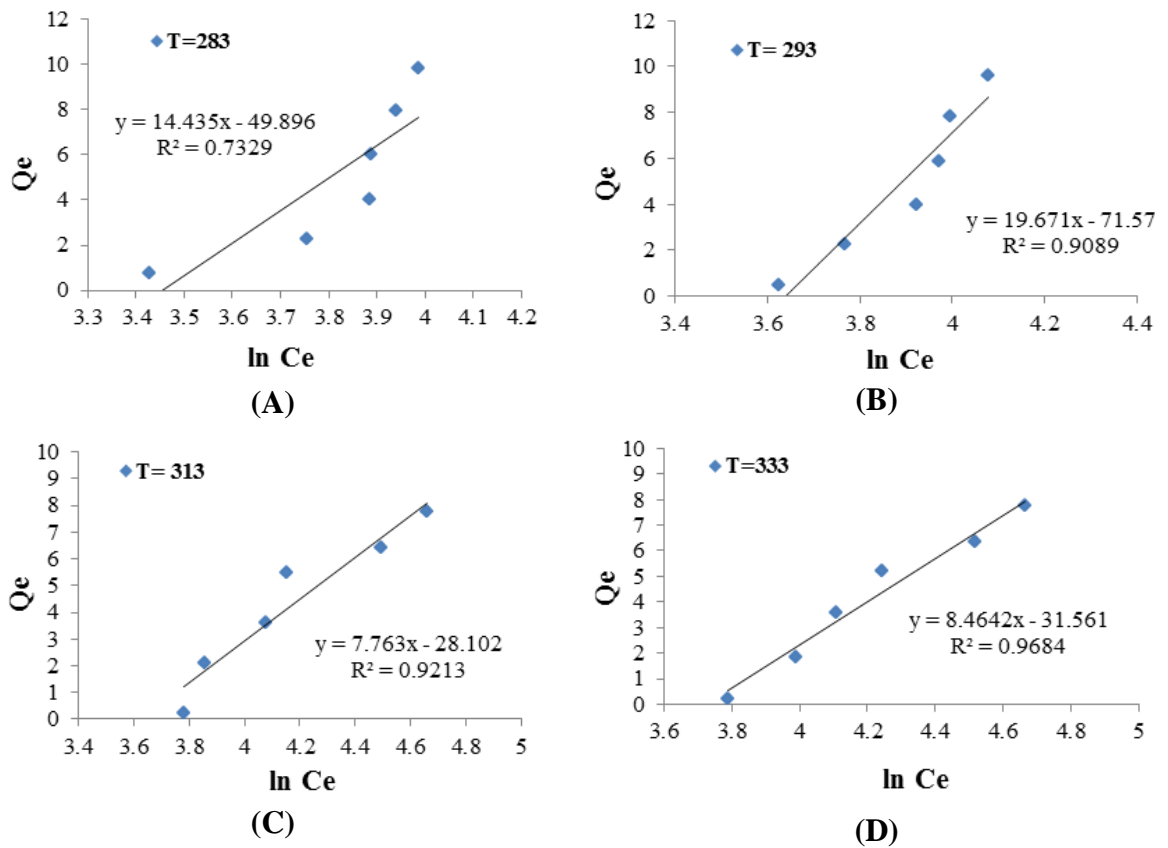
Fig. (3-21): The linear relationship of Temkin isotherm for the adsorption of o-xylene solutions on non-activated carbon at different temperatures

Table (3-9): The values of Freundlich, Langmuir and Temkin constants for o-xylene at different temperatures from Figs. (3-13), (3-14), (3-15), (3-16), (3-17), (3-18), (3-19), (3-20) and (3-21)

Samples	T (K)	Freundlich constants			Langmuir constants			Temkin constants		
		R^2	n	K_F	R^2	Q_o	K_L	R^2	B	A
MWCNT	283	0.927	1.374	2.350	0.981	5.111	55.556	0.919	1.126	953.06
	293	0.928	4.630	5.395	0.942	1.960	20.408	0.903	1.049	1168.7
	313	0.912	4.348	5.023	0.927	3.276	34.483	0.907	1.198	336.59
	333	0.984	0.954	0.738	0.973	0.032	0.866	0.900	5.384	0.492
A.C	283	0.9943	0.894	0.789	0.8329	-0.021	0.833	0.9005	5.736	0.5455
	293	0.9807	0.560	0.138	0.7781	-0.055	0.362	0.9486	9.347	0.255
	313	0.9596	0.549	0.101	0.6881	-0.051	0.299	0.9491	9.528	0.220
	333	0.9485	0.550	0.084	0.4970	-0.044	0.293	0.9154	9.748	0.195
N.A.C	283	0.9519	0.221	1.21×10^{-7}	0.9789	-0.018	0.012	0.7329	14.435	0.032
	293	0.9607	0.156	5.21×10^{-11}	0.7311	-0.017	0.006	0.9089	19.671	0.026
	313	0.8298	0.342	1.40×10^{-5}	0.2666	-0.010	0.007	0.9213	7.763	0.027
	333	0.8064	0.277	5.75×10^{-7}	0.3627	-0.010	0.006	0.9684	8.464	0.024

The adsorption rate of o-xylene increased with increasing concentration and the adsorption percentage decreases as temperature increases (Tables (3-10), (3-11), (3-12), (3-13), (3-14) and (3-15)). It is found that adsorption capacity increases until equilibrium concentration obtained. Almost a complete removal of o-xylene concentration was obtained for initial concentrations of (50,100) ppm and temperature of 283 K for MWCNT. Hence, it is clearly noted that the o-xylene adsorption by synthetic MWCNT agreed fair enough with the Langmuir, Freundlich and Temkin adsorption models, while, reduction of 96.51% was obtained in concentration of o-xylene at temperature of 283 K. It is expressly establish that o-xylene adsorption by synthetic activated carbon and non-activated carbon agreed fair enough with the Freundlich and Temkin adsorption models and poorly fit with Langmuir isotherm model. The correlation coefficient was very high throughout the experimental range of o-xylene concentrations.

Notes from the Tables (3-3) to (3-15) that the percentage of adsorption in the o-xylene is less compared to that of benzene non substituents due to the position and the type and the nature of the substituent group in addition to disability steric factor any size the substituent group has great effect on the adsorption ratio which hampers the process of adsorption in the o-xylene substituent methyl group in the ortho position compared to benzene non substituent.

Table (3-10): The adsorption percentage of o-xylene with concentration 50 ppm at different temperatures

Temp.	adsorption efficiency %											
	283K			293K			313K			333K		
Time (min)	N.A.C	A.C	CNT	N.A.C	A.C	CNT	N.A.C	A.C	CNT	N.A.C	A.C	CNT
0	0.00	0.00	0.00	0.00	0.00	0.00	0.00	0.00	0.00	0.00	0.00	0.00
10	17.24	84.29	85.43	10.67	74.57	76.19	7.52	71.14	74.95	6.10	68.76	74.19
20	21.81	85.24	86.45	11.71	79.81	83.33	8.57	78.57	81.43	6.67	76.10	78.48
30	25.52	87.06	87.22	18.57	82.38	84.00	9.33	80.57	82.95	7.33	77.43	81.05
40	26.10	87.13	87.49	21.81	84.19	85.52	10.19	83.62	84.29	8.48	81.62	84.18
50	29.71	87.87	90.39	24.19	86.25	87.08	10.48	86.00	86.65	9.24	84.57	86.40
60	33.52	90.11	93.77	25.14	87.01	87.49	10.76	87.01	87.21	9.62	86.50	87.17
70	36.48	90.39	96.31	25.43	87.18	88.14	12.10	87.10	87.56	10.29	87.00	87.53
80	36.67	92.93	98.00	25.52	87.24	91.24	12.38	87.31	88.99	10.76	87.14	88.33
90	37.62	93.21	99.97	25.81	87.80	95.46	12.57	87.38	94.06	10.95	87.53	92.76
100	38.00	95.46	99.97	25.05	90.39	98.97	12.48	87.42	95.49	11.43	87.80	94.29
110	38.48	95.46	99.97	25.05	90.96	99.77	12.38	89.27	98.93	11.81	88.03	95.05
120	38.38	95.75	99.97	24.95	91.24	99.87	12.38	89.27	98.93	11.52	88.03	95.24

Table (3-11): The adsorption percentage of o-xylene with concentration 100 ppm at different temperatures

Temp.	adsorption efficiency %											
	283K			293K			313K			333K		
Time (min)	N.A.C	A.C	CNT	N.A.C	A.C	CNT	N.A.C	A.C	CNT	N.A.C	A.C	CNT
0	0.00	0.00	0.00	0.00	0.00	0.00	0.00	0.00	0.00	0.00	0.00	0.00
10	31.86	84.00	88.67	31.14	74.71	84.86	30.43	73.19	83.91	29.43	69.86	81.24
20	36.00	87.43	89.38	35.67	79.29	87.05	30.86	75.43	85.05	29.76	73.91	83.05
30	40.10	89.48	90.76	37.14	83.81	89.71	31.57	78.57	86.43	30.10	76.05	83.52
40	46.67	91.05	93.23	42.81	86.33	90.81	32.91	82.91	86.91	31.95	79.57	85.00
50	48.14	92.10	93.76	45.81	89.00	92.29	34.48	86.91	88.05	33.48	82.95	85.86
60	50.33	93.10	94.63	50.95	91.33	93.28	35.48	88.95	88.71	34.86	86.00	87.10
70	53.10	94.49	96.32	51.91	93.33	93.55	44.95	90.81	90.81	35.14	88.43	90.38
80	54.62	95.06	97.73	54.95	93.51	93.71	48.81	93.05	92.86	37.14	91.86	92.67
90	56.48	95.48	98.72	56.24	93.62	95.90	52.62	93.45	93.52	44.52	93.23	93.48
100	56.62	95.76	99.99	56.95	93.69	98.58	52.86	93.61	93.76	45.24	93.56	93.61
110	57.33	95.76	99.99	56.67	93.69	99.42	52.81	93.64	95.62	45.86	93.57	94.35
120	57.24	95.76	99.99	56.67	93.71	99.99	52.62	93.62	96.89	45.95	93.56	94.63

Table (3-12): The adsorption percentage of o-xylene with concentration 150 ppm at different temperatures

Temp.	adsorption efficiency %											
	283K			293K			313K			333K		
Time (min)	N.A.C	A.C	CNT	N.A.C	A.C	CNT	N.A.C	A.C	CNT	N.A.C	A.C	CNT
0	0.00	0.00	0.00	0.00	0.00	0.00	0.00	0.00	0.00	0.00	0.00	0.00
10	29.05	72.41	91.27	27.81	68.44	88.89	27.59	66.98	88.13	22.44	66.76	87.24
20	35.90	75.68	91.46	33.68	71.27	89.30	29.05	71.75	88.86	25.90	70.57	88.13
30	43.84	77.94	92.06	38.41	75.97	90.60	36.06	73.27	89.49	29.52	72.67	88.67
40	48.25	80.35	92.35	42.79	80.06	90.73	38.44	79.87	90.03	34.57	78.63	89.14
50	52.32	83.90	92.92	44.10	82.38	91.59	40.44	82.44	91.02	38.32	81.52	90.32
60	57.46	86.63	93.43	46.25	86.44	92.03	42.63	85.87	91.62	42.89	84.86	90.98
70	59.43	88.79	94.19	52.03	87.56	92.63	44.95	87.05	92.29	44.51	86.06	91.71
80	63.56	90.76	95.14	58.57	90.06	93.62	48.89	89.81	93.17	51.46	88.89	92.76
90	66.35	93.08	95.55	63.87	92.86	94.22	52.48	92.32	93.84	53.24	91.46	93.68
100	66.51	95.21	95.83	65.78	93.97	94.98	55.52	92.73	94.70	58.60	92.70	94.48
110	67.56	95.79	96.42	66.70	94.48	95.70	60.54	93.97	95.52	59.27	93.81	95.21
120	67.59	95.79	97.74	66.32	94.54	95.85	60.60	93.97	95.71	59.37	93.81	95.68

Table (3-13): The adsorption percentage of o-xylene with concentration 200 ppm at different temperatures

Temp.	adsorption efficiency %											
	283K			293K			313K			333K		
Time (min)	N.A.C	A.C	CNT	N.A.C	A.C	CNT	N.A.C	A.C	CNT	N.A.C	A.C	CNT
0	0.00	0.00	0.00	0.00	0.00	0.00	0.00	0.00	0.00	0.00	0.00	0.00
10	41.60	73.43	91.76	45.48	72.67	91.02	39.21	72.07	89.93	38.17	69.17	89.81
20	51.74	74.14	92.41	49.83	73.83	91.62	42.02	72.62	90.60	41.05	72.19	90.33
30	55.81	79.43	92.67	51.12	78.95	92.10	43.33	77.26	91.38	42.29	76.36	90.64
40	60.74	83.24	93.45	56.93	81.86	92.93	45.21	79.74	92.17	44.21	78.26	91.31
50	62.00	86.71	94.36	59.57	86.57	93.07	45.74	85.60	92.76	45.21	83.52	91.79
60	66.91	89.36	94.67	62.45	88.86	93.67	46.74	85.74	93.52	46.26	84.83	92.21
70	69.45	91.45	95.41	63.98	90.45	94.24	51.41	89.93	93.91	50.19	89.26	92.64
80	72.14	92.74	95.98	66.88	92.43	94.60	52.21	91.76	94.36	51.48	89.83	93.17
90	72.69	94.79	96.48	68.91	93.60	95.67	57.52	93.00	95.10	55.14	92.45	93.67
100	73.19	95.67	96.78	71.21	94.62	96.05	62.24	94.50	95.62	57.26	93.50	94.98
110	75.52	96.19	96.89	73.46	95.45	96.50	68.29	94.52	96.36	65.17	93.55	95.55
120	75.57	96.19	97.97	73.46	95.48	96.73	68.29	94.52	96.64	65.24	93.55	96.05

Table (3-14): The adsorption percentage of o-xylene with concentration 250 ppm at different temperatures

Temp. Time (min)	adsorption efficiency %											
	283K			293K			313K			333K		
	N.A.C	A.C	CNT	N.A.C	A.C	CNT	N.A.C	A.C	CNT	N.A.C	A.C	CNT
0	0.00	0.00	0.00	0.00	0.00	0.00	0.00	0.00	0.00	0.00	0.00	0.00
10	50.99	75.16	92.97	50.57	74.34	92.34	50.08	73.85	91.47	49.79	72.30	91.03
20	54.48	76.32	93.64	52.02	76.10	92.90	51.56	74.48	91.87	51.16	73.22	91.54
30	60.59	80.88	93.89	56.88	80.13	93.41	53.73	78.08	92.32	52.13	76.13	91.98
40	63.20	85.12	94.15	60.59	84.53	94.02	54.90	80.21	92.74	53.81	77.96	92.65
50	67.79	86.59	94.48	63.07	85.92	94.17	56.08	83.33	93.10	55.37	81.10	93.14
60	71.62	87.89	95.07	67.64	87.79	94.72	57.12	84.46	93.33	56.30	82.99	93.35
70	74.13	90.27	95.35	70.40	90.17	94.90	57.20	85.94	93.70	56.90	84.46	93.75
80	75.60	91.56	95.89	73.49	91.52	95.22	60.19	87.43	94.02	59.22	86.74	93.92
90	77.35	92.55	96.53	74.72	92.42	95.37	61.26	88.59	95.25	60.29	89.90	94.44
100	77.58	94.11	96.93	76.70	93.56	96.17	62.53	92.02	95.84	62.04	91.92	94.78
110	79.33	96.25	97.26	78.32	95.66	96.63	64.21	95.05	96.58	63.28	94.51	95.62
120	79.43	96.28	98.41	78.29	95.71	97.27	64.19	95.03	96.96	63.33	94.55	96.45

Table (3-15): The adsorption percentage of o-xylene with concentration 300 ppm at different temperatures

Temp. Time (min)	adsorption efficiency %											
	283K			293K			313K			333K		
	N.A.C	A.C	CNT	N.A.C	A.C	CNT	N.A.C	A.C	CNT	N.A.C	A.C	CNT
0	0.00	0.00	0.00	0.00	0.00	0.00	0.00	0.00	0.00	0.00	0.00	0.00
10	58.87	77.95	93.70	58.50	77.57	92.83	58.05	77.35	92.32	57.73	73.76	91.10
20	60.27	80.95	94.35	59.25	78.71	93.16	58.51	78.38	92.79	58.27	75.87	91.73
30	63.95	84.13	94.59	59.65	82.51	93.46	59.32	79.29	93.19	59.24	78.24	92.35
40	67.33	86.87	94.79	64.05	85.83	93.92	59.83	81.54	93.70	59.95	80.02	92.94
50	71.03	89.84	95.24	66.76	87.54	94.25	60.81	84.62	93.95	61.21	82.22	93.21
60	75.89	91.97	95.49	69.86	89.60	94.44	61.54	86.19	94.22	61.79	84.57	93.70
70	77.83	93.06	95.71	73.14	90.78	94.89	62.56	87.40	94.54	62.90	85.81	93.95
80	79.51	94.64	95.90	76.67	91.84	95.17	63.08	88.44	94.81	63.29	88.33	94.29
90	80.22	95.43	96.64	77.73	93.22	95.38	63.48	89.94	94.97	63.75	89.51	94.62
100	80.87	96.10	96.95	79.78	94.57	96.87	64.02	93.24	96.52	63.95	93.00	94.79
110	82.00	96.51	97.36	80.30	95.98	97.14	64.69	95.54	96.70	64.46	95.29	96.02
120	82.05	96.51	98.61	80.32	95.98	97.44	64.76	95.56	97.19	64.52	95.27	96.67

3.3.1.3. *Sulfide Removal*

This investigation is dealing with adsorption of sulfide ion from aqueous solution using non activated carbon, activated carbon and MWCNT at temperature of 298 K. Effects of adsorption time and solution volume (10, 25, 50 and 100) ml on removal of sulfide ion rate during treatment by N.A.C, A.C and MWCNT for sulfide concentration was performed in 90 min as shown in Table (3-16). The table indicates that sulfide adsorption onto carbon increases when increasing treatment time starting from (30 - 90) min and by decreasing solution volume. The percentages of sulfide ion removal by MWCNT, A.C, and N.A.C were 99.00 %, 88.14% and 80.16% respectively at solution volume of 10 ml (Table 3-17). The table showed that a new MWCNT high efficiency in all times and solution volumes for removal of sulfide ion compared to that of activated carbon and non-activated carbon.

Table (3-16): Sulfide concentration after treated with carbon

| Time (min) | Concentration after treatment , ppm | | | | | | | | | | | |
| | MWCNT | | | | A.C | | | | N.A.C | | | |
	10 ml	25 ml	50 ml	100 ml	10 ml	25 ml	50 ml	100 ml	10 ml	25 ml	50 ml	100 ml
0	1183.96	1183.96	1183.96	1183.96	1183.96	1183.96	1183.96	1183.96	1183.96	1183.96	1183.96	1183.96
30	101.13	134.6	170.50	247.02	223.27	282.67	297.33	346.02	287.47	294.83	307.52	395.96
60	30.57	64.16	96.95	156.72	196.76	232.87	244.95	275.61	253.34	273.30	302.38	382.83
90	11.79	29.30	45.04	110.94	140.46	188.64	225.16	240.85	234.84	253.34	282.67	354.88

Table (3-17): Sulfide removal efficiency percentage on carbon

| Time (min) | Removal efficiency % | | | | | | | | | | | |
| | MWCNT | | | | A.C | | | | N.A.C | | | |
	10 ml	25 ml	50 ml	100 ml	10 ml	25 ml	50 ml	100 ml	10 ml	25 ml	50 ml	100 ml
0	0.00	0.00	0.00	0.00	0.00	0.00	0.00	0.00	0.00	0.00	0.00	0.00
30	91.46	88.63	85.60	79.14	81.14	76.13	74.89	70.77	75.72	75.10	74.03	66.56
60	97.42	94.58	91.81	86.76	83.38	80.33	79.31	76.72	78.60	76.92	74.46	67.67
90	99.00	97.53	96.20	90.63	88.14	84.07	80.98	79.66	80.16	78.60	76.13	70.03

3.4. Thermodynamic Parameters

The ΔH^o and ΔS^o values were calculated from slope ($-\Delta H^o/R^*$) and intercept ($\Delta S^o/R^*$) of the linear plot, of ln K vs. 1/T as shown in Figs. (3-22) and (3-23) for benzene and o-xylene respectively. The corresponding values of thermodynamic parameters are presented in Tables (3-18) and (3-19) for benzene and o-xylene respectively. The negative values of ΔG^o indicated that the benzene and o-xylene adsorption processes are spontaneous and feasible and this is consistent with the fact that the interaction exothermic. The negative value of ΔH^o shown that adsorption process is exothermic in nature and all the observed values of ΔH^o are smaller than 40 kJ.mol^{-1} (Tables (3-18) and (3-19)). This means that the adsorption of benzene and o-xylene on carbon be physisorption process [209, 210]. The negative ΔS^o indicated that a decrease in randomness at the solid/liquid interface during adsorption of benzene and o-xylene on carbon. The values of equilibrium constants (K) decrease in general with a high temperature may be due to breaking bonds between adsorbate molecules and surface adsorbent causing the return of material adsorbed from the surface adsorbent to solution which is called desorption and thus decreases material adsorbed considerably and decreases K value accordingly. All values show that the adsorption is more favorable at lower temperature.
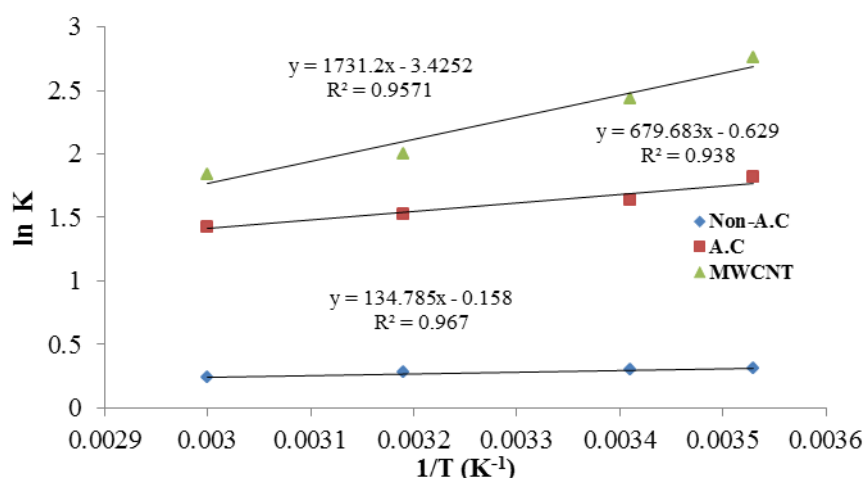
Fig. (3-22): The plot of ln K vs. 1/T for benzene with MWCNT, activated carbon and non-activated carbon
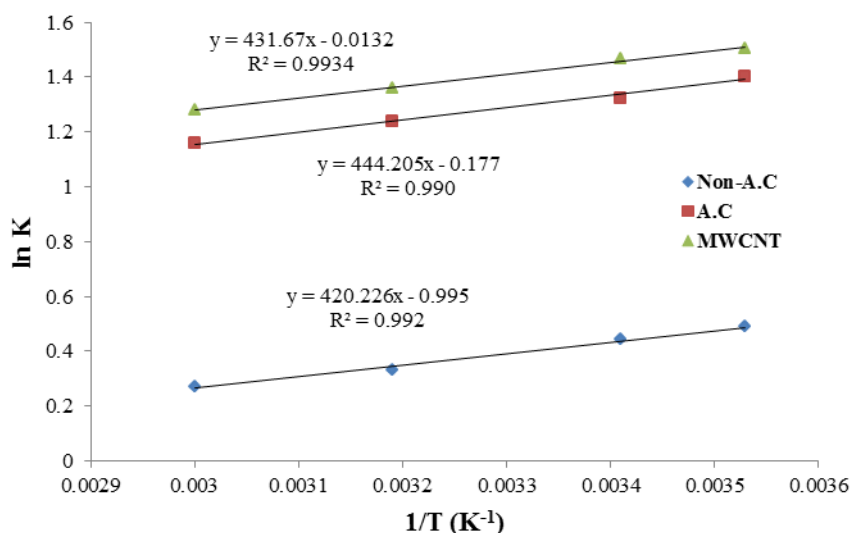
Fig. (3-23): The plot of ln K vs. 1/T for o-xylene with MWCNT, activated carbon and non-activated carbon

Table (3-18): Thermodynamic functions of benzene adsorption process in Fig.(3-22)

Samples	Initial Conc.(ppm)	T (K)	K	ΔH^o kJ.mol^{-1}	ΔS^o J.mol^{-1}.k^{-1}	ΔG^o kJ.mol^{-1}
MWCNT	200	283	572.066	-33.148	-64.343	-14.939
MWCNT	200	293	270.396	-33.148	-66.577	-13.641
MWCNT	200	313	99.770	-33.148	-67.636	-11.978
MWCNT	200	333	69.497	-33.148	-64.282	-11.742
A.C	200	283	65.161	-13.014	-11.261	-9.827
A.C	200	293	43.372	-13.014	-13.075	-9.183
A.C	200	313	33.680	-13.014	-12.339	-9.152
A.C	200	333	26.830	-13.014	-11.733	-9.107
N.A.C	200	283	2.065	-2.580	-3.088	-1.706
N.A.C	200	293	2.002	-2.580	-3.037	-1.690
N.A.C	200	313	1.906	-2.580	-2.881	-1.678
N.A.C	200	333	1.744	-2.580	-3.123	-1.540

Table (3-19): Thermodynamic functions of o-xylene adsorption process in Fig. (3-23)

Samples	Initial Conc.(ppm)	T (K)	K	ΔH^o kJ.mol^{-1}	ΔS^o J.mol^{-1}.k^{-1}	ΔG^o kJ.mol^{-1}
MWCNT	200	283	31.949	-8.265	-0.403	-8.151
MWCNT	200	293	29.534	-8.265	-0.061	-8.247
MWCNT	200	313	22.803	-8.265	-0.409	-8.137
MWCNT	200	333	19.192	-8.265	-0.255	-8.180
A.C	200	283	25.250	-8.505	-3.208	-7.597
A.C	200	293	21.104	-8.505	-3.676	-7.428
A.C	200	313	17.261	-8.505	-3.492	-7.412
A.C	200	333	14.450	-8.505	-3.336	-7.394
N.A.C	200	283	3.094	-8.046	-19.042	-2.657
N.A.C	200	293	2.767	-8.046	-19.000	-2.479
N.A.C	200	313	2.153	-8.046	-19.329	-1.996
N.A.C	200	333	1.877	-8.046	-18.928	-1.743

3.5. Adsorption Kinetics

Adsorption kinetic models can be useful to determine the mechanism of adsorption and the efficiency of the adsorbents for the removal of pollutants [207, 211]. In this study, the adsorption data of benzene and o-xylene by MWCNT, activated carbon and non-activated carbon were fitted through kinetic model of pseudo-first order kinetic as shown in equation (2-5).

Where q_e (mg/g) is the amount of benzene and o-xylene at equilibrium time while q_t (mg/g) is the amount of benzene or o-xylene at any time (t) and k (min^{-1}) is the pseudo-first order rate constant. Values of k and q_e were determined from the slope (- k) and intercept (lnq_e) of the linear plot of ln (q_e-q_t) against time, as shown in Figs. (3-24) and (3-25) respectively.
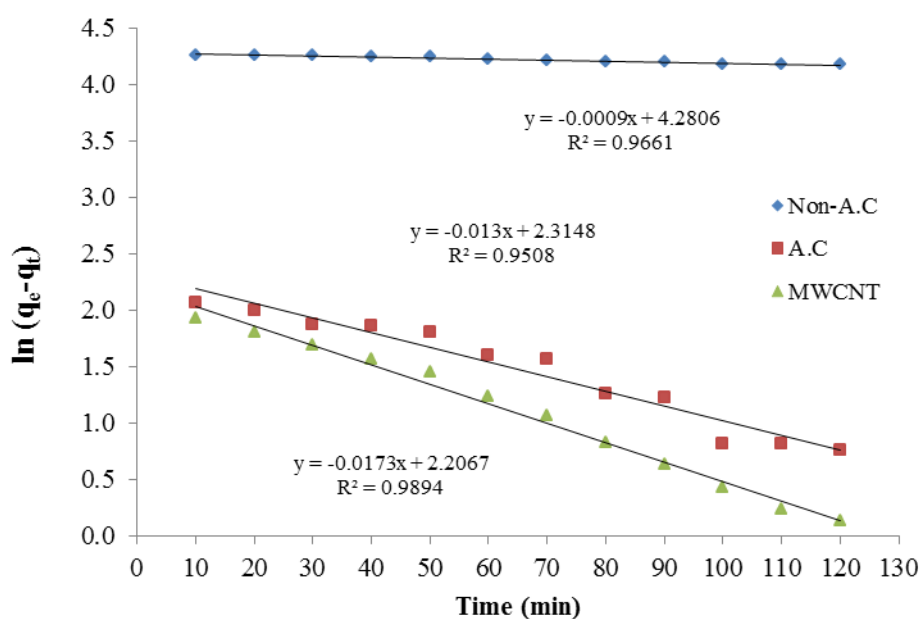
Fig. (3-24): Relationship between ln (q_e-q_t) vs. Time for adsorption of benzene solutions at temperature of 283K and conc. (200 ppm) on MWCNT, activated carbon and non-activated carbon
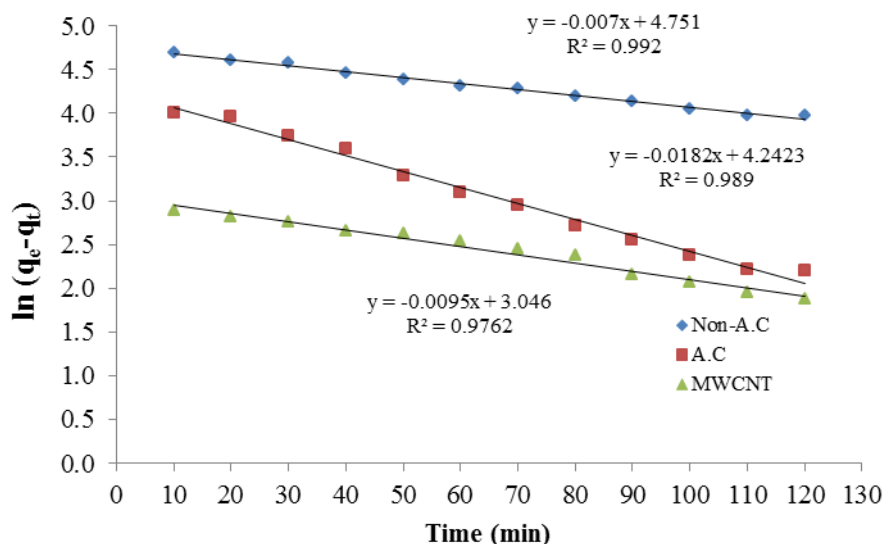
Fig. (3-25): Relationship between ln (q_e-q_t) vs. Time for adsorption of o-xylene solutions at temperature of 283K and conc. (200 ppm) on MWCNT, activated carbon and non-activated carbon

3.6. Removal of Organic Pollutant by Ultrasonic

Sonolysis is the breaking of chemical bonds or formation of radicals using ultrasound. In recent years, considerable interest has been shown in the application of ultrasound as an advanced oxidation process for the treatment of hazardous contaminants in water. Sonochemistry has been demonstrated as a promising method for the destruction of aqueous pollutants [212]. The action of ultrasound allows for the creation of micro bubbles in water at high temperature and pressure, leading to localize transient supercritical conditions. This leads to the production of active radicals (H$^.$ and $^.$OH) that take part in the degradation of organic matter.

In this study, sonodegradation of benzene and o-xylene were applied for different periods of time; 0, 10, 20, 30, 40, 50, 60, 70, 80, 90, 100, 110, 120, 130, 140 and 150 min. Also, sonodegradation experiments of benzene and o-xylene were carried out in the presence of various concentrations to observe if there was any effect on the degradation rates of benzene and o-xylene. Sonodegradation were performed at initial concentrations of

100 ppm and 200 ppm, electric power, liquid volume and temperatures at (283, 293, 313 and 333) K.

3.6.1. *Benzene Removal*

3.6.1.1. *Effect of Initial Concentration*

Experiments were conducted at various times to see if there was any synergistic effect on the degradation of benzene. Increasing the concentration from 100 ppm to 200 ppm showed a decrease in degradation of benzene. Experiments showed that about 100% and 97.94% degradation of benzene occurred after 150 min at 283 K respectively with sonochemical reactor. But only 89.48% and 78.62% degradation of benzene was observed within 10 min, as shown in Table (3-20).Therefore, results obtained from the sonochemical degradation of benzene at various concentrations indicated that removal rates were found to be decreased with increasing of benzene concentration.

Table (3-20): The degradation of benzene by ultrasonic percentage with concentrations of (100, 200) ppm at different temperatures

Time (min)	% of degradation at temperature (K)							
	283K		293K		313K		333K	
	100 ppm	200 ppm	100 ppm	200 ppm	100 ppm	200 ppm	100 ppm	200 ppm
0	0.00	0.00	0.00	0.00	0.00	0.00	0.00	0.00
10	89.48	78.62	81.24	76.48	81.00	70.43	74.00	69.12
20	90.50	83.98	83.71	81.48	83.52	76.98	76.76	71.98
30	91.43	88.38	86.05	84.50	85.86	78.76	78.33	74.81
40	93.05	90.62	87.33	86.21	86.62	82.88	78.76	76.71
50	93.47	91.67	89.10	88.29	88.14	85.64	79.38	78.26
60	93.67	92.41	89.68	89.31	89.19	87.29	79.91	79.48
70	93.95	94.74	91.48	90.45	90.57	88.74	80.38	80.10
80	94.49	96.10	93.16	91.43	91.64	91.05	84.48	81.88
90	95.05	96.63	94.33	93.76	92.28	92.76	86.94	87.50
100	95.54	96.77	95.37	95.08	93.65	93.12	89.82	89.61
110	96.42	96.98	96.23	96.60	94.49	93.77	92.28	91.44
120	97.47	97.30	97.35	96.94	95.28	95.59	93.86	92.79
130	98.84	97.49	98.09	97.24	96.28	96.59	94.65	94.15
140	99.86	97.78	99.79	97.51	97.19	97.07	95.38	95.30
150	100.00	97.94	100.00	97.79	98.02	97.31	96.63	96.02

3.6.1.2. *Effect of Sonication Time*

In order to observe the effect of sonication time on the benzene degradation rate during treatment, sonodegradation (sonication time) for aqueous benzene concentrations were performed in 150 min. As clearly seen, by increasing of the sonication time, considerable levels of benzene degradation can be expected after 150 min. It was observed that the degradation efficiency of acoustic frequency was increased when sonication time increased, as shown in Table (3-20). Therefore, the statistical study indicated that when sonication time is increased, there is an increase in removal percentage. This effect is due to the increase in the exposure time between the benzene solution and the acoustic cavitation process as the time of sonication is increased [213, 214].

3.6.1.3. *Effect of Temperature*

Increasing the temperature is causing a decrease in degradation ratios of benzene (Table 3-20). The reason is possibly coming from the decrease of the surface tension and viscosity of the solution, so that the generations of bubbles become easier. However, the increase in solution temperature results in a dramatic increase of the vapor pressure of the liquid, which gives a higher vapor content of the cavitating bubble. In general, increased temperature is likely to facilitate bubble formation due to an increase of the equilibrium vapor pressure. However, the sonochemical effect of such bubbles may be reduced. During the bubble growth, complete collapse may not occur and the bubble may oscillate in the applied field if some gas or vapor has diffused into the bubble [215-218].

The results showed that pH values have been affected through degradation of benzene. The pH values during the sonodegradation are shown in Table (3-21). These values indicated that a surfactant will accumulate on a surface independent of whether it is protonated or deprotonated, the effect of pH value on degradation [219]. Also, this conclusion was confirmed by other researchers [183] who predicted that the

pH value was a key parameter affected by the sonodegradation of surfactant.

Table (3-21): The effect of temperatures on pH values for degradation of benzene by sonication

Time (min)	Temp.(K)	pH	
		100 ppm	200 ppm
0	Standard	6.33	6.21
150	283	6.90	5.19
150	293	6.84	5.34
150	313	6.72	5.50
150	333	5.16	5.67

3.6.1.4. *Proposed Mechanism of Benzene Sonolysis*

The sonolytic benzene is involved in the degradation pathways and the primary degradation products of phenol. The experimental results have showed that the oxidation reaction of hydroxyl radicals with phenol is the most important among three main sonochemical degradations. The reaction of phenol with OH radicals leads to the formation of dihydroxyl cyclohexadienyl radicals as shown in equation (1) (sketch A). In the presence of oxygen, subsequent reaction of the dihydroxyl cyclohexadienyl radicals leads to the formation of peroxyl radicals by the addition of molecular oxygen as indicated by equation (2) (sketch A). Peroxyl radicals are known to form hydroquinone and catechol after eliminating superoxide radicals and rearranging the aromatic system [220]. These compounds further are degraded into biodegradable products, such as carboxylic acids, which is finally complete mineralized into CO_2 and H_2O [221].
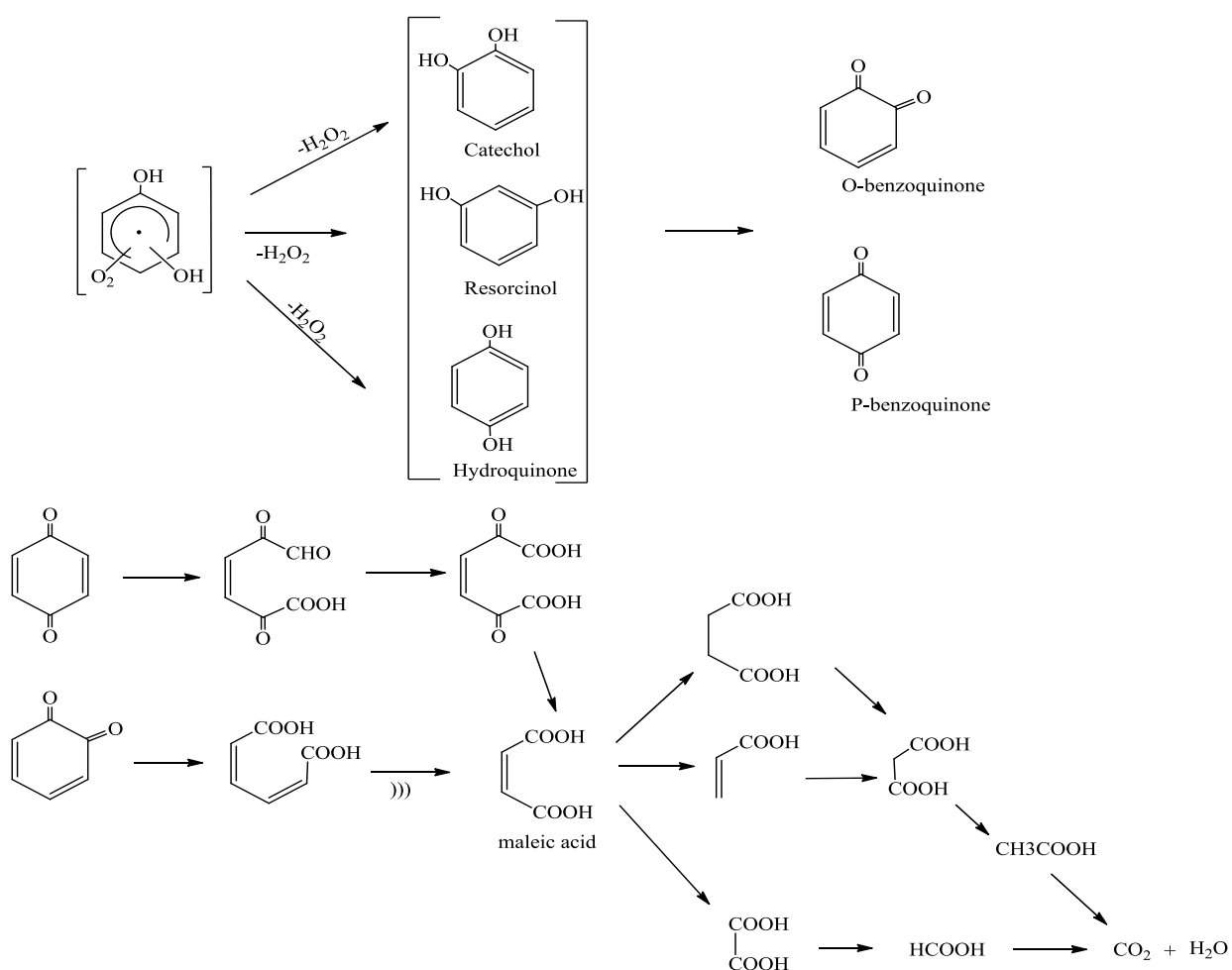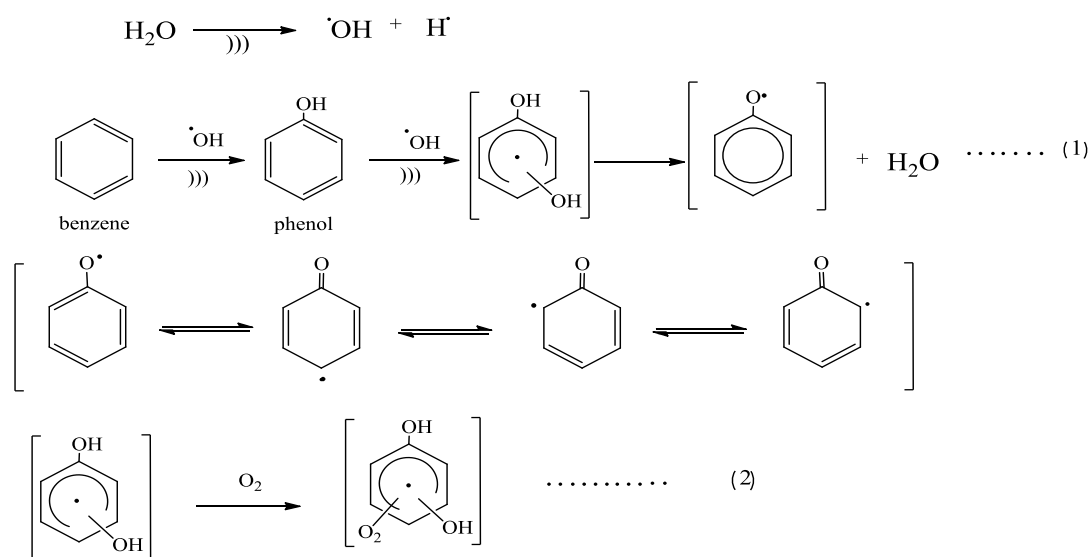
Sketch (A): Proposed Mechanism of Benzene sonolysis

Pyrolysis of benzene inside the cavities formed in the ultrasonic field has also given a minor contribution, because acetylene, which is a product of sonochemical destruction of volatile aromatic compounds, was detected in a low yield [222].

3.6.2. *O-xylene Removal*

3.6.2.1 *Effect of Initial Concentration*

The effect of concentration on o-xylene degradation by ultrasonic experiments was conducted in various times to see if there was any synergistic. Increasing the concentration from 100 ppm to 200 ppm showed a decrease in degradation of o-xylene. Experiments showed that about 97.88% and 95.52% degradation of o-xylene occurred after 150 min respectively at 283 K with sonochemical reactor. But only 86.43% and 68.39% degradation of o-xylene was observed within 10 min, as shown in Table (3-22). Therefore, results obtained from the sonochemical degradation of o-xylene at various concentrations indicated that removal rates were found to be decreased with increasing of o-xylene concentration.

Table (3-22): The degradation of o-xylene by ultrasonic percentage with concentrations of (100, 200) ppm at different temperatures

Time (min)	% of degradation at temperature (K)							
	283K		293K		313K		333K	
	100 ppm	200 ppm	100 ppm	200 ppm	100 ppm	200 ppm	100 ppm	200 ppm
0	0.00	0.00	0.00	0.00	0.00	0.00	0.00	0.00
10	86.43	68.39	76.26	63.77	70.75	59.32	61.01	54.78
20	89.05	76.35	78.47	70.33	73.89	64.49	65.75	57.07
30	89.57	82.45	79.82	71.78	77.79	67.67	69.06	59.57
40	90.83	85.29	82.62	77.62	80.67	73.43	72.62	61.69
50	91.92	88.30	85.33	80.55	82.11	76.27	75.75	67.54
60	92.59	89.70	87.36	85.33	84.48	82.33	77.11	74.02
70	92.98	92.91	89.82	87.67	87.36	84.87	79.74	78.00
80	93.54	93.43	91.81	90.55	90.08	86.86	82.96	81.22
90	93.98	93.95	92.19	93.55	91.99	88.81	86.33	86.02
100	94.49	94.21	93.52	94.00	92.99	91.78	86.91	86.88
110	94.88	94.50	93.95	94.17	93.78	93.52	87.57	87.55
120	95.48	94.79	94.78	94.38	94.00	93.81	87.91	88.74
130	95.99	95.17	95.30	94.69	94.15	93.91	88.33	89.19
140	96.39	95.36	95.92	94.81	94.39	94.07	89.71	89.62
150	97.88	95.52	96.53	94.98	94.91	94.29	93.76	93.05

3.6.2.2. *Effect of Sonication Time*

The effect of sonication time on removal of o-xylene by ultrasonic during treatment, sonodegradation (sonication time) for aqueous o-xylene concentrations was performed in 150 min. As clearly seen, by increasing of the sonication time, considerable levels of o-xylene degradation can be expected after150 min. It was observed that the degradation efficiency of acoustic frequency was increased when sonication time increased, as shown in Table (3-22). Therefore, the statistical study indicated that when sonication time is increased, there is an increasing in removal percentage. This effect is due to the increase in the exposure time between the o-xylene solution and the acoustic cavitation process as the time of sonication is increased [213, 214].

3.6.2.3. *Effect of Temperature*

The effect of temperature on o-xylene degradation by ultrasonic was investigated in the temperatures of (283, 293, 313 and 333) K. The results are presented in Table (3-22) showed that increasing the temperature causing a decrease in degradation ratios of o-xylene. The reason is possibly coming from the decrease of the surface tension and viscosity of the solution, so that the generations of bubbles become easier. However, the increase in solution temperature results in a dramatic increase of the vapor pressure of the liquid, which gives a higher vapor content of the cavitating bubble. In general, increased temperatures are likely to facilitate bubble formation due to an increase of the equilibrium vapor pressure. However, the sonochemical effect of such bubbles may be reduced. During the bubble growth, complete collapse may not occur and the bubble may oscillate in the applied field if some gas or vapor has diffused into the bubble [215-218].

Notes from the Tables (3-21) and (3-22) that the percentage of degradation in the o-xylene is less in compared with benzene non substituent due to the position and the type and the nature of the substituent

group in addition to disability steric factor any size the substituent group has great effect on the degradation ratio which hampers the process of degradation in the o-xylene substituent methyl group in the ortho position compared with benzene.

The results showed that pH values have been affected through degradation of o-xylene. The pH values during the sonodegradation are shown in Table (3-23). These values indicated that a surfactant will accumulate on a surface independent of whether it is protonated or deprotonated, the effect of pH value on degradation [219]. Also, this conclusion was confirmed by other researchers [183] who predicted that the pH value was a key parameter affected by the sonodegradation of surfactant.

Table (3-23): The effect of temperatures on pH values for degradation of o-xylene by sonication

Time (min)	Temp.(K)	pH	
		100 ppm	200 ppm
0	Standard	5.694	5.512
150	283	6.690	6.443
150	293	5.967	6.367
150	313	5.715	6.251
150	333	5.511	6.126

3.6.2.4. *Proposed Mechanism of O-xylene Sonolysis*

From the detailed analysis of the intermediate product, we propose that the reaction of o-xylene with the hydroxyl radical might have led to the formation of benzene, methyl benzene, o-methyl phenol, ortho dioxybenzene, benzoquinone and so on as the primary products. As the sonolysis went on, some carboxylic acids such as formic, oxalic and malonic acids and so on were formed. In the end, all of the carboxylic acids were decomposed into inorganic carbon, which might exist as bicarbonate or carbon dioxide. These results were in agreement with others [223, 224]. The variation of

intermediate products suggests that the degradation of o-xylene proceeded as shown in (Sketch B).

$$H_2O \xrightarrow{)))} {}^\bullet OH + H^\bullet$$
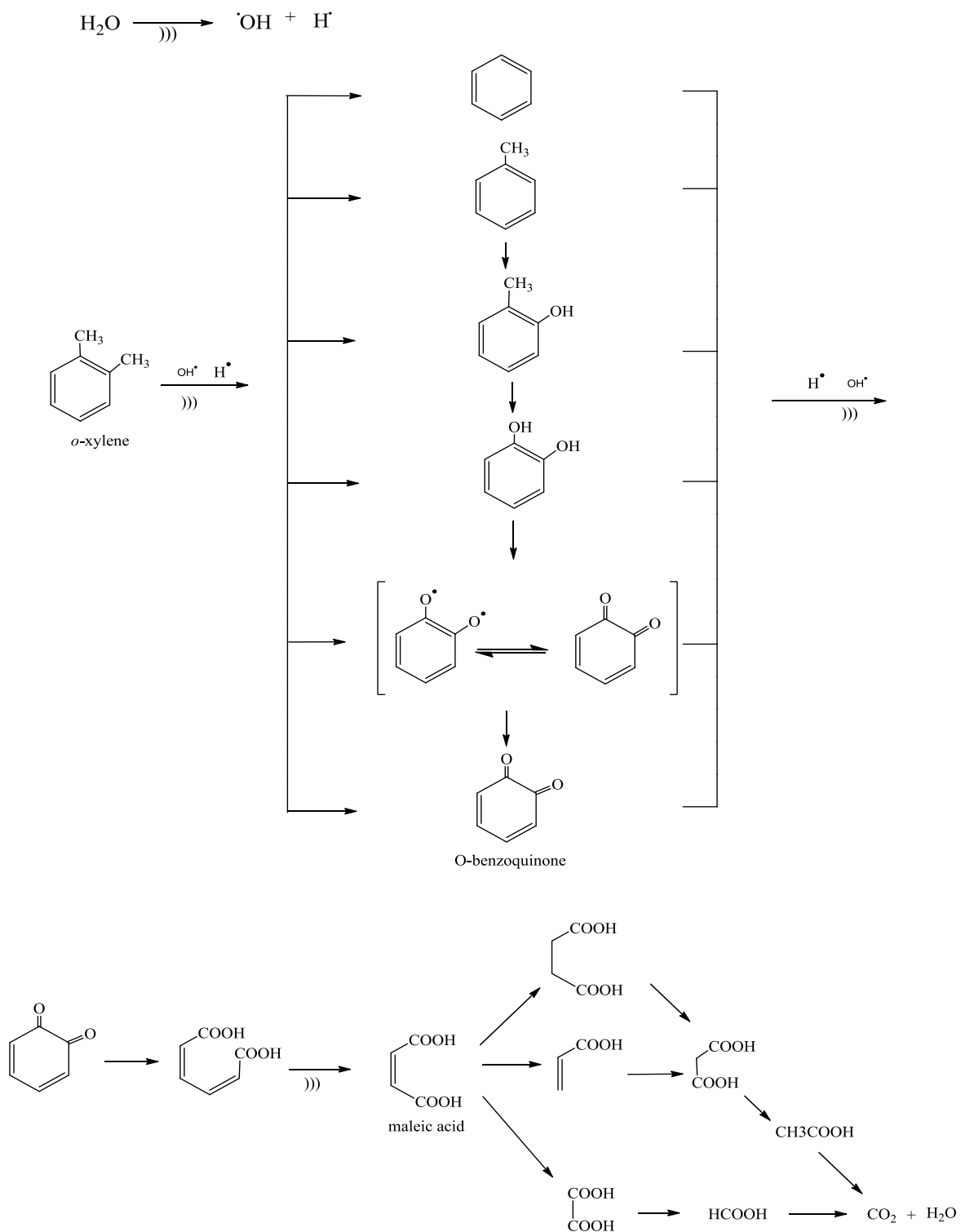
Sketch (B): Proposed Mechanism of O-xylene sonolysis

3.7. Thermodynamic Parameters

The thermodynamic parameters (ΔG^o, ΔH^o and $\Delta S^`$) for the degradation processes are determined by using equations (2-6) and (2-7) as mentioned previously [201]. The ΔH^o and ΔS^o values were calculated from slope and intercept of the linear plot, of ln K vs. 1/T as shown in Figs. (3-26) and (3-27) for benzene and o-xylene respectively. The corresponding values of thermodynamic parameters are presented in Tables (3-24) and (3-25) for benzene and o-xylene respectively. The negative values of ΔG^o indicate that the benzene and o-xylene degradation process are spontaneous and feasible, while the negative value of ΔH^o shown an exothermic degradation process in nature and the observed values ΔH^o is smaller than 40 kJ.mol^{-1} (Tables (3-24) and (3-25)), this means that the degradation of benzene and o-xylene be physisorption process [209,210]. The positive values of ΔS^o may indicate an increase in degree of freedom during degradation of benzene and o-xylene and the values of the equilibrium constants (K) decreased with increasing temperature. All values show that the degradation is more favorable at lower temperature.
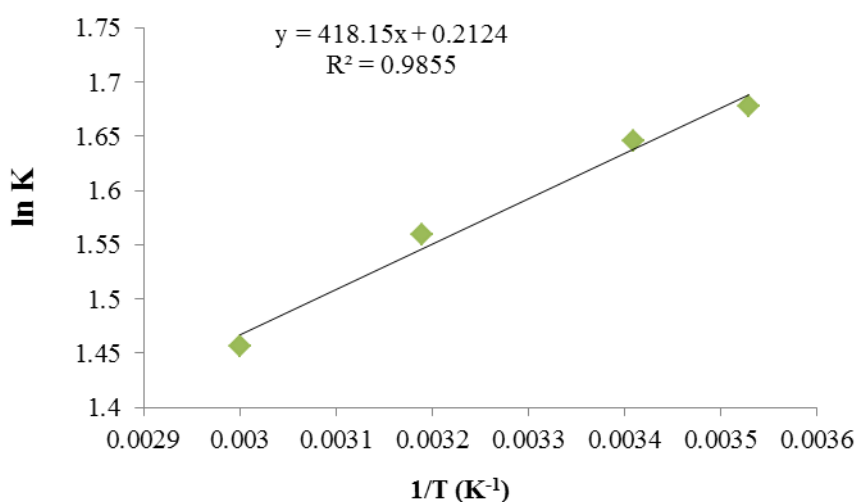
Fig. (3-26): The plot of ln K vs. 1/T for degradation of benzene by ultrasonic technique
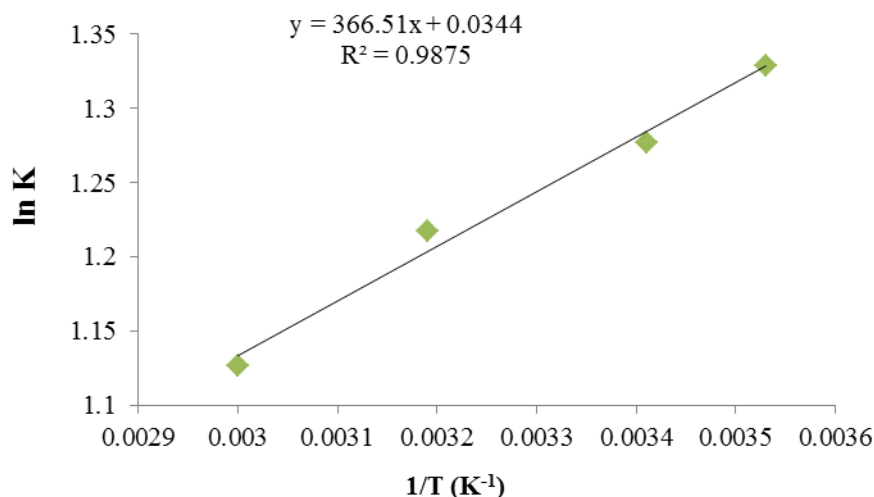
Fig. (3-26): The plot of ln K vs. 1/T for degradation of o-xylene by ultrasonic technique

Table (3-24): Thermodynamic functions of the benzene degradation process using ultrasonic at the concentration of 200 ppm

T(K)	K	ΔH^0 kJ.mol^{-1}	ΔS^0 J.mol^{-1}.k^{-1}	ΔG^0 kJ.mol^{-1}
283	47.591		3.827	-9.089
293	44.259	-8.006	4.184	-9.232
313	36.230		4.268	-9.342
333	28.656		3.853	-9.289

Table (3-25): Thermodynamic functions of the o-xylene degradation process using ultrasonic at the concentration of 200 ppm

T(K)	K	ΔH^0 kJ.mol^{-1}	ΔS^0 J.mol^{-1}.k^{-1}	ΔG^0 kJ.mol^{-1}
283	21.341		0.647	-7.201
293	18.904	-7.018	0.485	-7.160
313	16.499		0.885	-7.295
333	13.384		0.492	-7.182

3.8. Degradation Kinetics

Kinetic model studies on the sonocatalytic degradation rate of the benzene and o-xylene are useful to determine the mechanism of degradation and the efficiency of the removal of pollutants. The degradation data of benzene and o-xylene by ultrasonic were fitted through kinetic model including pseudo-first order kinetic as shown in Figs. (3-28)

and (3-29) for benzene and o-xylene respectively and as shown in equation (2-5) [207, 211].

(A)   **(B)**
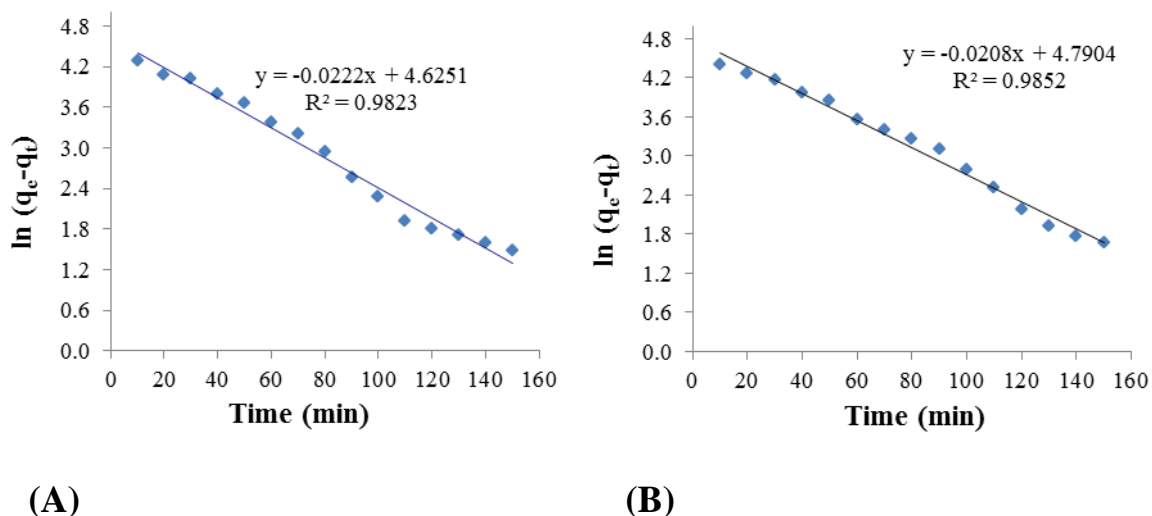
Fig. (3-28) Linear relationship between ln $(q_e - q_t)$ vs. Time for degradation of benzene solutions at temperatures **(A)** 293 K and **(B)** 313 K by conc. (200 ppm) using ultrasonic technique

(A)   **(B)**
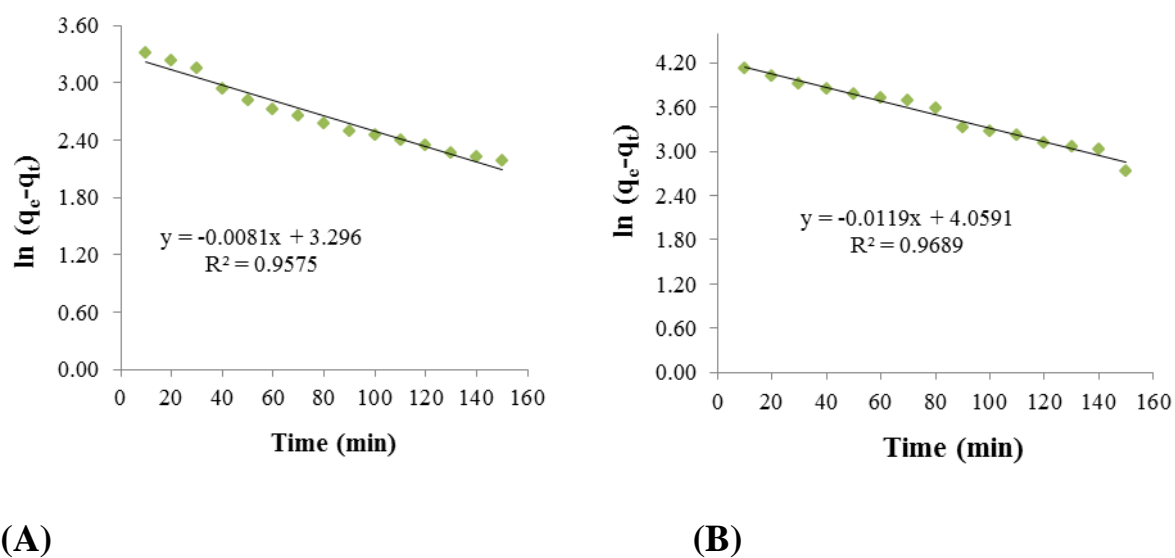
Fig. (3-29) Linear relationship between ln $(q_e - q_t)$ vs. Time for degradation of o-xylene solutions at temperatures **(A)** 283K and **(B)** 333K by conc. (200 ppm) using ultrasonic technique

Conclusions & Recommendations

I. Conclusions

Depending on the procedural steps followed and the discussion conducted it can be concluded that:

1. Multi-walled carbon nanotubes were prepared succefully with high surface area and high capacity for adsorption processes.

2. The adsorption capacity of pollutants increases with the decreasing of flow rate, particle size and increasing concentration.

3. The removal of benzene and o-xylene decrease with increasing solution temperature, which indicates that the adsorption of benzene and o-xylene onto carbon is exothermic process.

4. The kinetic results showed that benzene and o-xylene adsorptions onto carbon can be described by pseudo-first-order model.

5. A new circulating system showed high efficiency by adsorption treatments.

6. The adsorption process on carbon powder is fitting the Freundlich and Temkin isotherm models with very high correlation coefficients.

7. Fuel oil waste power plant used in this work as a new source for preparation of MWCNT by ultrasonic technique for the first time has high adsorption capacity. Therefore, it can be used in commercial production of MWCNT.

8. The advantages of the invention feature the followings:

   A. It does not need catalysts.

   B. It does not need high techniques but uses a simple ultrasonic technique.

   C. It uses by-products coming from fuel oil power plant.

   D. It follows the rules of environment cleaning.

9. MWCNT powder as an absorbent to an aqueous samples reduces benzene and o-xylene concentration dramatically with value of 100%.

Therefore, a complete reduction in concentrations of benzene and o-xylene respectively were obtained.

10. Results obtained from this study demonstrate that sonochemical reactor is capable to some degree of benzene and o-xylene degradation in waste waters produced by chemical processes.

11. The sonodegradation of benzene and o-xylene follows a pseudo-first order kinetic models. The degradation rate of benzene and o-xylene increased with decreasing the temperature and initial concentration.

II. Recommendations

In the light of the present study, the following recommendations can be helpful for further studies:

1. The MWCNT produced should be tested against different contaminants from industrial waste water, like dyes, polymers, metal ions and other organic compounds.

2. Emphasizing the fact that the modification of MWCNT surface has been succeeded, and this may pave the way for researchers to focus their attention toward modifying surfaces for different application, like biosensor for DNA or protein detection.

3. Using low cost catalysts, like titanium oxide TiO_2 in removal of many industrial contaminants (organic or inorganic), and to increase the efficiency of removal by irradiation using short or medium waves as well.

4. Sonochemical reactors alone may not be useful for reducing completely complex waste waters of high surfactant load. Hence, effectiveness may improve coupling acoustical reactors with other treatment processes including ozone, UV, chlorination and H_2O_2.

References

1. Abbas, A., Tayyebeh, M. and Ziba, K., "The effect of acid treatment of carbon cloth on the adsorption of nitrite and nitrate ions", *J. Hazardous Materials*, **144**, 427-431 (2007).

2. Rezaee, A., Godini, H., Dehestani, S. and Khavanin, A., "Application of impregnated almond shell activated carbon by zinc and zinc sulfate for nitrate removal from water", *Iran. J. Health. Sci. Eng.*, **5**, 125-130 (2008).

3. Emighaus, G., "Manual on Hydrocarbon Analysis", 6th Edition. A. W. Drews (Editor). American Society for Testing and Materials, West Conshohocken, PA. Chapter 3, p. 20 (1998).

4. Warne, T.M., "Manual on Hydrocarbon Analysis", 6th Edition. A.W. Drews (Editor). American Society for Testing and Materials, West Conshohocken, PA. Chapter 3, p. 33 (1998).

5. Charlot, J. C. and Claus, G., "Modern Petroleum Technology", Volume 2: Downstream. A.G. Lucas (Editor). John Wiley & Sons, New York. Chapter 21, p. 24 (2000).

6. Heinrich, H. and Duee, D., "Modern Petroleum Technology", Volume 2: Downstream. A.G. Lucas (Editor). John Wiley & Sons, New York. Chapter 10, p. 11 (2000).

7. Tran, T.V., Jae, H.L., Fanzhong, M., Gyung, R.K., IK, S.A. and Chang, H.L., "Hydrocracking of petroleum vacuum residue with activated carbon and metal additives in a supercritical m-xylene solvent", *Fuel*, **103**, 553-561 (2013)

8. Suntud, S., Soydoa, V. and Waree, C., "Removal of organic matters and phenol compounds from the waste water by using granular activated carbon-sequence batch reactor system", *Journal science Technology*, **4** (1), 38-48 (1999).

9. Mitra, S. and Roy, P., "BTEX: a serious ground-water contaminant", *Res. J. Environ. Sci.*, **5**, 394-398 (2011).

10. Su, F., Lu, C. and Hu, S., "Adsorption of benzene, toluene, ethyl benzene and p-xylene by NaOCl-oxidized carbon nanotubes", *Colloids Surf. A*, **353**, 83 -91 (2010).

11. Chenju, L. and Yan-Jyun, C.," Evaluation of activated carbon for remediating benzene contamination: Adsorption and oxidative regeneration ", *Journal of Hazardous Materials*, **182**, 544-551 (2010).

12. Yao, X., Liu, J., Gong, G., Jiang, Y. and Xie, Q.," Preparation and modification of activated carbon for benzene adsorption by steam activation in the presence of KOH", *International Journal of Mining Science and Technology*, **xxx**, xxx-xxx (2013).

13. World health organization, guidelines for drinking-water quality: world health organization, distribution and sales, Geneva 27, CH-1211 Switzerland, (2004).

14. Houghton, S. and Hall, S., "Simultaneous high throughput and quantitative analysis of MTBE and BTEX by P&T-GCMS using a Precept (R) autosampler", *Mineral. Mag*., **69,** 677-686 (2005).

15. Dan, W., Xie, Q., Yazhi, Z. and Shuo, C., "Removal of p-xylene from an air stream in a hybrid biofilter", *Journal of Hazardous Materials*, **136**, 288-295 (2006).

16. Alberici, R.M., Zampronio, C.G., Poppi, R.J. and Eberlin, M.N., "Water solubilization of ethanol and BTEX from gasoline: on-line monitoring by membrane introduction mass spectrometry", *The Analyst*, **127**, 230-242 (2002).

17. Asghar, M. D. and Mahmoud, K., "Adsorption of xylene isomers on Na-BETA Zeolite: Equilibrium in batch adsorber", *Microporous and Mesoporous Materials*, **172**, 136-140 (2013).

18. Chiou, C.T., Schmedding, D.W. and Manes, M., "Partitioning of organic-compounds in octanol-water systems", *Environmental Science and Technology*, **16**, 4-10 (1982).

19. Carpenter A.B. and *et. al.*, "Influence of mineralogy and microorganisms on iron and sulfide concentrations in groundwater. Springfield", VA, US National Technical Information Service, 38 (NTIS PB 205773), (1971).

20. Agency for Toxic Substances and Disease Registry (ATSDR). "Toxicological profile for hydrogen sulfide (Draft for Public Comment). Atlanta, GA: U.S.", Department of Health and Human Services, Public Health Service. Chapter 2, p.1, (2004).

21. Legator, M. S. and *et. al.*, "Health effects from chronic low-level exposure to hydrogen sulfide", *Archives of Environmental Health*, **56** (2), 123-131 (2001).

22. Knight, L. D. and Erin Presnell, S. M., "Death by Sewer Gas: Case Report of a Double Fatality and Review of the Literature" The American Journal of Forensic Medicine and Pathology, p.183 (2005).

23. Camacho-Munoz, D., Martin, J., Santos, J. L., Aparicio, I., and Alonso, E., "Effectiveness of conventional and low-cost wastewater treatments in the removal of pharmaceutically active compounds", *Water, Air & Soil Pollution*, **223**(5), 2611- 2621 (2012).

24. Shourian, M., Noghabi, K., Zahiri, H., Bagheri, T., Karaballaei, G., Mollaei, M., Rad, I., Ahadi, S., Raheb, J. and Abbasi, H.," Efficient phenol degradation by a newly characterized pseudomonas SP.SA01 isolated from pharmaceutical wastewaters", *Desalination*, **246**, 577-594 (2009).

25. El-Naas, M., Al-Zuhair, S. and Makhlouf, S., "Bath degradation of phenol in a spouted bed bioreactor system" , *J. Ind. Eng. Chem.*, **16**, 267-272 (2010).

26. Wang, Y., Gu, B. and Xu, W., "Electro-catalytic degradation of phenol on several metal-oxide anodes", *Hazard. Mater.*, **162**, 1159-1164 (2009).

27. Agrios, A., Gray, K. and Weitz, E.,"Photo catalytic transformation of 2, 4, 5-trichlorophenol on TiO_2 under sub-band-gap illumination", *Langmuir*, **19**, 1402-1409 (2003).

28. Pandit, A.B., Gogate, P.R. and Mujumdar, S.,"Ultrasonic degradation of 2, 4, 6 trichlorophenol in presence of TiO_2 catalyst", *Ultrason. Sonochem.*, **8**, 227-231 (2001).

29. Buchanan, I.D. and Micell, J.A.,"Peroxidase catalyzed removal of aqueous phenol", *Bio technol. Bio. eng.*, **54**, 251-261 (1997).

30. Busca, G., Berardinelli, S., Resini, C. and Arrighi, L.,"Technologies for the removal of phenol from fluid streams: A short review of recent developments", *J. Hazard. Master.*, **160**, 265-288 (2008).

31. Yang, C., Qian, Y. and Zhang, L., "Solvent extraction process development and on-site trial-plant for phenol removal from industrial coal-gasification wastewater", *Chem. Eng. J.*, **117**,179-185 (2006).

32. Mohd Din, A., Hameed, B.H. and Ahmad, A.L.," Batch adsorption of phenol onto physic-chemical-activated coconut shell", *J. Hazard. Master.*, **161**, 1522-1529 (2009).

33. Waid, O. and Hossam, I., "Removal of Pb^{+2} ions from aqueous solution by adsorption on kaolinite clay" , *American Journal of Applied Sciences*, **4** (7), 502-507 (2007) .

34. QU, J., "Research progress of novel adsorption processes in water purification: A review", *J. Environmental Sciences*, **20**, 1-13 (2008).

35. Al-Khalid, T. T., Haimour, N. M., Sayed, S. A. and Akash, B. A., "Activation of olive-seed waste residue using CO_2 in a fluidized-bed reactor", *Fuel Processing Technology*, **57**, 55-64 (1998).

36. El-Hamouz, A., Hilal, H. S., Nassar, N. and Mardawi, Z., "Solid olive waste in environmental cleanup: Oil recovery and carbon production for water purification", *J. Environmental Management*, **84**, 83-92 (2007).

37. Reha, Y., Hanife, A., Nilgun, K. and Eda, C., "Influence of preparation conditions on porous structures of olive stone activated by H_3PO_4", *Fuel Processing Technology*, **91**, 80-87 (2010).

38. Guojun, Y., Zhenyu, L., Qingya, L. and Weize, W., "The role of different properties of activated carbon in CO_2 adsorption", *Chemical Engineering Journal*, **230**, 133-140 (2013).

39. Karthikeyan, S., Sivakumar, P. and Palanisamy, P., "Novel activated carbons from agricultural wastes and their characterization", *E-Journal of Chemistry*, **5**, 409-426 (2008).

40. Cheremishinoff, N. P. and Moressi, A. C., "Carbon adsorption applications, in Cheremisinoff NP and F Ellerbusch (EDS.)", Carbon Adsorption Handbook, Ann Arbor: Ann Arbor Science, 1-53 (1978).

41. Smisek, M. and Cerny, S., "Active carbon: Manufacture, properties, and applications", Amsterdam: Elsevier, (1970).

42. Stavropoulos, G. G., "Precursor materials suitability for super activated carbons production", *Fuel Processing Technology*, **86**, 1165-1173 (2005).

43. El-Sheikh, A. H., Newman, A. P., Al-Daffaee, H. K., Phull, S. and Cresswell, N., "Characterization of activated carbon prepared from a single cultivar of Jordanian olive stones by chemical and physicochemical techniques", *J. Anal. Appl. Pyrolysis*, **71**, 151-164 (2004).

44. Baccar, R., Bouzid, J., Feki, M. and Montiel, A., "Preparation of activated carbon from Tunisian olive-waste cakes and its application for adsorption of heavy metal ions", *J. Hazardous Materials*, **162**, 1522-1529 (2009).

45. Joanna, S., Weronika, K., Beata, M. and Zvi C, K., "Production, characterization and methane storage potential of KOH-activated carbon

from sugarcane molasses", *Industrial Crops and Products*, **47**, 153-159 (2013).

46. Geoffrey, M., Kilian, S., Arno, R., Anne, W., Stefan, T. and Ulrich, K., "Impact of activated carbon, biochar and compost on the desorption and mineralization of phenanthrene in soil", *Environmental Pollution*, **181**, 200-210 (2013).

47. George Z. K., Nikolaos, K. L. and Eleni, A. D., "Oxidation time effect of activated carbons for drug adsorption", *Chemical Engineering Journal*, **xxx**, xxx-xxx (2013).

48. Kutahyal, C. and Eral, M., "Sorption studies of uranium and thorium on activated carbon prepared from olive stones: Kinetic and thermodynamic aspects", *J. Nuclear Materials*, **396**, 251-256 (2010).

49. Chafia, B., Mohamed, S., Odile, B. and Jean-Pierre, B., "Preparation and characterization of activated carbon from date stones by physical activation with steam", *J. Anal. Appl. Pyrolysis*, **82**, 70-77 (2008).

50. Nese, O. and Ennil, K., "A kinetic study of nitrite adsorption onto sepiolite and powdered activated carbon", *Desalination*, **223**, 174-179 (2008).

51. Walid, K. L., "Production of activated carbon from acorns and olive seeds", *Biomass and Bioenergy*, **20**, 57-62 (2001).

52. Reffas, A., Bernardet, V., David, B., Reinert, L., Lehocine, M., Dubois, M., Batisse, N. and Duclaux, L. "Carbons prepared from coffee grounds by H_3PO_4 activation: Characterization and adsorption of methylene blue and Nylosan Red N-2RBL", *J. Hazardous Materials*, **175**, 779-788 (2010).

53. Yang, T. and Lua, A., "Textural and chemical proprieties of zinc chloride activated carbons prepared from pistachio-nut shells", *Materials Chemistry and Physics*, **100**, 438-444 (2006).

54. Stavropoulos, G. G. and Zabaniotou, A. A., "Minimizing activated carbons production cost", *Fuel Processing Technology*, **90**, 952-957 (2009).

55. Amina, A. A., Badie, S. G. and Nady, A. F., "Removal of methylene blue by carbons derived from peach stones by H_3PO_4 activation: Batch and column studies", *Dyes and Pigments*, **76**, 282-289 (2008).

56. Gergova, K. and Eser, S., "Effect of activation method on the pore structure of activated carbons from apricot stones", *Carbon*, **34** (7), 879-888 (1996).

57. Valle, C. J., Corzo, M. G., Villegas J. P. and Serrano,V. G., "Study of cherry stones as raw material in preparation of carbonaceous adsorbents", *Analytical and Applied Pyrolysis*, **73** (1) , 59-67 (2005).

58. Al-Khateeb, I.I. and Al-Mehemdy, A.A., "Adsorption of orange II dye using activated carbon produced from Iraqi date-palm stones", *J. Chem. Eng.*, **5**, 715-723 (2011).

59. Alonso, A. M. and Tascon, J. M., "Pyrolysis of apple pulp: Chemical activation with phosphoric acid", *Analytical and Applied Pyrolysis*, **63** (2), 283-301 (2002).

60. Guoans, Y. and Rockstraw, D., "Physicochemical properties of carbons prepared from pecan shell by phosphoric acid activation", *Bioresour. Technol*, **98**, 1513-1522 (2007).

61. Hu, Z. and Vansant, E., "Carbon molecular sieves produced from walnut shell", *Carbon*, **33** (5), 561-567 (1995).

62. Toles, C. A., Marshall, W. E., Wartelle, L. H. and Johns, M. M., "Acid activated carbons from almond shells: Physical, chemical and adsorptive properties and estimated cost of production", *Bioresource Technology*, **71** (1), 87-92 (2000).

63. Tan, I. A., Ahmad, A. L. and Hameed, B. H., "Adsorption of basic dye on high surface area activated carbon prepared from oil palm shell: Batch and fixed bed studies", *Desalination*, **255** (1-3), 13-28 (2008).

64. Chuah, T. G., Jumasiah, A., Azni, I., Katayon, S. and Choong, S. Y., "Rice husk as a potentially low-cost biosorbent for heavy metal and dye removal: An overview", *Desalination*, **175**, 305-316 (2005).

65. Emine, Y., Meryem, O. and Zeki, A., "A novel method for production of activated carbon from waste tea by chemical activation with microwave energy", *Fuel*, **87**, 3278-3285 (2008).

66. El-Hendawy, A. A., Samara, S. E. and Girgis, B. S., "Adsorption characteristics of activated carbons obtained from corncobs", *Colloids Surf. A: Physicochem. Eng. Aspects*, **180**, 209-221 (2001).

67. Ersan, P., Basak, B. U. and Ayse, E. P., "Fixed-bed catalytic pyrolysis of cotton-seed cake: Effects of pyrolysis temperature, natural zeolite content and sweeping gas flow rate", *Bioresource Technology*, **97** (5), 701-710 (2006).

68. Roman, S., Gonzalez, J. F., Gonzalez-Garcia, C. M. and Zamora, F., "Control of pore development during CO_2 and steam activation of olive stones", *Fuel Processing Technology*, **89**, 715-720 (2008).

69. Alkhamis, T. M. and Kablan, M. M., "Olive cake as an energy source and catalyst for oil shale production of energy and its impact on the environment", *Energy Conversion and Management*, **40**, 1863-1870 (1999).

70. Turkan, K. and Atakan, T., "Preparation of activated carbons from Zonguldak region coals by physical and chemical activations for hydrogen sorption", *International Journal of Hydrogen Energy*, **32**, 5005- 5014 (2007).

71. Suat, U., Murat, E., Turgay, T. and Selhan, K., "Preparation and characterization of activated carbon produced from pomegranate seeds by $ZnCl_2$ activation", *Applied Surface Science*, **255**, 8890-8896 (2009).

72. Khalilia, N. R., Campbella, M., Sandib, G. and Golasc, J., "Production of micro- and mesoporous activated carbon from paper mill sludge. Effect of zinc chloride activation", *Carbon*, **38**, 1905-1915 (2000).

73. Jiaojiao, K., Qinyan, Y., Bo, W., Lihui, H., Baoyu, G., Yan, W. and Qian, L., "Preparation and characterization of activated carbon from leather waste microwave-induced pyrophosphoric acid activation", *Journal of Analytical and Applied Pyrolysis*, **xxx**, xxx-xxx (2013).

74. Turmuzi, M., Daud. R. M., Tasirin, S.M., Takriff, M.S. and Iyuke, S.E., "Production of activated carbon from candlenut shell by CO_2 activation", *Carbon*, **42**, 423-460 (2004).

75. Rio, S., Faur, C., Le Coq, L., Courcoux, P. and Le Cloirec, P., "Experimental design methodology for the preparation of carbonaceous sorbents from sewage sludge by chemical activation: Application to air and water treatments", *Chemosphere*, **58**, 423-437 (2005).

76. Williams, P. T. and Reed, A. R., "Development of activated carbon pore structure via physical and chemical activation of biomass fiber waste", *Biomass and Bioenergy*, **30**, 144-152 (2006).

77. Mehmet, U., Ahmet, G. and Metin, A., "Comparison of textile dyeing effluent adsorption on commercial activated carbon and activated carbon prepared from olive stone by $ZnCl_2$ activation", *Microporous and Mesoporous Materials*, **111**, 228-235 (2008).

78. Martín-Lara, M. A., Pagnanelli, F., Mainelli, S., Calero, M. and Toro, L.,"Chemical treatment of olive pomace: Effect on acid-basic properties and metal biosorption capacity", *Hazardous Materials*, **156** (3), 448-457 (2008).

79. Caturla, F., Molina-Sabio, M. and Rodriguez-Reinoso, F., "Preparation of activated carbon by chemical activation with $ZnCl_2$", *Carbon*, **29**, 999-1007 (1991).

80. Tzong-Horng, L., "Development of mesoporous structure and high adsorption capacity of biomass-based activated carbon by phosphoric acid and zinc chloride activation", *Chemical Engineering Journal*, **158** (2), 129-142 (2010).

81. El-Sayed, Y. and Bandosz T., "Adsorption of valeric acid from aqueous solution onto activated carbons: Role of surface basic sites", *J. Colloid Interf. Sci.*, **273**, 64-72 (2004).

82. Shen, W., Li, Z. and Liu, Y., "Surface chemical functional groups modification of porous carbon", *Recent Patents on Chemical Engineering*, **1**, 27-40 (2008).

83. Moreno-Castilla, C., "Adsorption of organic molecules from aqueous solutions on carbon materials", *Carbon*, **42**, 83-94 (2004).

84. Derylo-Marczewska, A., Swiatkowski, A., Biniak, S. and Walczyk, M., "Effect of properties of chemically modified activated carbon and aromatic adsorbate molecule on adsorption from liquid phase", *Colloids and Surfaces A: Physicochem. Eng. Aspects*, **327**, 1-8 (2008).

85. Kim, B. J., Park, S. J., "Effects of carbonyl group formation on ammonia adsorption of porous carbon surfaces", *J. Colloid Interface Sci.*, **311**, 311-314 (2004).

86. Huang, C., Li, S. and Chen, H., "Effect of surface acidic oxides of activated carbon on adsorption of ammonia", *J. Hazard. Mater.*, **159** (2-3), 523-527 (2008).

87. Stoeckli, F., Hugi-Cleary, D.,"On the mechanisms of phenol adsorption by carbons", *Russ. Chem. B*, **50**, 2060-2063 (2001).

88. Erlangung, D.,"Carbon Nanotube Composites-Mechanical Electrical and Optical Properties", Ph.D. Thesis, Rheinischen Friedrich, Wilhelms-University Bonn (2006).

89. Donglin, Z., Weimeng, Z., Changlun, C. and Xiangke, W.," Adsorption of methyl orange dye onto multi-walled carbon nanotubes", *Procedia Environmental Sciences*, **18**, 890-895 (2013).

90. Dekker, C., "Physics Today" 52 (22), (1999).

91. Dresselhaus, M. S., Dresselhaus, G. and Eklund, P. C., "Science of Fullerenes and Carbon Nanotubes", Academic Press, San Diego, 2 C (1996).

92. Meei, M. G., Yan, X. Y., Siang, P.C. and Abdul Rahman, M.," Multi-walled carbon nanotubes modified with (3-aminopropyl) triethoxysilane for effective carbon dioxide adsorption", *International Journal of Greenhouse Gas Control*, **14**, 65-73 (2013).

93. Ajayan, P. M., "Carbon Nanotubes, Handbook of Nanostructure Materials and Nanotechnology", 5, 375- 403 (2000).

94. Onur, G. A., Qiliang, W., Yang, Z. and Tanju, K., "Adsorption of aromatic organic contaminants by graphene nanosheets: Comparison with carbon nanotubes and activated carbon", *Water Research*, **47**, 1648 -1654 (2013).

95. Ajayan, P.M. and Ebbesen, T.W., "Nanometer-size tubes of carbon", *Rep. Prog. Phys.*, **60**, 1025-1062 (1997).

96. Fei, Y., Yanqing, W., Jie, M. and Chi, Z., "Adsorption of lead on multi-walled carbon nanotubes with different outer diameters and oxygen contents: Kinetics, isotherms and thermodynamics", *Journal of Environmental Sciences*, **25**(1), 195-203 (2013).

97. Paul, L. M., Michael, S. F. and Hongkun, P., "Single-walled carbon nanotube electronic", *IEEE Transactions on Nanotechnology*, **1**(1), 78-85 (2002).

98. Meyyappan, M., "Carbon nanotubes science and applications"; CRC Press: Boca Raton, FL, (2005).

99. Daenen, M., Fouw, R.D., Hamers, B., Janssen, P.G., Schouteden, K. and Veld, M.A., "The Wondrous Word of Carbon Nanotubes" Eindhoven University of Technology, (2003).

100. Adedeji, E. A., "Development and Model Formation of Scalable Carbon Nanotube Processes HiPCO and CoMoCAT Process Models ", M.S. of Science in Chemical Engineering, Louisiana State University and, Mechanical College (2005).

101. Rahmanian, S., Suraya, A.R., Zahari, R. and Zainudin, E.S., "Synthesis of vertically aligned carbon nanotubes on carbon fiber", *Applied Surface Science*, **271**, 424-428 (2013).

102. Jong, Y. S., Hyunwook, S., "Molecular scale electronic devices using single molecules and molecular monolayers", *Current Applied Physics*, **xxx**, 1-15 (2013).

103. Terrones, M., "Science and technology of the Twenty-First century: Synthesis, properties and applications of carbon nanotubes", *Annual Review of Materials Research*, **33**, 419-509 (2003).

104. Baughman, R. H., Zakhidov, A. A. and Heer, W. A., "Carbon nanotubes - the route toward applications", *Science Compass Review*, **297**, 787-792 (2002).

105. Wu, Y., Lun, W., Haiyan, W., Xiaolei, Z., Ling, L., Na, Z., Le, P. and Nannan, X.," An electrochemiluminescent DNA sensor based on nano-gold enhancement and ferrocene quenching", *Biosensors and Bioelectronics*, **40**, 356-361 (2013).

106. Mccabe, L. and Smith, C., "Unit Operation of Chemical Engineering", Peter Harriott.

107. Jalal, M. S., "Surface Chemistry and Catalyst" 1st, addition, Baghdad University Press (1980).

108. Maron, S.H. and Lando, J.B., "Fundamentals of Physical Chemistry" Macmillan pulishing Co., London (1974).

109. Doming, M., Fernandez, I. and Morals, F.G., *J. Chromatog.*, **29**, 14-21 (1984).

110. Anthony, L. H. and Robert, N. M., "Mass Transfer Fundamentals and Applications", Prentice-Hall Inc., p.458, 460 (1985).

111. Durgananda, C.," Adsorption-Filtration Hybrid System in Wastewater Treatment and reuse" Ph.D. Thesis University of Technology Sydeny, Australia, (2003).

112. Oscik J.O. and Cooper I.L., "Adsorption ", 15th edition Wiely and Sons, New York, (1982).

113. Al Duri, B., "Adsorption modeling and mass transfer, use of adsorbents for the removal of pollutants from waste waters", CRC, N. Y., 133-140, (1996).

114. Haghseresht, F. and Lu, G., "Adsorption characteristics of phenolic compounds onto coal-reject-derived adsorbents", *Energy Fuels*, **12**, 1100-1107 (1998).

115. Fytianos, K., Voudrias, E. and Kokkalis, E., "Sorption-desorption behavior of 2, 4-dichloriphenol by marine sediments", *Chemosphere*, **40**, 3-6 (2000).

116. Mehdi, V., Marjan, A., Marjan, Z., and Bita, J., "Application of the Freundlich, Langmuir, Temkin and Harkins-Jura Adsorption Isotherms for Some Amino Acids and Amino Acids Complexation with Manganese Ion (II) on Carbon Nanotube", *International Conference on Nanotechnology and Biosensors*, **2** , 117-119 (2011).

117. Amarnath, R.K, Ultrasonic chemistry, A survey and energy assessment, TR-109974, Finareport, April, (1998).

118. Joost, R., Evgeny, V. R., Jaap, C. S. and Jos, T.K.," Dissolved gas and ultrasonic cavitation - A review", *Ultrasonics Sonochemistry*, **20**, 1-11 (2013).

119. Abolfazl, Z., Javad, S. and Sahar, R., "Sonochemically synthesis of pyrazolones using reusable catalyst CuI nanoparticles that was prepared by sonication", *Ultrasonics Sonochemistry*, **20**, 1069-1075 (2013).

120. Ince, N.H., Tezcanli, G., Belen, R.K. and Apikyan, I.G., "Ultrasound as a catalyzer of aqueous reaction systems: The state of the art and environmental applications", *Appl. Catal. B-Environ.*, **29**, 167-176 (2001).

121. Suslick, K.S., "The chemistry of ultrasound. Chicago: Encyclopedia Britannica", 138-155 (1994).

122. Gong, C. and Hart, D.P, "Ultrasound induced cavitation and sonochemical yields", *J. Acoustic Society of America*, **104**, 1-16 (1998).

123. Chen, Y.C, "Enhancement on photocatalytic degradation of phenol by ultrasound" 10-31 (2002).

124. Dehghani, M.H. and Changani, F., "The effect of acoustic cavitation on chlorophyceae from effluent of wastewater treatment plant", *Environmental Technology*, **27**, 963-968 (2006).

125. Praveena, J. D and Palanivelu, K., "Sonochemical degradation of p-chlorophenol in aqueous solution using hypervalent iron", *Indian Journal of Chemical Technology*, **17**, 111-119 (2010).

126. Rosello, I.R, "Waste treatment by sonochemical, electrochemical and sonoelectrochemical technology", Universidad de Alicante, (1999).

127. O'Grady, T. M. and Wennerberg, A. N., "High-surface area active carbon", ACS Symposium Series 303, Publ. ACS, Washington D.C., USA, p. 302-309 (1984).

128. Massoud, R.A., Jian, S., M. and Daniel, B., "Novel carbons from Illinois coal for natural gas storage", ICCI Project Number: 95-114 (1996).

129. Gracia, A., Gregorio, A., Boavida, D. and Gulyurtlu, I., "Preparation and characterization of activated carbon from pine wastes gasified in a pilot reactor", Department of Inorganic Chemistry, University of Alicante, Spain, (2003).

130. Aweed, K.A., "Study effect of structural modifications on the production of the activated carbon from heavy crude oil residues by chemical treatment". Ph.D. Thesis, University of Mosul (2003).

131. Prinsloo, F.F. and Jager, S., "Preparation of active carbon from coke by chemical activation", Sastech, R. & D, Po. Box.1, Sasolburg 9570, Rep. of South Africa, (2003).

132. Kim, M.S., Hong, J.C. and Lim, Y.S., "Preparation and properties of activated carbon from rice hulls" Myong J., University, Korea, 104-105 (2003).

133. Aweed, K.A., "Production of activated carbon from some agricultural wastes by chemical treatment", *National Journal of Chemistry*, **17**, 138-142 (2004)

134. Rhamadhan, O.M., Hamdon, A.A. and Al-Ghanam, K.A., *J. Sci. & Edu.*, **16** (2), (2004).

135. Al-Ghanam, K.A., Rhamadhan, O.M. and Hamdon, A.A., *J. Sci. & Edu.*, **16** (3), (2004).

136. Al-Ghanam, K.A., Al-Neaime, K.I. and Hamdon, A.A., *J. Sci. & Edu.*, **16** (3) (2004).

137. Al-Ghannam, K.A., Al-Neaime, K.I and Hamdon A.A. , "Study of adsorption some organic acids from aqueous solutions by activated carbon production by chemical treatment". *J. Sci. & Edu.*, **16**, 3-15 (2004).

138. Gonzalez, S., "Removal of water pollutants with activated carbons prepared from H_3PO_4 activation of Lignin from kraft black liquors", *Water Res.*, **38** (13), 3043 -3050 (2004).

139. Ichcho, S., Khouya, E., Abourriche, A., Ezzine, M., Hannache, H., Naslain R. and Pailler R., "Phosphoric acid activation of Morrocan oil shale of timahdit: Influence of the experimental conditions on yield and surface area of adsorbents", *J. Phys. IV France*, **123**, 81-85 (2005).

140. Hamdon, A.A., Aweed, K.A. and Al-Dubony, S.A., "Production of activation carbon by chemical treatment and study effect of Gamma rays on its", *J. Edu. Sci.*, **12**, 17- 22 (2005).

141. Dusart, O., Bouabane, H. and Mozet, M., *J. Chimie Physique Etde. Physico-Chimie Biologique*, **88**, 243-252 (1991).

142. Ryabukhova, V.O., Arzamaa, S., Okishevana, A.B. and Konovalova, S.N., *Russian J. of Physical Chemistry*, **74**, 272- 281 (2000).

143. Al-Hyali, A.A., Ramadhan, O.M. and Al-Dubony, S.A., *J. Rafiden Science*, **10**, 12-22 (2004).

144. Punjaporn, W., Onanong, K. and John, F., "Benzene removal from waste water using aqueous surfactant two-phase extraction with cationic and anionic surfactant mixtures" *J. of Chemosphere*, **72**, 1043-1048 (2008).

145. Valente, J.M., Gomes, N. J., Carrott, S. P., Laginhas, C. and Roman, S., "Phenol removal onto novel activated carbons made from lingocellulosic precursors: Influence of surface properties", *J. of Hazardous Materials*, **167**, 904-910 (2009).

146. Chen, D.Z., Zhang, J.X. and Chen, J.M.," Adsorption of methyl tert-butyl ether using granular activated carbon: Equilibrium and kinetic analysis*", Int. J. Environ. Sci. Tech.*, **7**(2), 235-242 (2010).

147. Muftah, H. E., Sulaiman, A. and Manal, A., "Removal of phenol from petroleum refinery wastewater through adsorption on data-pit activated carbon", *Chemical Engineering Journal*, **162**, 997-1005 (2010).

148. Sze, M. and McKay, G., "An adsorption diffusion model for removal of para-chlorophenol by activated carbon derived from bituminous coal", *Environmental Pollution*, **158**, 1669-1674 (2010).

149. Salman, J.M., Njokua, V.O. and Hameed, B.H, "Batch and fixed-bed adsorption of 2, 4-dichlorophenoxy acetic acid onto oil palm frond activated carbon", *Chemical Engineering Journal*, **174**, 33-40 (2011).

150. Natalia, G.A, Patricia, A., Marcos, G., Clara, B., Ricardo, S. and Rosa, M., "High performance activated carbon for benzene/toluene adsorption from industrial wastewater", *J. of Hazardous Materials*, **192**, 1525-1532 (2011).

151. Nourmoradi, H., Nikaeena, M. and Khiadani, M., "Removal of benzene, toluene, ethylbenzene and xylene (BTEX) from aqueous solutions by montmorillonite modified with nonionic surfactant: Equilibrium, kinetic and thermodynamic study", *Chemical Engineering Journal*, **191**, 341-348 (2012).

152. Iijima, S., "Helical microtubules of graphitic carbon", *Nature*, **354**, 56-58 (1991).

153. Ebbesen, T.W. and Ajayan, P.M., "Large scale synthesis of carbon nanotubes", *Nature*, **358**, 220-222 (1992).

154. Bethune, D. S., Klang, C. H., Gorman, G., Savoy, R., Vazquez, J. and Beyers, R., "Cobalt-catalysed growth of carbon nanotubes with single-atomic-layer walls", *Nature*, **363**, 605-607 (1993).

155. Smalley, R. E., Thess, A., Lee, R., Nikolaev, P. and Scuseria, G., *Science*, **273**, 483-487 (1996).

156. Journet, C., Maser, W., Bernier, P., Lefrant, S., Denlard, P. and Lee, R., "Large-scale production of single-walled carbon nanotubes by electric-arc technique", *Nature*, **388**, 756-758 (1997).

157. Huang, Z., Ling, Z., Guangming, H. and Rongsheng, S.,"Synthesis of various forms of carbon nanotubes by AC arc-discharge", *Carbon*, **36** (3), 259-261 (1998).

158. Kazaoui, S., Minami, N., Yamawaki, H., Kataura, H. and Achiba, Y. "Pressure dependence of the optical absorption spectra of single-walled carbon nanotube films", *Phys. Rev*., **62** (3), 123-132 (2000).

159. Park, Y. S., Choi, Y. C., Kim, K. S., Chung, D. C., Zhu, X. Y. and Lee, Y. H., "High yield purification of multi-walled carbon nanotubes by selective oxidation during thermal annealing", *Carbon*, **39**, 655-661 (2001).

160. Lee, S.J., Baik, H.K. and Han, J.H., "Large scale synthesis of carbon nanotubes by plasma rotating arc-discharge technique", *Diamond and Related Materials*, **11**, 914-917 (2002).

161. Yu, J., Lucas, J., Strezov, V. and Wall, T., "Coal and carbon nanotube production", *Fuel*, **82**, 2025-2032 (2003).

162. Debasis, B., Suresh, C., Matthem, M. and Sudipta, S., "In-situ synthesizes of palladium nanoparticals-filled carbon nanotubes using

arc-discharge in solution", *Chemical Physics Letter*, **4386**, 364-368 (2004).

163. Ambrosio, A., Ambrosio, M., Ambrosone, G., Passacantando, M. and Santucci, S., "Use of carbon nanotubes as radiation detectors" (2005).

164. Hitoshi, Y. and Tetsu, W., "X-Ray diffraction of multi-walled carbon nanotube under high pressure: Structural durability on static compression", *Carbon*, **43**, 519-523 (2005).

165. Pekker, A., Borondics, F., Kamaras, K., Rinzler, A. and Tanner, D., "Calculation of optical constants from carbon nanotube transmission spectra", *Phys. Stat. Sol.*, **243** (13), 3485-3488 (2006).

166. Bryan, H., Stephanie, G. and David, A.," Diode properties of nanotube networks", Materials Engineering, N283 ESC, Provo, UT 84602, Provo, UT, 84606, 1-16 (2007).

167. Roy, D., Angeles, E., Brown, R., Spencer, S., Fry, T., Young, T. and Miltn, M., "Synthesis and Raman spectroscopic characterization of carbon nano-scrolls", *Chemical Physics Letter*, **465**, 254-257 (2008).

168. Liao, Q., Sun, J. and Gao, L., "The adsorption of resorcinol from water using multi-walled carbon nanotubes", *Coll. And Surf. A. Physicochem. Eng. Aspects*, **312**, 160-165 (2008).

169. Yang, K. and Xing, B., "Adsorption of fulvic acid by carbon nanotubes from water", *Environmental pollution*, **157**, 1095-1100 (2009).

170. Arasteh, R., Masoumi, M., Rashidi, A., Moradi, L., Samimi, V. and Mostafavi, S., "Adsorption of 2-nitrophenol by multi-wall carbon nanotube from aqueous solutions" *Applied Surface Science*, **256**, 4447-4455 (2010).

171. Yu, F., Ma, J. and Wu, Y., "Adsorption of toluene, ethyl-benzene and m-xylene on multi-walled carbon nanotubes with different oxygen contents from aqueous solutions", *J. Hazar. Mater.*, **192**, 1370-1379 (2011).

172. Yao, Y., He, B., Xu, F. and Chen, X., "Equilibrium and kinetic studies of methyl orange adsorption on multi walled carbon nanotubes", *Chem. Eng. J.*, **170**, 82-89 (2011).

173. Bina, B., Amin, M., Rashidi, A. and Pourzamani, H., "Benzene and toluene removal by carbon nanotubes from aqueous solution", *Archi. of Envi.*, **38**, 3-25 (2012).

174. Donglin, Z., Weimeng, Z., Changlun, C. and Xiangke, W., "Adsorption of methyl orange dye onto multi-walled carbon nanotubes", *Procedia Environmental Sciences*, **18**, 890-895 (2013).

175. Maezawa, A., "Utilization of Ultrasonic energy in a photocatalytic oxidation process for treating waste water containing surfactants", Department of Materials Science and Chemical Engineering, Shizuoka University, Hamamatsu 432-8561, Japan (2000).

176. Kulkarni, A.A. and *et. al.*, "Techniques of wastewater treatment", 56-68 (2000).

177. Selli, E., "Synergistic effects of sonolysis combined with photocatalysis in the degradation of an azo dye", Physical Chemistry Chemical Physics, 19, I 20133, Italy (2002).

178. Vajnhandl, S. and Marechal, A., "Ultrasound in textile dyeing and the decolouration-mineralization of textile dyes". *Dyes and Pigments*, **65** (2), 89-101(2005) .

179. Zeng, L. and James, W.M., "Degradation of pentachlorophenol in aqueous solution by audible-frequency sonolytic ozonation" , *J. Hazar. Mater.*, **35** (3), 218-225 (2006).

180. Yano, J., Matsuura, J., Ohura, H. and Yamasaki, S., "Complete mineralization of propyzamide in aqueous solution containing TiO_2 particles and H_2O_2 by the simultaneous irradiation of light and ultrasonic waves", *Ultrason. Sonochem*, **12** (3), 197-203 (2005).

181. Berberidou, C., "Sonolytic, photocatalytic and sonophotocatalytic degradation of malachite green in aqueous solutions", *Environmental*, **74**, 63-72 (2007).

182. Selli, E., "Efficiency of 1,4-dichlorobenzene degradation in water under photolysis, photocatalysis on TiO_2 and sonolysis", *Journal of Hazardous Materials*, **153**, 1136-1141 (2008).

183. Mahvi, A.H., "Application of ultrasonic technology for water and wastewater treatment", *Iranian Journal of Public Health*, **38** (2), 1-17 (2009).

184. Qusay, J. R., Kannaiyan, P. and Karuppan, M., "Treatment of petroleum refinery wastewater by ultrasound-dispersed nanoscale zero-valent iron particles", *Ultrasonics Sonochemistry*, **18**, 1138-1142 (2011).

185. Xikui, W., Yuechang, W., Jingang, W., Weilin, G. and Chen, W., "The kinetics and mechanism of ultrasonic degradation of p-nitrophenol in aqueous solution with CCl_4 enhancement", *Ultrasonics Sonochemistry*, **19**, 32-37 (2012).

186. Meral, D. and Gonul, G., "Sonolytic degradation of butyric acid in aqueous solutions", *Journal of Environmental Management*, **129**, 564-568 (2013).

187. Standard Test Method for Distillation of Petroleum Products at Atmospheric Pressure, D 86 -07 (1986).

188. Standard Test Method for Flash and Fire Points by Cleveland Open Cup Tester, D 92-05 (1992).

189. ASTM-D2866-70, "Total ash content of activated carbon", Annal Book of ASTM standard   compyrigth ASTM rase street, (1970).

190. ISO, 5.62-1981, "Determination of volatile matter content of hard coal and coke", the full text can be obtained from ISO central secretarial cose postable 5G, CH-1211: Genera 20 or Any ISO member, (1981).

191. ASTM D2854-70, "Standard test method for apparent density of activated carbon", (1970).

192. Glasstone, S. and Lews, D.," Elements physical chemistry" 2nd Edition, Macmillan and Coltd, London, p.506-565, (1963).

193. Adamson, A. W. and Gast, A. P., "Physical Chemistry of Surfaces," 6th Edition, Jon Wiley and sons, New York, (2001).

194. Khursheed, A., "Scanning electron microscope optics and spectrometeras", World Scintific Publishing Co. Pte. Ltd., Singapor, (2011).

195. Bogner, A., Jouneau, P.H., Thollet, G., Basset, D. and Gauthier, C., "A history of scanning electron microscopy developments: Towards wet-TEM" imaging, Micron 38, 390-401 (2007).

196. Reimer, L., "Transmission electron microscopy", 5th, in, Springer Science Business Media, LLC., New York, USA (2008).

197. Schroder. D.K., "Semiconductor material and device characterization", New York, john Wiley & Sons. (1998).

198. Neha, B., Rajiv, V., and .Jani, R.A., "X-ray diffraction studies of NbTe2 single crystal", *Bulletin of Material Science*, **27**, 23-25 (2004).

199. Fogler, H.S., "Elements of chemical reaction engineering", Prentice-Hall, (1986).

200. Saroj, B., Surendra, D. and Pradip, R.," Hexavalent chromium removal from aqueous solution by adsorption on treated sawdust", *Biochemical Engineering Journal*, **31**(3), 216-222 (2006).

201. Purkait, M., Dasgupta, S. and De, S., "Determination of thermodynamic parameter for the cloud point extraction of different dyes using TX-100 and TX-114", *Desalination*, **244**, 130-138 (2009).

202. Abdullah, A.H., Kassim, A., Zainal, Z., Hussien, M.Z., Kuang, D., Ahmad, F. and Wooi, O.S., "Preparation and characterization of activated carbon from gelam wood bark (Melaleuca Cajuputi)", *Malaysian Journal of Analytical Sciences*, **7**, 65-76 (2001).

203. Saleh, N.J., Ismaeel, M.I. and Ibrahim, R.I., "Preparation activated carbon from Iraqi reed", *Eng. & Tech.*, **26** (3), 291-203 (2008).

204. Tongpoothorn, W., Sriuttha, M., Homchan, P., Chanthai, S. and Ruangviriyachai, C., "Preparation of activated carbon derived from Jatropha curcas fruit shell by simple thermo-chemical activation and characterization of their physico-chemical properties", *Chem. Eng. Res. Des.*, **89**, 335-340 (2011).

205. Yang, J. and Qiu, K., "Preparation of activated carbons from walnut shells via vacuum chemical activation and their application for methylene blue removal", *Chem. Eng. J.*, **165**, 209-217 (2010).

206. Zhang, Z., Xu, M., Wang, H. and Li, Z., "Enhancement of CO_2 adsorption on high surface area activated carbon modified by N_2, H_2 and ammonia", *Chem. Eng. J.*, **160**, 571-577 (2010).

207. Ozturk, N., and Bektaş, T. E., "Nitrate removal from aqueous solution by adsorption onto various materials", *J. Hazardous Materials*, **112**, 155-162 (2004).

208. Ramakrishna, K. R., and Viraraghavan, T., "Dye removal using low cost adsorbents", *Water Sci. Tech.*, **36** (2-3), 189-196 (1997).

209. Ramadhan, O. M. and Rigibi, M. A., "Activated carbon by modified carbonization", *Sciences and Educt.*, **46**, 110-121 (2000).

210. Fripiat, J.J. and Gatineau, L., "Multilayer physical adsorption on fractal surfaces", *Langmuir*, **2**(5), 562-567 (1986).

211. Ho, Y. S., "Citation review of Lagergren kinetic rate equation on adsorption reaction", *Scientometrics*, **59** (1), 171-177 (2004).

212. Francony, A. and Petrier, C., "Sonochemical degradation of carbon tetrachloride in aqueous solution at two frequencies: 20 kHz and 500 kHz", *J. Ultrason Sonochem.*, **3**, 77-82 (1996).

213. Ashokkumar, M., Niblett, T., Tantiongco, L. and Grieser, F., "Sonochemical degradation of sodium dodecyl benzene sulfonate in aqueous solutions", *Aust. J. Chem.*, **56** (10), 1045-1049 (2003).

214. Yim, B., Okuno, H., Nagata, Y., Nishimura, R. and Maeda, Y., "Sonolysis of surfactants in aqueous solutions: An accumulation of

solute in the interfacial region of the cavitation bubbles", *Ultrason. Sonochem.*, **9** (4) 209-213 (2002).

215. Dehghani, M.H., Mesdaghinia, A.R. and Mahvi, A.H., "Application of sonochemical reactor technology for degradation of reactive yellow dye in aqueous solution", *Water Qual. Res. J. Canada*, **43** (2-3) 183-187 (2008).

216. Dehghani, M.H. and Changani, F., "The effect of acoustic cavitation on chloro phyceae from effluent of wastewater treatment plant", *Environ. Technol.*, **27** (9) 963-968 (2006).

217. Nanzai, B., Okitsu, K., Takenaka, N., Bandow, H., Tajima, N. and Maeda, Y., "Effect of reaction vessel diameter on sonochemical efficiency and cavitation dynamics", *Ultrason. Sonochem.*, **16**, 163-168 (2009).

218. Villeneuve, L., Alberti, L., Steghens, J. P., Lanceline, J. M. and Mestas, J. L., "Assay of hydroxyl radicals generated by focused ultrasound", *Ultrason. Sonochem.*, **16**, 339-344 (2009).

219. Trabelsi, F., Ait-Lyazidi, H., Ratsimba, B., Wilhelm, A.M., Delmas, H., Fabre, P.L. and Berlan, J., "Oxidation of phenol in wastewater by sono electrochemistry". *Chem. Eng. Sci.,* **51**, 1857-1865 (1996).

220. Janet, D., Joern, T. and Detlef, W. B., "Formation of nitroaromatic compounds in advanced oxidation process: Photolysis versus photo catalysis", *Environ. Sci. Technol.*, **33**(2), 294-300 (1999).

221. Serpone, N. R., Terzan, P., Colarusso, P., Minerco, C., Pelizzetti, E. and Hidaka, H., "Sonochemical oxidation of phenol and three of its intermediate products in aqueous media: Catechol, hydroquinone, and benzoquinone, kinetic and mechanistic aspects", *Res. Chem. Intermediates*, **18**, 183-202 (1992).

222. Currell, D.L. and Zechmeister, L., "On the ultrasonic cleavage of some aromatic and heterocyclic rings", *J. Am. Chem. Soc.*, **80**, 205-208 (1958).

223. Ke, G. and Yan-Jie, D., "Plasma induced degradation of azobenzene in water", *J. Chin. Chem.* Soc., **52**, 273-276 (2005).

224. Gai, K., "Anodic oxidation with platinum electrodes for degradation of p-xylene in aqueous solution", *J. of Electrostatics*, **67**, 554-557 (2009).

الخلاصة

يتصف الكاربون المنشط بمواصفات ذات أهمية صناعية كبيرة ويستعمل في السيطرة على التلوث البيئي. تهدف الدراسة الحالية بصورة رئيسية الى متابعة إزالة الملوثات مثل البنزين والاورثو زايلين وأيون الكبريتيد بأستخدام مايلي:

1- الكاربون غير المنشط والكاربون المنشط وأنابيب الكاربون النانوية متعددة الجدران المنتجة من مخلفات النفط الأسود الخارج من محطات الطاقة الكهربائية.

2- تقنية الموجات فوق الصوتية.

ويتضمن الجزء الأول منها تحضير الكاربون غير المنشط والكاربون المنشط من مخلفات النفط الأسود بعمليات الكلسنة والتنشيط وبأستعمال 20% من كلوريد الزنك اللامائي. وقد تم تحضير أنابيب الكاربون النانوية متعددة الجدران بطريقة جديدة من الكاربون المنشط وبأستخدام تقنية الموجات فوق الصوتية ولأول مرة. كما جرى تشخيص أنابيب الكاربون النانوية متعددة الجدران بأستخدام تقنيات متطورة مثل المجهر الالكتروني الماسح عالي الكفاءة ، والمجهر الالكتروني الناقذ، ومجهر القوة الذرية ، وحيود الأشعة السينية، وطيف الأشعة تحت الحمراء. إضافة الى قياس وتقييم بعض الصفات الفيزيائية للنماذج المحضرة من الكاربون مثل المساحة السطحية والدالة الحامضية والكثافة والمحتوى الرطوبي والرماد.

إستعملت نماذج أنابيب الكاربون النانوية متعددة الجدران لإزالة البنزين والأورثو زايلين وأيون الكبريتيد من محاليلها المائية حيث تم استخدام طريقة التوازن الاعتيادي لأيون الكبريتيد بينما البنزين والاورثو زايلين فقد أستخدام نظام التدوير الجديد الذي تم تصميمه واقتراحه من خلال هذه الدراسة. أعتمدت معاير تقييم كفاءة أنابيب الكاربون النانوية متعددة الجدران ونماذج الكاربون المنشط وغير المنشط من خلال دراسة عملية الإمتزاز للبنزين والأورثو زايلين وأيون الكبريتيد

للتراكيـــــز (50, 100, 150, 200, 250, 300) ملغم/لتر وبأربع درجات حرارية مختلفة (283, 293, 313, 333) مطلقة وبفترات زمنية مختلفة. تم دراسة الإمتزاز المتوازن بوساطة نظام التدوير الجديد والموديلات الأيزوثرمية مثل لانكماير وفريندلش وتمكن ، كما تم حساب العوامل الثرموديناميكية وحركية عمليات الإمتزاز .

تتأثر نسب الإمتزاز النوعي للبنزين والأورثو زايلين بشكل كبير عند إضافة المنشط وتتخفض مع زيادة درجة الحرارة مقارنة مع ما يحدث في الكاربون غير المنشط. يزداد معدل الإمتزاز مع زيادة تراكيز البنزين والأوثو زايلين، وتحصل إزالة تامة لتراكيز البنزين والأورثو زايلين عند المستويين (50, 100) ملغم / لتر عند أستعمال أنابيب الكاربون النانوية متعددة الجدران بدرجة حرارة 283 مطلقة.

وهذا يؤكد وبشكل واضح بأن إمتزاز البنزين والأورثو زايلين بأستعمال أنابيب الكاربون النانوية متعددة الجدران يتطابق بشكل جيد مع موديلات الإمتزاز لانكماير وفريندلش وتمكن. كما أن أمتزاز البنزين والاورثو زايلين بأستعمال الكاربون المنشط وغير المنشط يتطابق بشكل مقبول مع موديلي فريندلش وتمكن للأمتزاز في حين يتطابق بشكل ضعيف مع موديل لانكماير. تشير القيم السالبة للانثالبي بأن عملية الإمتزاز تكون باعثة للحرارة وأن الامتزاز يكون فيزيائياُ بينما القيم السالبة للأنتروبي توضح بأن هناك نقصاً في درجات الحرية عند الإمتزاز. تبين القيم السالبة للطاقة الحرة بأن عملية الامتزاز هي عملية تلقائية. وتوضح الدراسة الحركية لإمتزاز على مركبات الكاربون المحضرة بأن التفاعل يتطابق تماماً مع الرتبة الأولى الكاذبة.

أما الجزء الثاني من الدراسة يتعلق بعملية تحلل البنزين والأورثو زايلين في المحاليل المائية بأستخدام تقنية الموجات فوق الصوتية إذ تم تعريض المحاليل للموجات فوق الصوتية عند درجات حرارية مختلفة وبتركيزين أوليين هما (100, 200) ملغم / لتر. تم حساب الحركية والدوال

الثرموديناميكية للتحلل المائي للبنزين والأورثو زايلين. كما تم اقتراح ومناقشة ميكانيكية التحلل الصوتي للبنزين والاورثو زايلين.

وقد لوحظ زيادة معدل سرعة تحلل البنزين والأورثو زايلين مع زيادة القدرة الكهربائية وزمن التعرض للموجات فوق الصوتية وتتخفض مع حجم السائل ودرجة الحرارة والتركيز الأولي للبنزين والأورثو زايلين حيث كان التحلل تاماً للبنزين في التركيز الابتدائي 100 ملغم / لتر. ويعتقد بأن التأثير المفيد للقدرة على معدل الإزالة يكون بزيادة فعالية الفجوة التي تحصل عند المستويات العالية من القدرة. وقد بينت الدوال الثرموديناميكية بأن عملية تحلل البنزين والأورثو زايلين هي عملية تلقائية وباعثة للحرارة في حين تشير النتائج المستحصلة من الدراسات الحركية الى أن التحلل يتبع موديل الرتبة الأولى الكاذبة.

جمهورية العراق

وزارة التعليم العالي والبحث العلمي

جامعة الأنبار

كلية العلوم – قسم الكيمياء

إزالة بعض الملوثات من محاليلها المائية باستخدام تقنية الموجات فوق الصوتية وأنابيب الكاربون النانوية متعددة الجدران المحضرة

أطروحة مقدمة الى

مجلس كلية العلوم – جامعة الأنبار

وهي جزء من متطلبات نيل شهادة الدكتوراه في فلسفة علوم الكيمياء

من قبل

أحمد مشعل محمد فرحان الكبيسي

| بكالوريوس علوم كيمياء | جامعة الأنبار – 2000 |
| ماجستير علوم كيمياء | جامعة الأنبار – 2002 |

بإشراف

أ.د. عدوية جمعة حيدر **أ.د. إسماعيل خليل الخطيب**

2013 م 1434 هـ